MASS SPECTROMETRY BASED TECHNIQUES FOR *IN VIVO* NEUROCHEMICAL MONITORING

by

Peng Song

A dissertation submitted in partial fulfillment

of the requirements for the degree of

Doctor of Philosophy

(Chemistry)

in the University of Michigan

2012

Doctoral Committee:

Professor Robert T. Kennedy, Chair

Professor Philip C. Andrews

Professor Zhan Chen

Associate Professor Kristina I. Håkansson

To family and friends

ACKNOWLEDGEMENTS

I am deeply grateful to my advisor, Professor Robert T. Kennedy, whose coaching and support guided me through the 5 demanding years of PhD program. I would also like to thank the Kennedy group members whom I was very fortunate to overlap or interact with, for the sharing of their ideas, inspiring discussions, cordial friendship and valuable career advice.

I acquired the bulk of my mass spectrometry knowledge from Professor Kristina Håkansson's Chem 647. It proved to be highly valuable for my later research. I was also lucky enough to spend one semester in her group where I got exposure to the state of art mass spectrometry research.

I thank Professor Zhan Chen very much for his kindness and confidence in me. He provided valuable input which prompted me to think deeper on my research. What I learned from his spectroscopy class laid a good foundation for my future industrial R&D needs.

I would like to thank Professor Philip Andrews for his keen interest in my research, insightful discussion and sharing his group's expertise and equipment.

I would also like to express my appreciation to faculties and staff from different departments and institutions of U of M who assisted me on various issues ranging from visa application to computer support.

It was a privilege to become friends with so many wonderful people in Ann Arbor. Although many have left to pursue different paths of life in other places and I will soon embark on my own journey, the time spent together with them will always be a cherished memory.

Last but not least, I want to thank my family, especially wife, the future Dr.Jing Nie, for their unconditional love and support.

TABLE OF CONTENTS

LIST OF FIGURES

LIST OF TABLES

LIST OF APPENDICES

LIST OF ABBREVIATIONS

3-MT	3-methoxyltyramine
5-HIAA	5-Hydroxyindoleacetic acid
5-HT	serotonin
AA	amino acid
ACh	acetylcholine
ACN	acetonitrile
aCSF	artificial cerebrospinal fluid
Ado	adenosine
Asp	aspartate
Bz	benzoyl group
BzCl	benzoyl chloride
CE	capillary electrophoresis
Ch	choline
DA	dopamine
DMSO	dimethyl sulfoxide
Dns	dansyl group
DnsCl	dansyl chloride
DOPAC	3,4-Dihydroxyphenylacetic acid
ESI	electrospray ionization
GABA	gama aminobutyric acid
Glu	glutamate
Gly	glycine
HPLC	high performance liquid chromatography
HVA	Homovanillic acid
i.d.	inner diameter
IS	internal standard
LC	liquid chromatography
LOD	limit of detection
m/z	mass to charge ratio
MALDI	matrix assisted laser desorption
MD	microdialysis

mPFC	medial prefrontal cortex
MRM	multiple reaction monitoring
MS	mass spectrometry
MW	molecular weight
NAc	nucleus accumbens
NE	norepinephrine
NM	normetanephrine
o.d.	outer diameter
PFD	perfluorodecalin
QqQ	triple quadrupole mass spectrometer
RSD	relative standard deviation
Ser	serine
STD	standard deviation
Tau	taurine
TOF	time of flight
UHPLC	ultrahigh pressure liquid chromatography

ABSTRACT

Neurotransmitter concentration *in vivo* reflects various behavioral and pharmacological events. Therefore, the measurement of neurochemical dynamics in live behaving animals' brain is of crucial importance for the fundamental understanding of the central nervous system and the development of therapies for neurological disorders.

Previously published neurochemical monitoring methods, although being capable of measuring one or one class of neurotransmitters, fall short of truly multiplexed neurochemical monitoring. We developed a liquid chromatography-tandem mass spectrometry based assay of all commonly studied small molecule neurotransmitters, detecting 17 neurotransmitters and metabolites sampled *in vivo* at basal level. Prior to LC-MS analysis, amine and phenol containing analytes were benzoylated using benzoyl chloride, significantly improving chromatographic separation and mass spectrometric sensitivity. Additionally, stable isotope labeled internal standard was produced for each analyte, by reacting with commercially available $^{13}C_6$ benzoyl chloride. The quantitative performance was enhanced. It demonstrated the ability to work with high spatial (1 mm) and high temporal resolution (1 min) monitoring.

A benzoylation UHPLC-MS method was further developed into a faster and scaled down version. A two-fold improvement in throughput and four-fold reduction in sample consumption was achieved using a capillary column packed with high efficiency

particles. It was suitable for high temporal resolution monitoring with conventional microdialysis sampling.

For the neurotransmitter, acetylcholine, *in vivo* monitoring, high temporal resolution and high sensitivity are strongly desired due to its low basal levels and rapid changes during neuroexcitation such as behavioral activation. Current technologies do not meet these specific characteristics well. Electrochemical sensors have high temporal resolution but lack sensitivity while the opposite holds true for HPLC based methods. We developed an online acetylcholine monitoring method using segmented flow microdialysis - mass spectrometry. This novel acetylcholine "sensor" combines 5 s temporal resolution with 5 nM detection limit capable of detecting basal levels. Additionally, other analytes such as choline and the acetylcholine esterase inhibitor, neostigmine can both be detected simultaneously, demonstrating the versatility of mass spectrometry for detection. Tested *in vivo*, this setup captured both acetylcholine increase in response to acetylcholine esterase inhibition and decrease due to neuronal inhibition by tetradotoxin.

CHAPTER 1

INTRODUCTION

Bioanalytical Mass Spectrometry

Mass spectrometry is one of the fastest growing fields in analytical science today. Its rapid development is to a large extent fueled by its broad application in bio-analysis, with increasingly high resolution and more varieties of tandem MS capabilities, mass spectrometry proves to be an invaluable tool for elucidating structures and determining the quantities of bio-molecules. In areas such as proteomics, metabolomics, lipidomics, and glycomics, mass spectrometry has become the central tool[1-3].

Mass spectrometry did not see large scale biological application until successful development of "soft" ionization methods such as electrospray ionization (ESI) and matrix assisted laser desorption ionization (MALDI) in the late 1980s. Previous ionization methods such as electron impact (EI) ionization tend to break the covalent bond of bio-molecules, causing extensive fragmentation which complicates data interpretation. "Soft" ionization techniques are able to convert bio-molecules from condensed phase to charged gas phase ions without breaking the intra-molecular chemical bonds. In some cases, even non-covalent inter-molecular interactions can be preserved while bio-molecules go through soft ionization processes. Compared to

MALDI, ESI is a continuous ionization method and is easier to couple with online purification methods such as chromatography and capillary electrophoresis. In the ESI process, as analytes pass through the spray needle, excess charge is created by the high voltage applied at the needle. A Taylor cone is formed as the result of solvent surface tension and the electric field. Charged liquid droplets coming off the tip of the Taylor cone fly towards the mass spectrometer's inlet which is the counter electrode in the closed circuit. Meanwhile, droplets shrink in size as solvent evaporates with the assistance of heat and gas. They split into smaller droplets as the Coulomb repulsion exceeds solvent surface tension. Eventually, charged droplets become gas phase ions without solvent molecules and some ions are sampled into the mass spectrometer (Figure 1.1). Commonly studied molecules in biology such as nucleotides, proteins, peptides, and a large number of metabolites can be readily ionized through ESI.

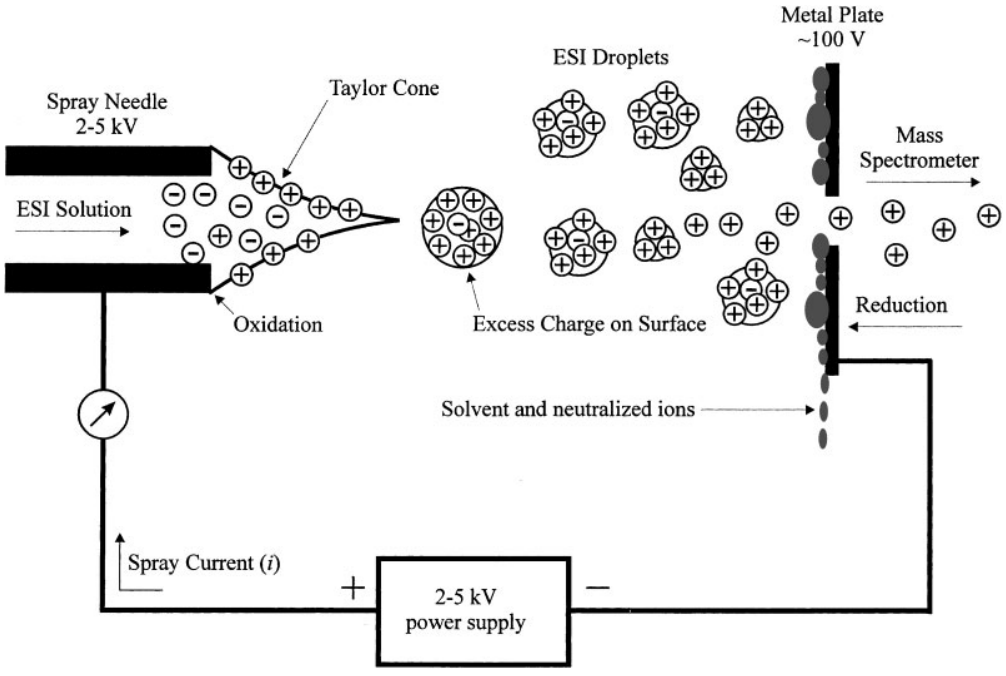

Figure 1.1 Schematic of the electrospray ionization process[4]. Reproduced with permission from John Wiley and Sons.

Although all mass spectrometers measure m/z of gas phase ions, their mass analyzers operate according to different physical principles, which determines the instruments' strengths and weaknesses[5]. The quadrupole mass analyzer is made of 4 parallel rods arranged as shown in Figure 1.2. DC voltage (U) superimposed with AC (V cos ωt) voltage is applied on the conductive rods. At a given U, V and ω, only ions of certain m/z will have stable trajectories in the resulting electric field. Ions with unstable trajectory will not make it through the analyzers and are unable to reach the detector. Quadrupole mass analyzers generate mass spectra by varying the electric parameters over time to allow ions of different m/z values to reach the detector. They are simple and robust but have low mass resolution (usually unit mass resolution) and limited m/z range (usually a few thousand). However, performance can be improved by coupling with additional mass analyzers in tandem and using multistage mass filtration, such as in triple quadrupole and Q-TOF mass spectrometers.

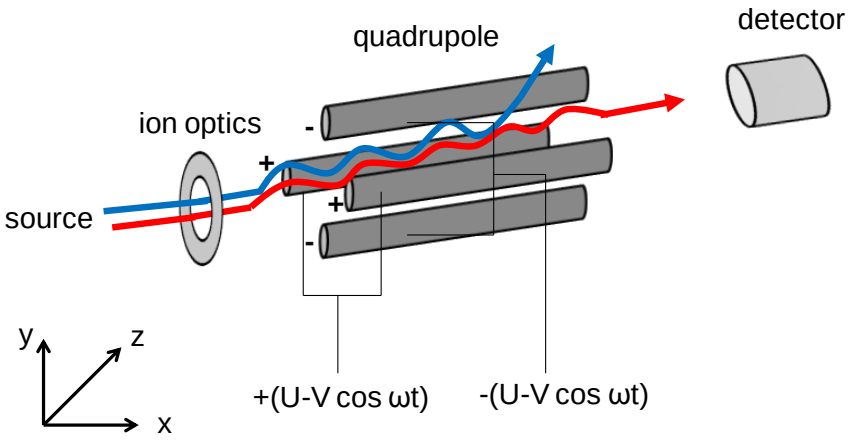

Figure 1.2 Operating principle of quadrupole mass analyzer. Ions with stable trajectory (red) will make through the analyzer while ions with unstable trajectory (blue) will not make to the detector.

In this dissertation, we describe several methods using ESI-triple quadrupole mass spectrometers coupled with different separation and sample manipulation techniques for continuous monitoring of neurochemical changes in the brains of live animals, and demonstrate the versatility, robustness, sensitivity and selectivity of using mass spectrometry for neurochemical analysis.

In Vivo Neurochemical Monitoring

Neurotransmitters are key components controlling nervous system function. Upon stimulation, neurons release pre-packaged neurotransmitters into the synapse. Some neurotransmitters subsequently bind to receptors located on the membrane of post synaptic neurons, inducing responses that promote or inhibit the post synaptic neuron's action potential. Neurotransmitters not binding with receptors are metabolized by extracellular enzymes or recycled by pre-synaptic neurons. Some neurotransmitters also bind to autoreceptors on the pre-synaptic membrane, becoming part of the feedback control mechanism[6] (Figure 1.3). Being involved in all kinds of brain functions and activities, the extracellular level of neurotransmitters and their metabolites reflects these events, providing clues for understanding the overall neuronal circuits and revealing the molecular basis of these processes. However, current analytical tools are not capable of measuring neurochemicals directly from the 20-50 nm wide[6] synaptic cleft of intact brains. Instead, existing technologies detect neurochemicals spilling over from the synaptic cleft into larger brain extracellular space. On one hand, it provides an averaged view of the multiple neurons' activity in that particular brain area, on the other hand, neurotransmitters diffusing out potentially affect other neurons and this extra-synaptic transmission is called volume transmission. Nevertheless, the measurement of extra-

synaptic neurochemicals provides invaluable information that allows scientists to gain substantial insight of the nervous system and facilitates the development of therapies for neurological disorders[7].

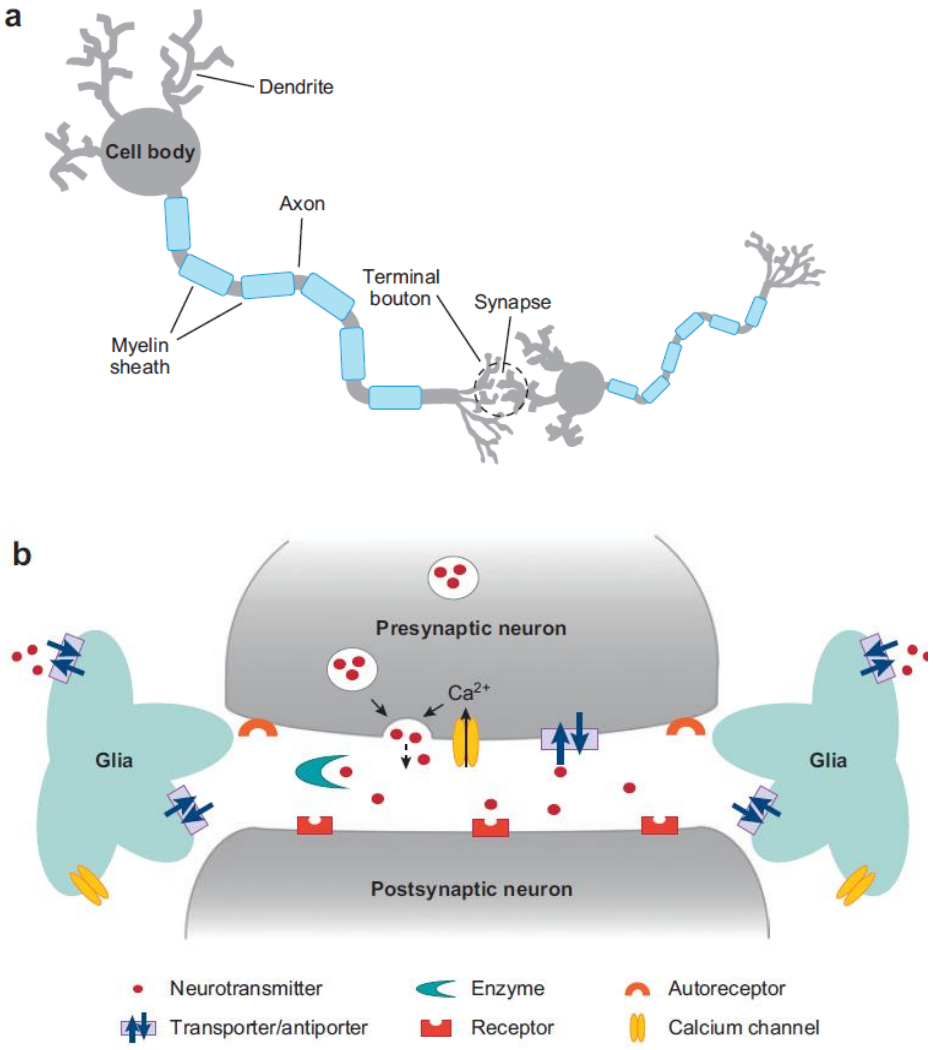

Figure 1.3 Structure of neurons and neurotransmission. (a) Neuronal structure and synaptic features. Dendrites collect chemical input from neighboring neurons, which influences the membrane potential of the neuron. Once the threshold membrane potential is reached, an action potential is generated and travels from the cell body down the axon toward the terminal boutons. Myelin ensheathment of neurons increases the speed of action potential propagation. (b) Neurotransmission at synapses. Neurotransmitters diffuse across the synapse to interact with and bind to receptors on the postsynaptic neuron. If a neurotransmitter binds to an autoreceptor on the presynaptic neuron, a

negative feedback loop is initiated to inhibit further release. Signaling is terminated via enzyme degradation or reuptake into the presynaptic terminal by transporters. Other supportive neuronal cells such as glia can also release and take up neurotransmitters[7]. Reproduced with permission from Annual Reviews.

Temporal and spatial resolution are two challenges for continuous monitoring of neurochemicals in live brains. Neurochemical events occur on vastly different time scales. Exocytosis and re-uptake processes happen at the millisecond levels, while sustained changes induced by pharmacological activation may last hours. Ideally the monitoring techniques will have adequate temporal resolution to be able to capture concentration dynamics across all time scales[8].

The brain is a highly heterogeneous organ. Brain regions 1 mm apart may perform entirely different functions. It is imperative for the analytical methods to be able to discern such small spatial differences, especially when small model animals such as mice and rats are used for *in vivo* studies. Electrochemical sensors represent an important class of *in vivo* monitoring tools and electrodes can have high temporal resolution thanks to the fast readout of electrical signals (millisecond level) and high spatial resolution due to the advancement of modern material science and manufacturing technologies. However, bare electrodes can only detect electrochemically active neurochemicals, such as the monoamines and some of their metabolites. For the non-electrochemically active species, catalytic enzymes are coated on the electrode surface to convert such analytes into redox products such as H_2O_2. One electrochemical sensor typically detects only one analyte. Microelectrode arrays allow multiplexed detection but at the expense of spatial resolution and are still far from exhaustive, in addition to other hurdles. Another disadvantage of using electrochemical sensors is their high background signal due to the presence of interferences. Endogenous redox species such as ascorbic acid and H_2O_2 are present in

the brain, and the lack of chemical separation comprises the specificity. In many cases, basal levels of neurochemicals cannot be reliably determined.

The major competing technologies to electrochemical sensors are sampling techniques such as microdialysis and low flow push-pull perfusion. After neurochemicals are collected from the brain, a myriad of analytical tools can be employed, offering more sensitivity and flexibility in determining the sample's chemical content. Microdialysis is the most prevalent *in vivo* sampling method. The key element of this technique is the microdialysis probe (Figure 1.4). After implantation in the brain, artificial saline solution is perfused through. The tip of the microdialysis probe is made of a piece of semi permeable membrane, which allows free diffusion of small molecules and ions. Bigger molecules, such as proteins and poly nucleotides are blocked from entering the probe. Because the neurochemical concentration is higher in the brain than within the probe, the chemical gradients drive the endogenous small molecules through the membrane into the probe. Continuously infusing saline solution then carries the collected analytes from the brain for analysis. The sample, called dialysate or microdialysate is either analyzed online by a fast analytical method, or more commonly, collected as temporally resolved fractions and analyzed offline, usually by slower but more powerful techniques.

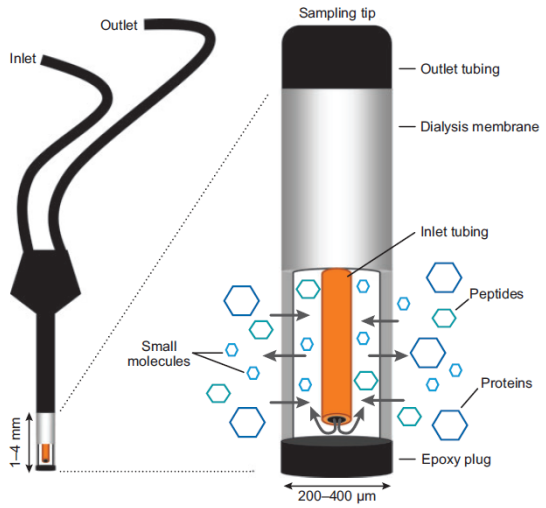

Figure 1.4 Depiction of a concentric microdialysis probe[7]. Reproduced with permission from Annual Reviews.

Using microdialysis coupled with online fast capillary electrophoresis system, a temporal resolution of ~ 10 s has been previously achieved for Glu and Asp monitoring[9]. Offline analysis allowed more flexibility. For example, using segmented flow microdialysis integrated with microfluidic CE system, temporal resolution as high as 2 s could be attained[10]. In another example, offline analysis permitted the use of a slower capillary HPLC method, but all amino acid neurotransmitters could be detected at 10 s temporal resolution[11].

Microdialysis is not an exhaustive sampling method. Its recovery depends on the analytes' property, membrane type and length, flow rate and *in vivo* environment. It typically has 0.5-3 mm of active membrane lengths, operate at 0.5-2 µL/min flow rate range. Longer membrane improves the recovery of analytes, but compromises the spatial resolution. Lower flow rate enhances relative recovery but decreases sample volume available for analysis and causes more mixing, also sacrificing temporal resolution[10] (Figure 1.5).

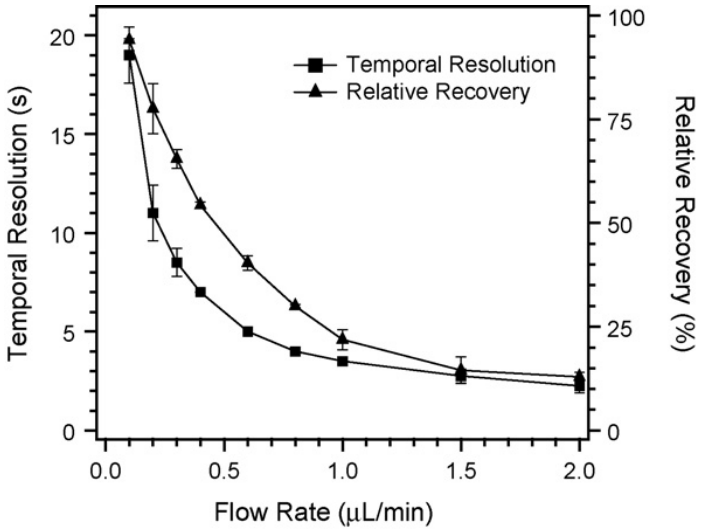

Figure 1.5 Dependence of temporal resolution and relative recovery on sampling flow rate using 2 mm microdialysis probes[10]. Reproduced with permission from Elsevier.

Technologies for Dialysate Analysis

HPLC based methods are popular for dialysate analysis. High sensitivity electrochemical (EC), fluorescence, and mass spectrometric detectors are typically used because of the low analyte concentration in dialysate. HPLC-EC methods have been the workhorse of monoamine neurotransmitter analysis for decades. Due to the intrinsic chemical structures of DA, NE, 5-HT and some of their metabolites, they can be easily oxidized and generate current on the electrode surface[12].

Amino acid neurotransmitters are routinely detected using fluorescence detectors. Amino acids do not produce strong intrinsic fluorescence, so a fluorescent tag is linked to their amine functional group prior HPLC separation. The pre-column derivatization serves two purposes. In addition to enhanced fluorescent signal, the label also increases hydrophobicity of highly hydrophilic amino acid neurotransmitters, facilitating reversed-phase LC separation.

Besides HPLC, capillary electrophoresis (CE) methods have seen wide application in brain dialysate analysis. Compared to HPLC, CE methods are usually much faster, resolving neurotransmitters in seconds rather than in minutes at high separation efficiency. Meanwhile, sample consumption in CE is minute compared to HPLC. These features are highly advantageous for high temporal resolution monitoring, which produces large numbers of low volume samples. With the addition of chiral selection agents like cyclodextrin, chiral separation can be achieved on CE. This is of special interest because D and L amino acids perform distinct biological functions and the ability to resolve them provides deeper insight of their respective roles[13]. The bulk of CE methods applied in neuroscience use laser induced fluorescence (LIF) due to its good sensitivity (low nM detection limit) and ease of implementation. The majority of CE-LIF methods have been used for analyzing amino acid neurotransmitters because of their relatively higher *in vivo* level. The much lower monoamine levels demand higher peak capacity to separate the interferences[14].

Immuno- and enzymatic assays have also been used to monitor chemicals in the brain, such as glucose, glutamate, and neuropeptides. These assays can be miniaturized and automated, and are therefore adaptable to be used on microfluidic devices with the goal of lower sample and reagent consumption, higher throughput and better temporal resolution[15]. Neuropeptides have traditionally been analyzed by enzyme or radio immunoassays[12]. Cross reactivity sometimes compromises the specificity in complex dialysate samples. Radio immunoassay also poses a potential safety hazard and suitable enzymatic or immuno assays have yet to be developed for some neurochemicals.

Liquid Chromatography- Mass Spectrometry

Today, the hyphenated technology of liquid chromatography and mass spectrometry is one of the most preferred analysis formats for complex biological samples. There have been a number of LC-MS methods dedicated for neurochemical measurement[16-19]. The mass spectrometer is a powerful LC detector, being relatively universal and providing additional information regarding the analytes' molecular structure (Figure 1.6). On the other hand, LC separation prior to MS is also a prerequisite for obtaining high quality mass spectra from complex biological samples. Most LC-MS is coupled via ESI as the ionization method and it has long been observed that ESI is highly susceptible to matrix effect[20]. Co-ionizing species in the sample matrix suppress or enhance ionization efficiency of analytes. For biological samples, high concentrations of salt results in severe signal suppression of bio-molecules. The LC step removes inorganic salt and separates other matrix components, partially alleviating the matrix effect[20, 21]. At its current stage of development, the resolving power of HPLC is still not adequate for completely separating all matrix components in biological samples and co-elution will still occur. The gold standard of correcting for remaining matrix effect and intrinsic ionization efficiency in LC-MS is through the use of stable isotope labeled internal standards.Chapter 2 and Chapter 4 describe the development of LC-MS methods for comprehensive neurochemical analysis. These methods employ stable isotope internal standard for every analyte, thus overcoming the Achilles Heel of LC-MS quantification.

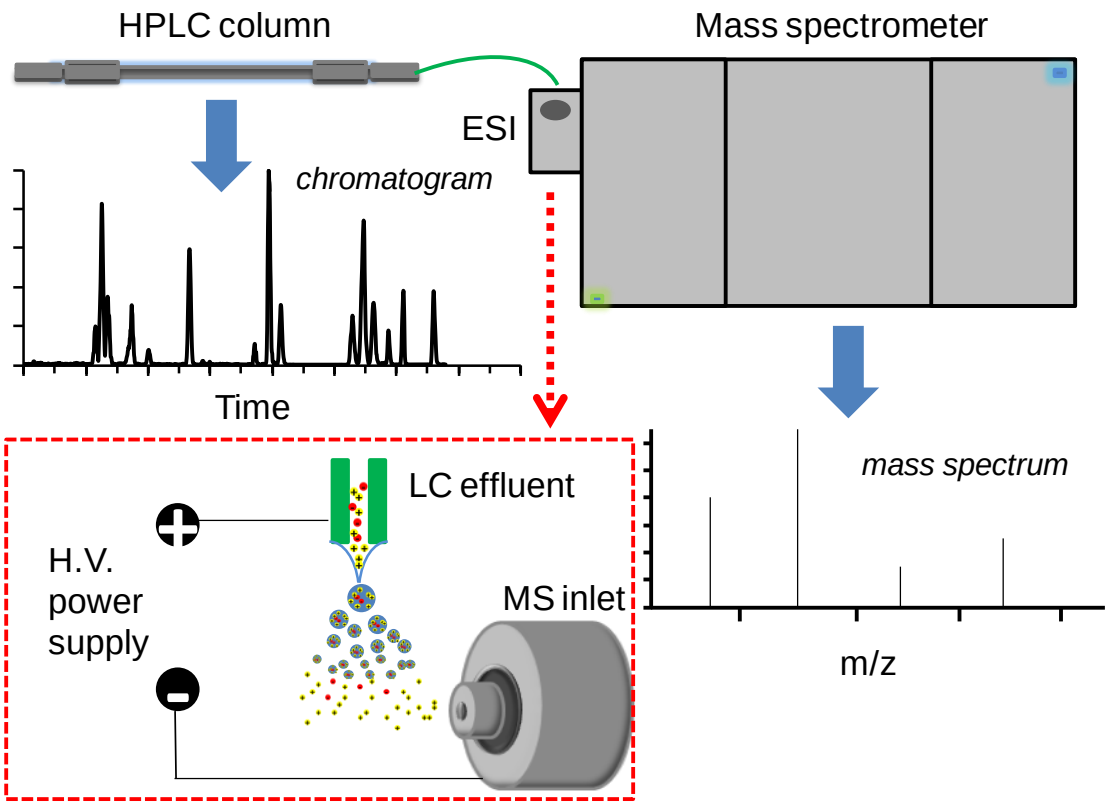

Figure 1.6 Online LC-MS setup using ESI as the ionization source.

High Speed Liquid Chromatography

In vivo monitoring experiments generate large numbers of samples. A single experiment can produce well over 100 samples per day. The requirement for analytical throughput and robustness is high, but conventional HPLC methods typically take 20 - 30 min per sample, significantly limiting analysis throughput.

In this work, we examined use of high-speed HPLC to the separate all classical neurotransmitters. Such work involved careful consideration of LC parameters such as gradient time, flow rate, column and particle size for the best balance of separation efficiency and analysis time.

Separation efficiency is often evaluated using plate height *H*, which is governed by the Van Deemter equation. It shows the relationship between separation efficiency and linear velocity *u*.

$H = A + B/u + Cu$ (Equation 1.1)

A is the term for Eddy diffusion, band broadening caused by different flow path in the column for analyte molecules. *B* is the term for longitudinal diffusion, band broadening caused by analyte molecules' diffusion in the longitudinal direction of the column. *C* is the term for resistance to mass transfer, band broadening due to the non-instantaneous equilibrium of analyte distribution between the stationary phase and mobile phase and between the stagnant intra-particle mobile phase and moving interstitial mobile phase.

High speed HPLC uses high linear velocity to drive separations faster. As the linear velocity increases, the plate height increases due to resistance to mass transfer (C term), leading to the loss of separation efficiency[23]. So the key for fast HPLC is to improve the mass transfer term so efficiency does not suffer excessively at high velocity. Several technologies are available to mitigate the adverse effect of the mass transfer limit at fast HPLC conditions.

Ultrahigh Pressure Liquid Chromatography

One way for improving LC efficiency at high velocity is to use smaller totally porous particles for packed columns. The mobile phase mass transfer resistance (between stagnant intra-particle mobile phase and moving the interstitial mobile phase) decreases proportionally to the square of particle size. Additionally, *A* term also drops

proportionally to the particle diameter. The advantages of using smaller particles for high speed separation are twofold: the optimum velocity is higher and the loss of efficiency is less at higher velocities (Figure 1.7). The drawback of this approach is that column backpressure is inversely proportional to the square of particle diameter. Going from 3 μm particles to 1.7 μm particles triples the column back pressure at the same flow rate. For fast separation, the back pressure of sub 2 micron particle columns easily exceed the 6000 psi limit of conventional HPLC instruments. So separation using this type of chromatographic media is often referred to as Ultrahigh Pressure Liquid Chromatography (UHPLC). The high operating pressure also exacerbates frictional heating. This phenomenon causes uneven radial and longitudinal heat distribution in the column. While the longitudinal thermal gradient tends not to harm the column efficiency, the radial one does. In this respect, narrow bore and capillary columns are more preferable due to their better heat dissipation[24]. Chapter 2 describes a UHPLC method for comprehensive high throughput analysis of all classical neurotransmitters. Operating at 8000 psi, 17 analytes of a large range of polarity are resolved within 8 min.

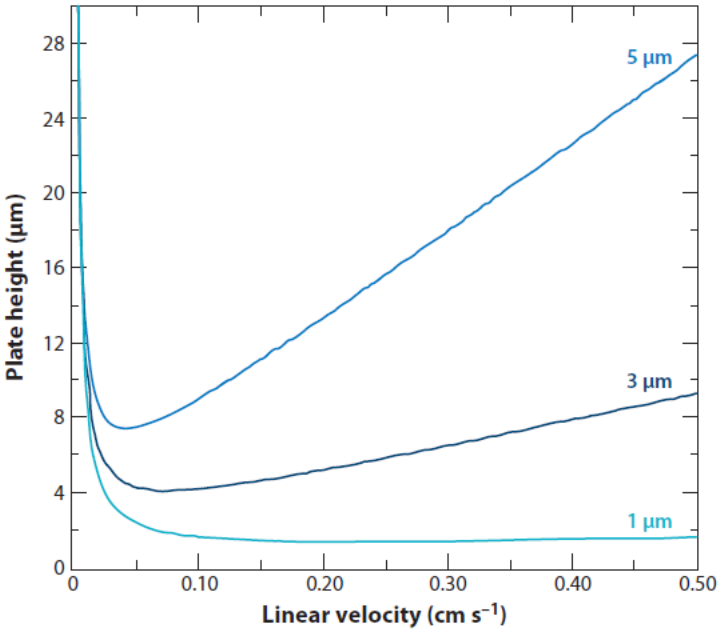

Figure 1.7 Hypothetical van Deemter curves of 5-, 3-, 1 µm particles[24]. Reproduced with permission from Annual Reviews.

Core-shell particles

Another approach to achieve fast and efficient LC separation is use of fused core particles with porous outer layer and solid inner core (Figure 1.8). The principle for high efficiency of such particles is similar to that of the sub 2 micron UHPLC particles, which lies in the shortened diffusion distance of analyte in the stagnant mobile phase, resulting in a smaller *C* term (Figure 1.9). The backpressure created by core-shell particles is much less than the totally porous counter sub 2 micron particles due to its bigger total size. Modern HPLC instruments are capable of operating columns packed with such particles for high throughput applications. In addition, the thermal conductivity of fused core particles is higher so the detrimental radial heating effect is reduced. Moreover, the size distribution of fused core particles is narrower, resulting in more uniform particles which

in turn facilitate homogenous packing leading to a smaller *A* term[25]. The disadvantage of this technology is the reduced loading capacity. The smaller surface areas of fused core particles resulted in more than 2 fold reduction in sample loading capacity[26]. Chapter 4 explores fused core particles for improved analysis throughput and successfully halves the analysis time of the UHPLC method described in Chapter 2.

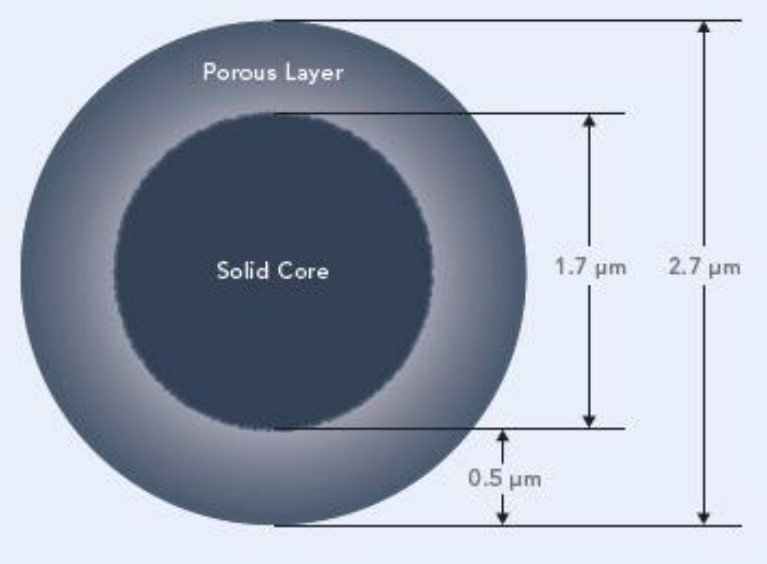

Figure 1.8 Schematic of the cross-section of a fused-core particle. Adapted from www.advanced-materials-tech.com.

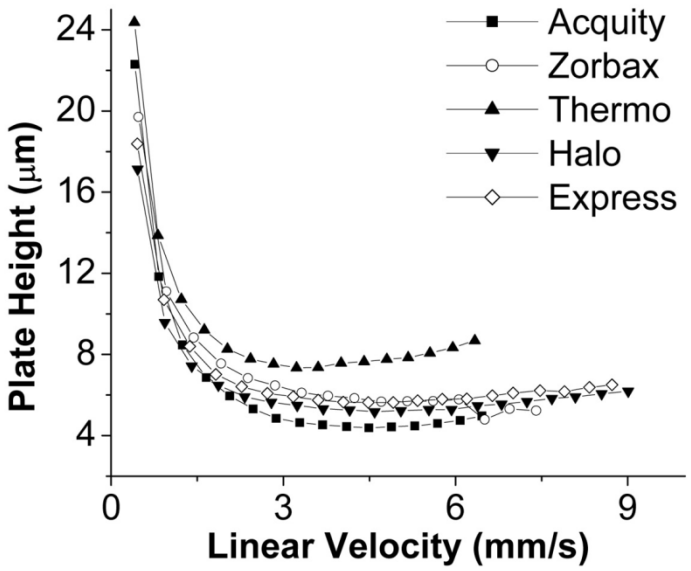

Figure 1.9 van Deemter plot for the five columns using naphthalene**.** The mobile phase was 50:50 ACN:water. Columns tested were 1) Waters Acquity BEH C18, 2.1 X 100 mm, 1.7 μm; 2) Agilent Zorbax Extended-C18, 2.1 X 100 mm, 1.8 μm; 3) Thermo Hypersil Gold, 2.1 X 100 mm, 1.9 μm; 4) Halo C18, 2.1 X 100 mm, 2.7 μm; 5) Supelco Ascentis Express C18, 2.1 X 100 mm, 2.7 μm[27]. Reproduced with permission from Wiley and Sons.

Monolith Column

Monolith columns use a piece of continuous porous material as the separation media. The monolith also has bimodal pore sizes, similar to its packed counterpart. The big through-pores form the fluid path and the small mesopores contribute most to the surface area critical for analyte retention and separation (Figure 1.10). The stationary phase is formed *in situ*, instead of being packed in place and this one piece material does not need frits to hold it in place. The overall porosity of monolith columns is higher than the packed ones, usually around 80% (69% external, 15% internal), resulting in less flow resistance. The separation performance of current commercial monolith columns is equivalent to that of packed columns with 3 – 5 μm particles, but their backpressure is comparable to 15 μm particles[28]. Interestingly, the *C* term of monolith columns was

repeatedly demonstrated to be smaller than their packed counterparts[29]. These findings support the notion that monolith columns possess faster mass transfer rates than packed columns. With the high permeability and fast mass transfer, monolith columns are suitable for fast LC separations. Unfortunately, only a few monolithic columns are currently commercially available (Merck Chromolith Phenomenex Onyx, and Dionex Pepswift) with limited options regarding column chemistry and size. This option was not explored in this dissertation.

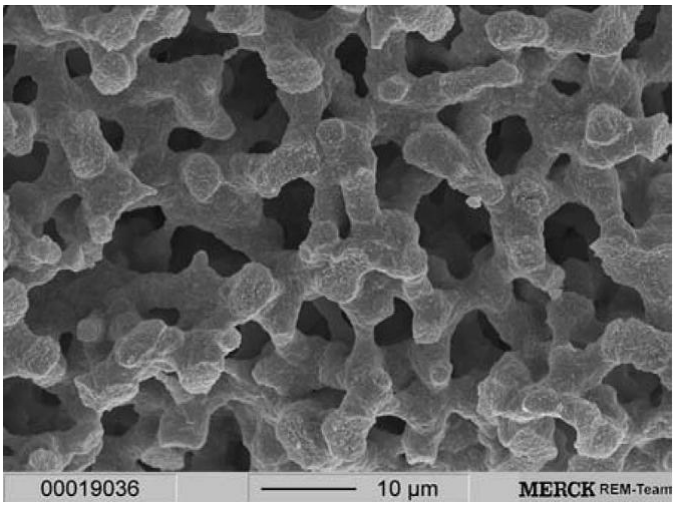

Figure 1.10 SEM-picture of the typical porous structure of monolithic silica columns[30]. Reproduced with permission from Wiley and Sons.

High temperature

Using elevated temperature is another way of achieving fast LC separation. Higher temperature reduces mobile phase viscosity, permitting the use of higher flow rate without exceeding the pressure limit (Figure 1.11)[31].

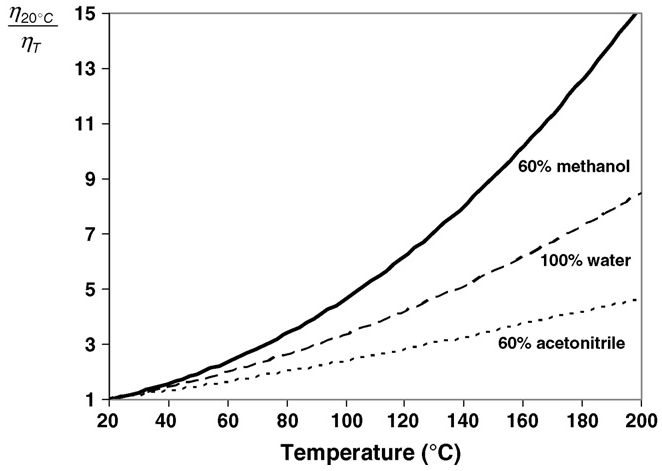

Figure 1.11 Effect of temperature on the reduction of viscosity for three different effluents[31]. Reproduced with permission from Elsevier.

At the same time, higher temperature also improves the rate of stationary phase and stagnant mobile phase mass transfer, resulting in a significantly smaller *C* terms (Figure 1.12)[32].

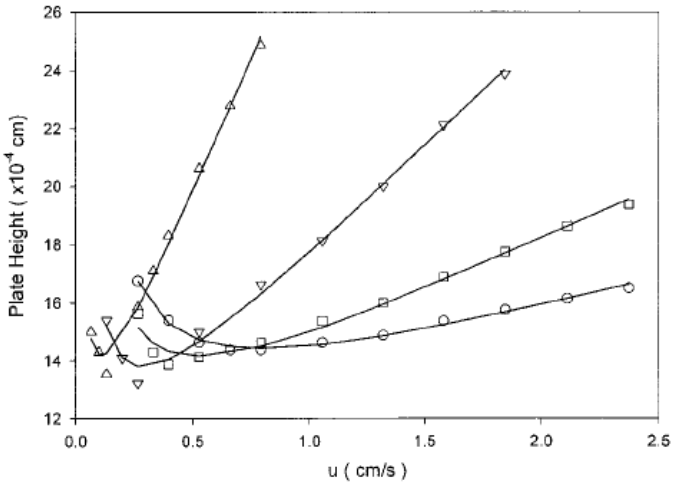

Figure 1.12 Plate height vs linear velocity at various temperatures for well-retained solutes. Δ, 25 ℃ (decanophenone, *k'*= 12.2); ▽,80 ℃ (dodecanophenone, *k'* = 7.39); □, 120 ℃ (tetradecanophenone, *k'*= 12.3); ○, 150°C (tetradecanophenone, *k'*= 7.00)[33]. Reproduced with permission from ACS.

In addition to reduced flow impedance and enhanced mass transfer, high temperature also decreases the retention of analytes on reversed phase columns. The effect of 4-5 ^{o}C increase in temperature roughly equals that of 1% increase in organic modifier for neutral compounds in RPLC[31]. In some cases, 100% water could be used as the sole mobile phase for separation under high temperatures, making HPLC "greener" by avoiding use of expensive and toxic organic modifiers. High temperature LC has not yet seen extensive applications due to several reasons. In addition to requirement for the temperature control element such as column heater, solvent pre-heater, solvent cooler, many analytes and most column stationary phase are not stable under high temperatures[34]. The few commercially available stationary phases that are capable of withstanding > 100 ^{o}C temperature include organic-silica hybrid (Waters BEH columns) and zirconia based columns (ZirChrom).

Tandem Mass Spectrometry and Triple Quadrupole Mass Spectrometer

Tandem mass spectrometry makes multi stage m/z measurements of selected analyte ions. When soft ionization is used, tandem MS first determines the m/z of molecular ions (parent ions), then fragments them into smaller pieces and analyzes the m/z of the fragment ions (daughter ions). This extra step provides more insight in the molecular structure, and adds an extra level of selectivity. The most commonly used tandem MS method is collision activated dissociation (CAD). It breaks up parent ions by colliding them with inert gas molecules. This technique usually breaks the labile covalent bonds with high efficiency. Novel tandem MS techniques such as electron capture dissociation (ECD), electron transfer dissociation (ETD), and negative ion electron capture dissociation (niECD) are capable of preserving labile functionalities, providing

additional, sometimes crucial information regarding parent ion's structure. Our study focused on quantitative analysis of known compounds, so the fragmentation with the highest yield, CAD, was used to achieve maximum sensitivity.

Triple quadrupole mass spectrometers (QqQ) are generally considered the most suitable instrument for targeted analysis. As its name indicates, the QqQ instrument consists of three quadrupoles, or more exactly, two quadrupole mass analyzers and a quadrupole (hexpole in many cases) collision cell. Ions selected in the first quadrupole collide with inert gas molecules in the collision cell and fragment into smaller pieces. The fragment ions then enter the second analyzer. There are several operating modes for the QqQ. MS1 utilizes only one of the two mass analyzers, either in full scan mode or dwells on a particular m/z. MS/MS mode requires the two mass analyzers to work in coordination. In daughter (product) ion scan mode, the first analyzer passes known parent ions of certain m/z. The collision cell fragments these ions and let all fragments to pass to the second mass analyzer where the daughter ions are scanned (Figure 1.13 A). The parent (precursor) ion scan mode is opposite of daughter ion scan mode. Here the second analyzer fixes on a certain daughter ion while the first analyzer scans all possible parent ions (Figure 1.13 B). The multiple reaction monitoring (MRM) is a unique mode of operation that makes the QqQ top choice for targeted analysis. In this mode, both mass analyzers dwell on specific m/z s. The first analyzer passes only certain parent ions while the second analyzer lets through only the corresponding daughter ions (Figure 1.13 C). Although fewer ions reach the detector, the dual filtering of both parent and daughter ions significantly reduces the noise. There are usually gains in signal to noise ratio which explains the higher sensitivity of MRM. Dwelling on ion pairs rather than scanning over

a certain range, MRM also has fast duty cycle, a feature important for online coupling with high efficiency separations. Another unique operating mode is the neutral loss scan. Certain molecules, when going through the CAD process, lose mass corresponding to a neutral molecule such as H_2O or CO_2. Neutral loss mode scans parent/daughter ion pairs at a constant m/z offset, the value of which is the molecular weight of the neutral molecule (Figure 1.13 D). For loss of water, the offset is 18.

For mass spectrometric detection of low level neurochemicals from large number of samples, both high sensitivity and fast readout are needed. All work described in this dissertation used MRM mode of QqQ to meet such demands.

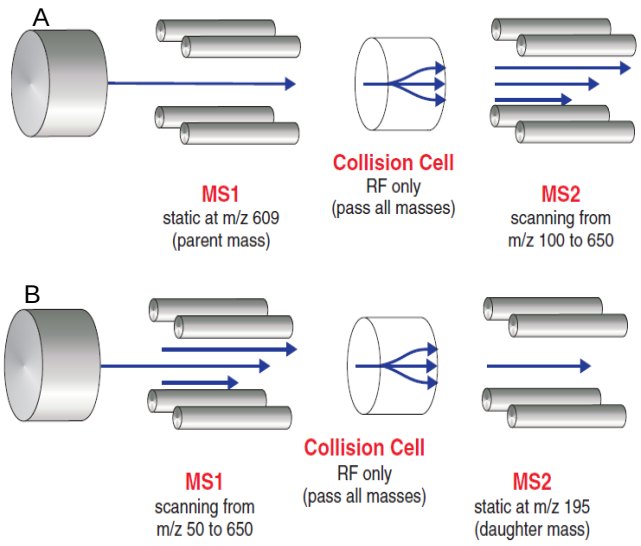

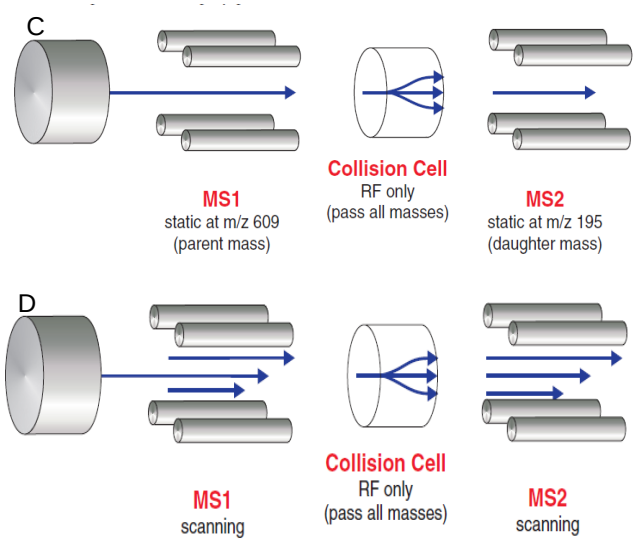

Figure 1.13 MS/MS mode of QqQ mass spectrometers. A. daughter ion scan; B. parent ion scan; C. multiple reaction monitoring; D. neutral loss scan. Figure from Waters Quattro Ultima user's guide (3rd issue).

Dissertation Overview

This dissertation describes development of novel mass spectrometry based tools to meet the demand unanswered in existing technologies for *in vivo* neurochemical monitoring. One was high throughput LC-MS approach (Chapter 2 and 4), the other was stand alone MS coupled to a unique sample handling technique with high temporal resolution (Chapter 3).

Chapter 2 describes a UHPLC-tandem MS method for comprehensive analysis of all classical neurotransmitters and commonly studied metabolites. Analytes were benzoylated prior to analysis to increase hydrophobicity, which greatly improved sensitivity for small hydrophilic neurochemicals. Good quantitative performance with average 7% RSD was achieved due to the method's inherent capability of incorporating stable isotope internal standard. It was demonstrated to be compatible with challenging

microdialysis sampling at high temporal and spatial resolution. With 17 analytes resolved in 8 min, this method was the highest throughput among all HPLC methodologies dedicated to comprehensive *in vivo* neurochemical monitoring.

Chapter 3 demonstrates the possibility of using only mass spectrometry to monitor low level neurotransmitter acetylcholine. An elaborate sample handling and introduction system was designed using segmented flow microdialysis with the goal of reducing sample dispersion during transport. After careful optimization of sample treatment, plumbing and detection parameters, this unique microdialysis-mass spectrometry system was capable of online monitoring of acetylcholine together with other molecules at 5 second temporal resolution. This mass spectrometry acetylcholine "sensor" was on par with existing electrochemical sensors, but excelled in sensitivity and multiplexed analyte capability.

Chapter 4 examines the feasibility of increasing the speed of the UHPLC-MS analysis described in Chapter 2 by capillary UHPLC-MS. Operating a capillary column packed with high efficiency fused core particles at very high linear velocity, a twofold improvement in throughput was achieved with adequate chromatographic resolution. Sample consumption was reduced to 0.5 μL and mobile phase consumption was also decreased four fold. The compromises in other areas under fast LC conditions is discussed and the causes are examined and proposals for further improvement are presented.

Chapter 5 discusses new possibilities originating from the knowledge and experience gained from previous method development. Preliminary data suggests the

feasibility of adding neuropeptides to the portfolio of the benzoylation UHPLC-MS method. The mass spectrometry "sensor" approach could be expanded to include more neurotransmitters and achieve higher temporal resolution using alternative sampling technique. The benzoylation reaction can be adapted to quantitative metabolomics due to the availability of stable isotope labeled reagent. A unique experimental setup using online LC-MS and segmented flow fraction collection is proposed for quantitative amine and phenol containing biomarker discovery.

CHAPTER 2.

COMPREHENSIVE CLASSICAL NEUROTRANSMITTER ANALYSIS USING BENZOYLATION UHPLC-MS

Introduction

Monitoring neurotransmitter concentration dynamics in the living brain is a critically important tool in neuroscience. *In vivo* measurements enable study of the relationship between neurotransmitter concentrations in relevant brain nuclei and behavior, drug effects, or disease states. Since its inception, microdialysis sampling has been the preeminent tool for making such measurements [35-37]. In this approach, a semi-permeable membrane probe is inserted into the brain and perfused with artificial cerebral spinal fluid (aCSF). Molecules in the extracellular space diffuse across the membrane according to their concentration gradient and are collected into fractions which are analyzed for neurotransmitter or metabolite content. This tool has been invaluable for neuroscience, e.g. it has been used to demonstrate that all drugs of abuse activate the mesolimbic dopamine (DA) system [38], glutamate (Glu) sustains drug seeking behavior [39, 40],and adenosine (Ado) is a modulator of sleep [41]. The technique is also used clinically for

studying epilepsy [42] and brain trauma [43, 44] and plays a prominent role in the pharmaceutical industry when screening novel neurological and psychiatric therapeutics.

A key to using microdialysis is analysis of sample fractions [12]. Many assays for neurotransmitters have been developed using high performance liquid chromatography (HPLC)-electrochemical detection [45, 46], HPLC-fluorescence detection [47], capillary electrophoresis-laser induced fluorescence [48, 49], immunoassay[50] and more recently, HPLC-mass spectrometry (MS) [18, 19, 51]. Despite extensive research into methods for chemical analysis of dialysate, all methods presently in use can only determine a subset of common small molecule neurotransmitters. Therefore, studies that require monitoring different types of neurotransmitters must use multiple assays which increases costs and time required for equipment maintenance, method development and analysis. Use of multiple assays also increases sample volume requirements and animal usage. Assays that measure only a single or few neurotransmitters also preclude discovering involvement of unanticipated neurotransmitter systems. A comprehensive analytical method for neurotransmitter measurements would be of great value to the neurosciences by revealing previously unknown neurotransmitter interactions. Such a method could also accelerate neurological drug development by allowing rapid evaluation of the effect of novel compounds in the brain. Any such method must be sensitive enough for dialysate samples and have sufficient throughput for the many samples generated from *in vivo* experiments.

Here we report a HPLC-MS method for the measurement of 12 of the most commonly studied neurotransmitters or neuromodulators (Figure 2.1A) including ACh, Ado, DA, norepinephrine (NE), serotonin (5-HT), histamine (Hist), Glu, glycine (Gly), aspartate (Asp), γ-aminobutyric acid (GABA), serine (Ser), and taurine (Tau). The

method also assays the metabolites homovanillic acid (HVA), 5-hydroxyindole-3-acetic acid (5-HIAA), 3,4-dihydroxyphenylacetic acid (DOPAC), normetanephrine (NM) and 3-methoxytyramine (3-MT). The method is compatible with challenging experiments which generate low concentration samples such as using small microdialysis probes for high spatial resolution and fast sampling rates (60 s/sample) for high temporal resolution *in vivo* monitoring.

A major difficulty to overcome in developing such an assay is identifying chromatographic conditions that can resolve the highly polar neurochemicals while remaining compatible with MS detection. We discovered that derivatization with benzoyl chloride renders the compounds more hydrophobic so that they can be separated by reversed phase chromatography. Derivatization also increases sensitivity and provides a convenient way to improve quantification by stable-isotope labeled internal standards generated using $^{13}C_6$ benzoyl chloride. Importantly, benzoyl chloride reacts with primary and secondary amines, phenols, and ribose-hydroxyl groups (Figure 2.1B) allowing nearly all small organic molecule neurotransmitters to be labeled. ACh, which cannot be labeled by benzoyl chloride, is directly detected in this method. Rapid derivatization and an 8 min separation time give the method sufficient throughput for the large number of samples generated by microdialysis experiments. The method uses commercial instrumentation and readily available reagents; therefore, it can easily be adopted by other laboratories.

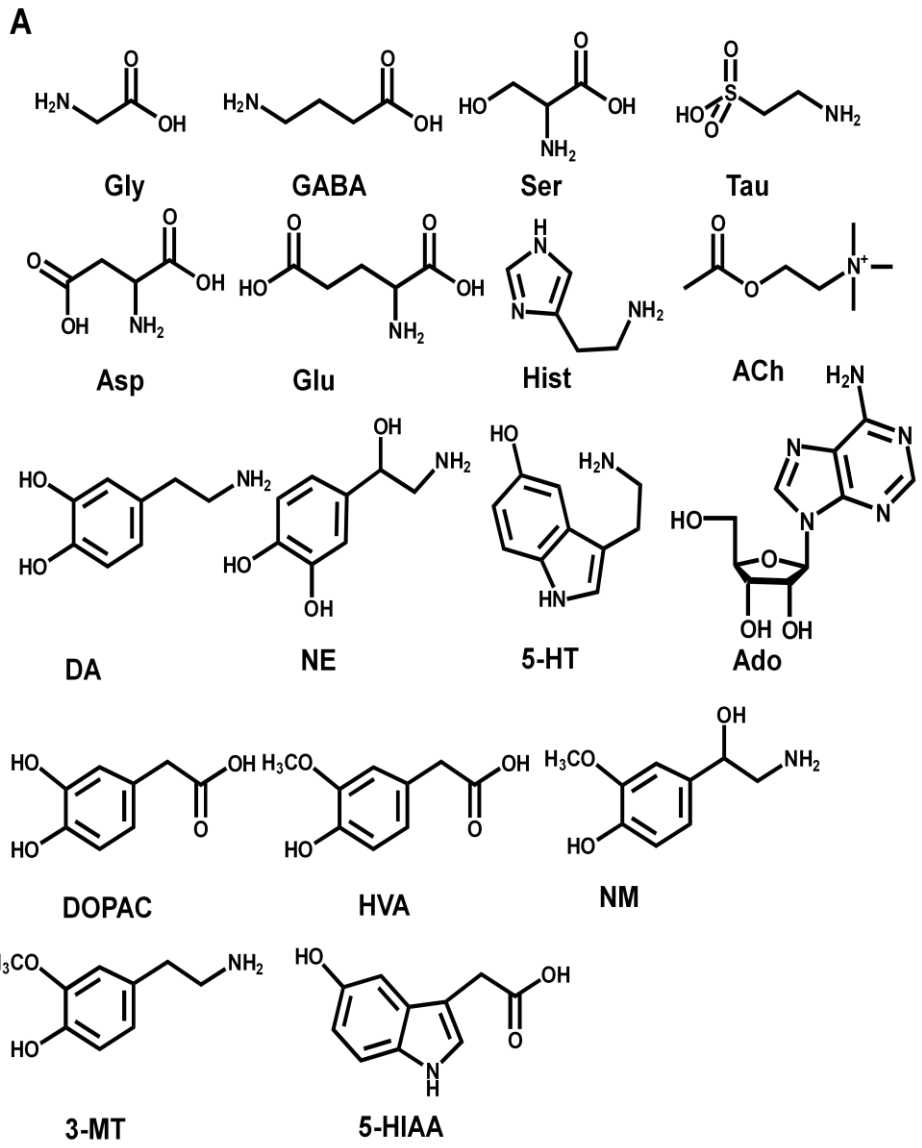
A
Gly
GABA
Ser
Tau
Asp
Glu
Hist
ACh
DA
NE
5-HT
Ado
DOPAC
HVA
NM
3-MT
5-HIAA

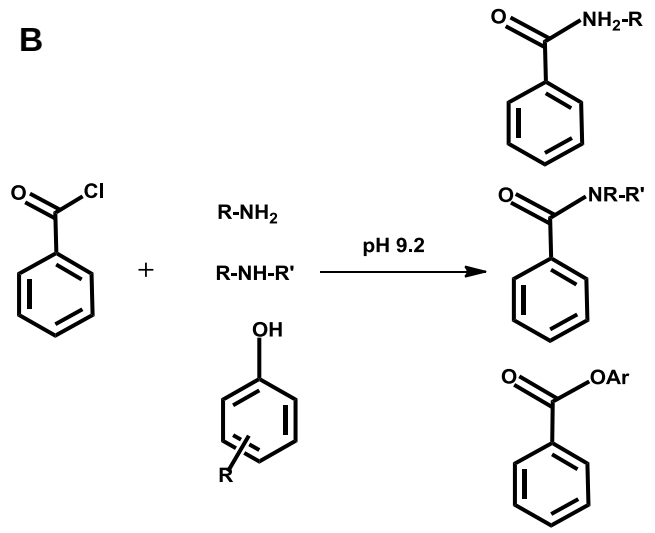

Figure 2.1 Chemical structure of targeted neurotransmitters and metabolites (A). Reaction scheme of benzoylation using benzoyl chloride (B)

Experimental Section

Chemicals and Reagents

All chemicals, drugs and reagents were purchased from Sigma Aldrich (St. Louis, MO) unless otherwise noted. Water and acetonitrile are Burdick & Jackson HPLC grade purchased from VWR (Radnor, PA). 10 mM stock solution of each analyte was made in HPLC water and kept at -80 ^{o}C. Standard mixture was diluted from stock using aCSF consisting of 145 mM NaCl, 2.68 mM KCl, 1.10 mM $MgSO_4$, 1.22 mM $CaCl_2$, 0.50 mM NaH_2PO_4, and 1.55 mM Na_2HPO_4, adjusted pH to 7.4 with 0.1 M NaOH. Calibration curves were made using standards at 50 nM, 500 nM, 1000 nM, 5000 nM, 10000 nM for Gly, Ser and Tau; 5 nM, 50 nM, 100 nM, 500 nM, 1000 nM for Asp, Glu, GABA, Hist, Ado, HVA, 5-HIAA and DOPAC; 0.5 nM, 5 nM, 10 nM, 50 nM, 100 nM for ACh, 5-HT, NE, DA, NM and 3-MT. Internal standard was 1 mM Gly, Ser and Tau, 100 µM Asp, Glu, GABA, Hist, Ado, HVA, 5-HIAA, and DOPAC and 10 µM 5-HT, NE, DA, NM and 3-MT derivatized with $^{13}C_6$ benzoyl chloride using the same procedure as ^{12}C reagent,

then diluted 100 fold in DMSO containing 1% formic acid. d4-ACh (C/D/N isotopes, Pointe-Claire, Canada) was spiked into the reaction mixture to a final concentration of 100 nM.

Microdialysis

Adult male Sprague-Dawley rats (Harlan, Indianapolis, IN) weighing between 295 and 355 g were used. Ketamine (65 mg/kg i.p.) and dexdormitor (0.25 mg/kg i.p.) were used for operative anesthesia. For dual probe experiments, concentric microdialysis probes (250 m diameter) were implanted unilaterally in both the VTA (1 mm long probe) and NAc (1.5 mm long probe) according to following coordinates from bregma and dura: anterior-posterior (AP) -5.3, medial-lateral (ML) $\pm$ 0.5, dorsal-ventral (DV) – 8.0 mm and AP + 1.2, ML $\pm$ 1.4 and DV -7.8 mm, respectively. For single probe experiments, probes (3 mm long) were implanted into the mPFC from bregma and dura: AP +3.0, ML $\pm$ 0.5, DV – 4.0 (Paxinos and Watson 2007). Probes were secured to the skull by acrylic dental cement and metallic screws. Following surgery, rats were allowed to recover and experiments were performed later. Animals were awake and freely moving with access to food and water throughout the experiment. Microdialysis probes were flushed at 1.5 µL/min with aCSF for 3 h using a Chemyx (Stafford, TX) Fusion 400 syringe pump. Perfusion flow rate was reduced to 0.6 µL/min and samples were collected every 20 min for VTA-NAc experiments. For mPFC experiments, perfusion flow rates were reduced to 1 µL/min to generate 1 µL samples. 1 µL fractions were diluted with 4 µL aCSF, then treated same way as 5 µL sample described below. Following collection of basal fractions, VTA lines were switched to aCSF containing 50 µM bicuculline for the duration (2 h) of experiments. Though 12 µL of dialysate were collected per fraction,

only 5 µL of total volume was used for analysis. For mPFC, following 20 min of basal fraction collections, 1 µM neostigmine was perfused through the probe for 5 min.

Benzoylation reaction

5 µL of standard or sample was mixed with 2.5 µL borate buffer (sodium tetraborate, 100 mM) and 2.5 µL benzoyl chloride (2% in acetonitrile, v/v). The mixture was vortexed and 2.5 µL internal standard was added before LC-MS analysis.

HPLC-MS analysis

The HPLC system was a Waters (Milford, MA) nanoAcquity HPLC. A Waters BEH C18 column (1 mm X 100 mm, 1.7 µm, 130 Å pore size) was used for separation. Mobile phase A was 10 mM ammonium formate, 0.15% (v/v) formic acid in water. Mobile phase B was acetonitrile. The mobile phase gradient for all 17 analytes was: initial, 0% B; 0.1 min, 15% B; 2 min, 20% B; 2.3 min, 25% B; 2.31 min, 50% B; 5.31 min, 50% B; 5.57 min, 65 % B; 6.57 min, 65%B; 6.58 min, 0% B; 8.0 min, 0% B.

The flow rate was 100 µL/min and sample injection volume was 9 µL in partial loop injection mode. Autosampler was kept at ambient temperature and column was maintained at 27 ^{o}C. A Waters/Micromass Quattro Ultima triple quadrupole mass spectrometer was used for detection. Atmospheric pressure ionization source was operated in positive ESI mode at 3 kV. Source temperature was 140 ^{o}C and desolvation temperature was 400 ^{o}C. Cone gas and desolvation gas flowed at 150 L/h and 500 L/h, respectively.

MRM conditions are listed in Table 2.1. Interchannel delay and intercycle delay were both 10 ms. Automated peak integration was performed using Waters Masslynx version 4.1. All peaks were visually inspected to ensure proper integration. Calibration

curves were constructed based on peak area ratio ($P_{analyte}/P_{I.S.}$) versus concentrations of internal standard by linear regression.

Statisical analysis

Data were transformed to percent of baseline measurement to normalize pretreatment levels to 100 percent. All analyses were performed in Graphpad (La Jolla, CA) Prism 5. The measurements were all continuous variables and the Kolmogorov-Smirnov test was used to assess normality of the residuals for each individual repeated measurement and this assumption was met. A two-tailed repeated measures analysis of variance (RM ANOVA) was performed on all microdialysis data followed by a post-hoc Tukey test to test the pairwise difference between every time point and baseline (i.e. 100%). Although animal numbers were relatively small (n = 8 for the bicuculline study and n = 5 for the neostigmine study), following baseline we collected 7 (for bicuculline) and 60 (for neostigmine) measures over time on each animal, enabling analyses of variation in the outcomes both between and within animals. In addition, with 8 animals in one group and 5 in the other, and 8 repeated measures on each animal, a RM ANOVA will have more than 90% power to detect a mean difference of 50 percentage points between the two groups at a 0.05 level of significance (assuming correlations of 0.25 of the repeated measures, and standard deviations of 10 percentage points in each group). RM ANOVA is the primary statistical test used for such continuous measurements. Since the two experiments (i.e. bicuculline and neostigmine) were performed independently, and did not contain control groups since basal levels were taken as control, no randomization was necessary. However, the individual who processed the data was blind to any expected outcomes for each measure.

Results and Discussion

HPLC-MS of benzoylated neurotransmitters

All analytes of interest were benzoylated (except ACh), resolved by reversed phase HPLC, and detected by MS/MS (Figure 2.2). Amino acids were singly benzoylated while monoamines containing phenolic groups were doubly or triply labeled as determined by the mass detected. Protonated benzoylation products (MW+1) were observed by positive electrospray ionization (ESI) for primary, secondary amines and ribose hydroxy groups. For analytes containing only phenol groups (HVA, DOPAC, 5-HIAA), the ammonium adduct of their products (MW+18) was detected. For ACh, the unlabeled molecular ion was used for detection.

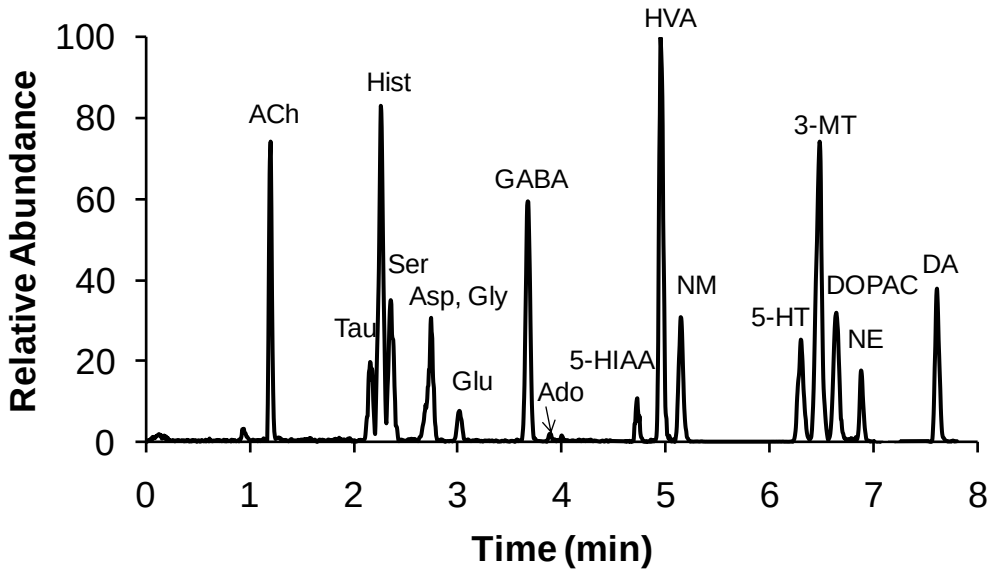

Figure 2.2 Ion chromatogram for all 17 analytes. The concentration of each analyte was: ACh (10 nM); Tau (1000 nM); Hist (100 nM); Ser (1000 nM); Asp (100 nM); Gly (1000 nM); Glu (100 nM); GABA (100 nM); Ado (100 nM); 5-HIAA (100 nM); HVA (100 nM); NM (10 nM); 5-HT (10 nM); DOPAC (100 nM); 3-MT (10 nM); NE (10 nM); and DA (10 nM).

Analytes were detected by MS/MS under collision activated dissociation (CAD) conditions; therefore, the fragmentation of each analyte was examined to determine the best product ions to use for quantification (Table 2.1). For most benzoylated analytes, the benzoyl fragment (m/z 105) was the most abundant product ion (Figure 2.3, top) and was subsequently used for multiple reaction monitoring (MRM). 5-HT generated additional fragment ions (m/z 160, m/z 264) besides the benzoyl fragment (Figure 2.3, bottom). The unique fragment (m/z 264) was selected for MRM of 5-HT. Most analytes were fully labeled yielding a single chromatographic peak; however, benzoylated Ado produced two peaks corresponding to N6-benzoyl-Ado and 3'-O-benzoyl-Ado. The latter product is a result of activity of the 3'-hydroxy group on the ribose ring in nucleophilic substitutions[52, 53]. Besides m/z 105, both N6-benzoyl-Ado and 3'-O-benzoyl-Ado generated a characteristic m/z 136 fragment corresponding to an adenine moiety under MS/MS conditions. The 3'-O-benzoyl-Ado produced more abundant fragment ions and was chosen for MRM quantification. For ACh, the quanternary ammonium residue (m/z 87) after loss of acetyl ester was used for quantification.

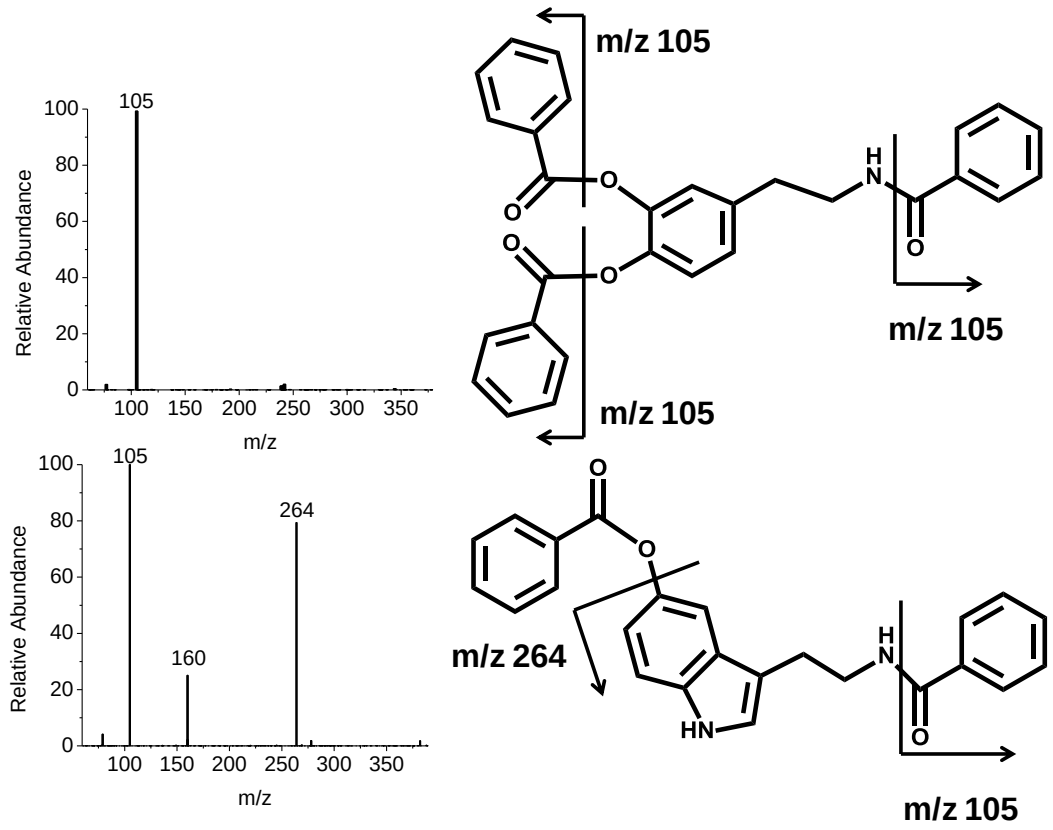

Figure 2.3 MS/MS spectra of benzoylated DA (top) and 5-HT (bottom). Benzoylated 5-HT gave a unique fragment of 264 m/z besides the characteristic 105 m/z (benzoyl group). Most other benzoylated analytes like DA produced only 105 m/z in CAD.

Table 2.1 MRM conditions of 17 benzoylated neurotransmitters and metabolites and their internal standards.

analyte	precursor m/z	product m/z	cone voltage (V)	collision energy	dwell time (ms)
ACh	146	87	35	15	150
d_4-ACh	150	91	35	15	150
Bz-Gly	180	105	35	10	75
$^{13}C_6$Bz-Gly	186	111	35	10	75
Bz-GABA	208	105	35	20	150
$^{13}C_6$Bz-GABA	214	111	35	20	150
Bz-Ser	210	105	35	20	50
$^{13}C_6$Bz-Ser	216	111	35	20	50
Bz-Hist	216	105	35	20	50
$^{13}C_6$Bz-Hist	222	111	35	20	50
Bz-Tau	230	105	35	10	50
$^{13}C_6$Bz-Tau	236	111	35	10	50
Bz-Asp	238	105	35	10	75
$^{13}C_6$Bz-Asp	244	111	35	10	75
Bz-Glu	252	105	35	20	150
$^{13}C_6$Bz-Glu	258	111	35	20	150
Bz-Ado	372	136	35	30	75
$^{13}C_6$Bz-Ado	378	136	35	30	75
Bz-5HT	385	264	60	20	150
$^{13}C_6$Bz-5HT	397	270	60	20	150
Bz-NE	482	105	60	30	150
$^{13}C_6$Bz-NE	500	111	60	30	150
Bz-DA	466	105	70	30	150
$^{13}C_6$Bz-DA	484	111	70	30	150
Bz-HVA	304	105	35	15	150
$^{13}C_6$Bz-HVA	310	111	35	15	150
Bz-5HIAA	313	146	35	15	150
$^{13}C_6$Bz-5HIAA	319	146	35	15	150
Bz-NM	374	105	60	15	150
$^{13}C_6$Bz-NM	386	111	60	15	150
Bz-3MT	376	105	35	20	150
$^{13}C_6$Bz-3MT	388	111	35	20	150
Bz-DOPAC	394	105	35	20	150
$^{13}C_6$Bz-DOPAC	406	111	35	20	150

Besides enhancing retention on reversed phase columns, benzoylation also enhanced sensitivity for ESI-MS. For example, signal (peak area) was increased 22-fold for 5-HT, 23-fold for Glu, 37-fold for DA, 460-fold for 3-MT, and 1,400-fold for GABA compared to their respective native form. Analytical performance of benzoylation HPLC-MS method was satisfactory, with average relative standard deviation (RSD) of 7% for analysis of samples made in triplicate, linear response ($R^2 > 0.99$), biologically relevant limits of detection (LOD), and adequate analyte stablity (Table 2.2**)**. Use of isotopically labeled internal standard improved measurement precision with RSD of repeated analysis of the same sample reduced from 4-6% to 2% (Figure 2.4**)**.

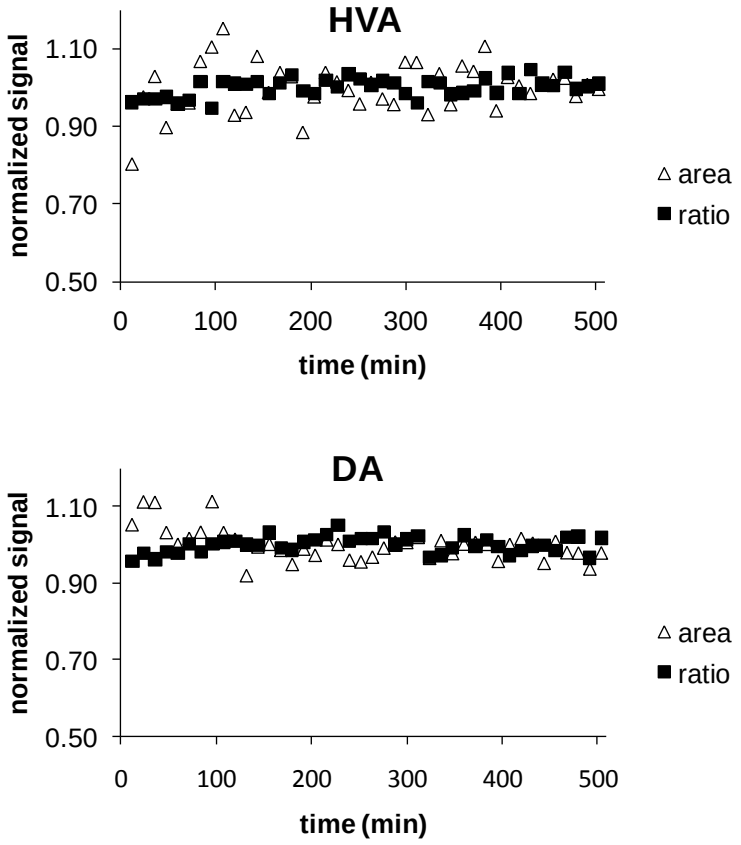

Figure 2.4 Peak area and peak area ratio of HVA (top) and DA (bottom) in a repeatedly analyzed standard solution. Signals were normalized to their respective averages. RSD was 6% for HVA and 4% for DA using only peak area. It was reduced to 2% for both HVA and DA when peak area ratio to internal standard was used for quantification.

Table 2.2 Figures of merit for benzoylation-HPLC-MS method

analyte	RSD (n = 3)	LOD (nM)	R^2	% remaining after storage (n = 3)	basal *in vivo* dialysate concentration		
					VTA (n = 8)	NAc (n = 8)	mPFC (n = 5)
Gly	5	500	0.9933	80 ± 18	4 ± 2 µM	7 ± 2 µM	7 ± 1 µM
GABA	5	2	0.9989	114 ± 10	0.04 ± 0.01 µM	0.03 ± 0.01 µM	44 ± 8 nM
Ser	11	250	0.9975	94 ± 21	6.4 ± 0.8 µM	20 ± 6 µM	10 ± 4 µM
Tau	7	250	0.9995	86 ± 21	12 ± 4 µM	4 ± 1 µM	4.3 ± 0.6 µM
Asp	10	50	0.9987	109 ± 19	0.6 ± 0.1 µM	0.7 ± 0.1 µM	n.d.
Glu	8	5	0.9995	107 ± 14	0.9 ± 0.2 µM	1.9 ± 0.3 µM	0.7 ± 0.3 µM
DA	4	0.03	0.9981	109 ± 14	3 ± 1 nM	8 ± 2 nM	2.2 ± 0.4 nM
NE	10	0.2	0.9997	97 ± 7	1.4 ± 0.2 nM	2.0 ± 0.5 nM	2.0 ± 0.4 nM
5-HT	4	0.1	0.9998	118 ± 19	0.36 ± 0.06 nM	0.32 ± 0.08 nM	0.36 ± 0.08 nM
Hist	13	2	0.9961	118 ± 14	1.2 ± 0.5 nM	0.8 ± 0.2 nM	1.0 ± 0.4 nM
Ado	4	25	0.9974	102 ± 15	18 ± 3 nM	28 ± 5 nM	n.d.
3-MT	1	0.05	0.9999	116 ± 18	2.2 ± 0.3 nM	1.7 ± 0.4 nM	n.d.
DOPAC	5	2	0.9973	103 ± 5	0.8 ± 0.1 µM	5 ± 1 µM	110 ± 9 nM
HVA	4	0.5	0.9973	108 ± 3	0.12 ± 0.01 µM	0.7 ± 0.2 µM	49 ± 9 nM
NM	2	0.1	0.9996	102 ± 2	0.8 ± 0.1 nM	0.46 ± 0.03 nM	2.7 ± 0.9 nM
5-HIAA	7	5	0.9999	115 ± 20	1.1 ± 0.1 µM	0.67 ± 0.07 µM	0.26 ± 0.04 µM
ACh	7	0.5	0.9963	non-labeled	8 ± 2 nM	15 ± 2 nM	3.8 ± 0.6 nM

Note: RSDs were calculated by comparing peak area of 3 individually derivatized standards at approximate *in vivo* concentrations, thus evaluating both reaction and analytical variability. Dynamic range tested for linearity was 500 – 10,000 nM for Gly, Ser and Tau; 5 – 100 nM for HVA, 5-HIAA, NM, 3-MT and DOPAC; 50 – 1000 nM for GABA, Asp, Glu, Hist and Ado; 0.5 – 100 nM for ACh,5-HT, NE and DA. Percent remaining was calculated by comparing peak area of stored standard solution (room temperature for a week) to a freshly derivatized standard solution. Basal concentration of each analyte in dialysate from different brain regions is listed. These values are not corrected for microdialysis probe recovery.

Microdialysis

To demonstrate utility of the method under conditions requiring good spatial resolution, we performed dual probe microdialysis experiments in the mesolimbic pathway, i.e. the ventral tegmental area (VTA) and the nucleus accumbens (NAc). Though probes were only 1 mm and 1.5 mm in length, respectively, we detected all

expected neurochemicals in these samples (Figure 2.5). Basal neurotransmitter concentrations in VTA and NAc dialysate, reported in Table 2.2, are within the expected range [54, 55].

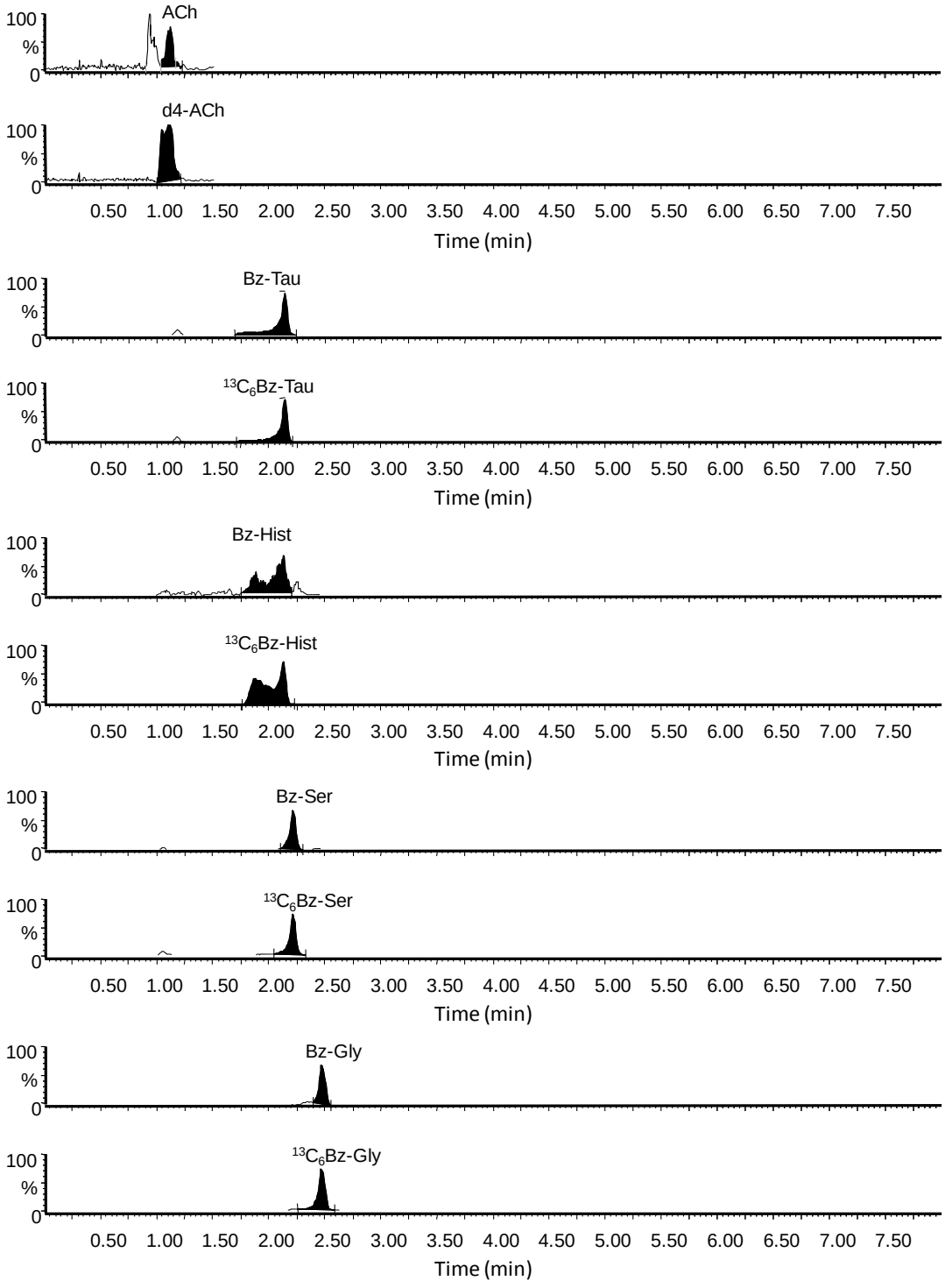

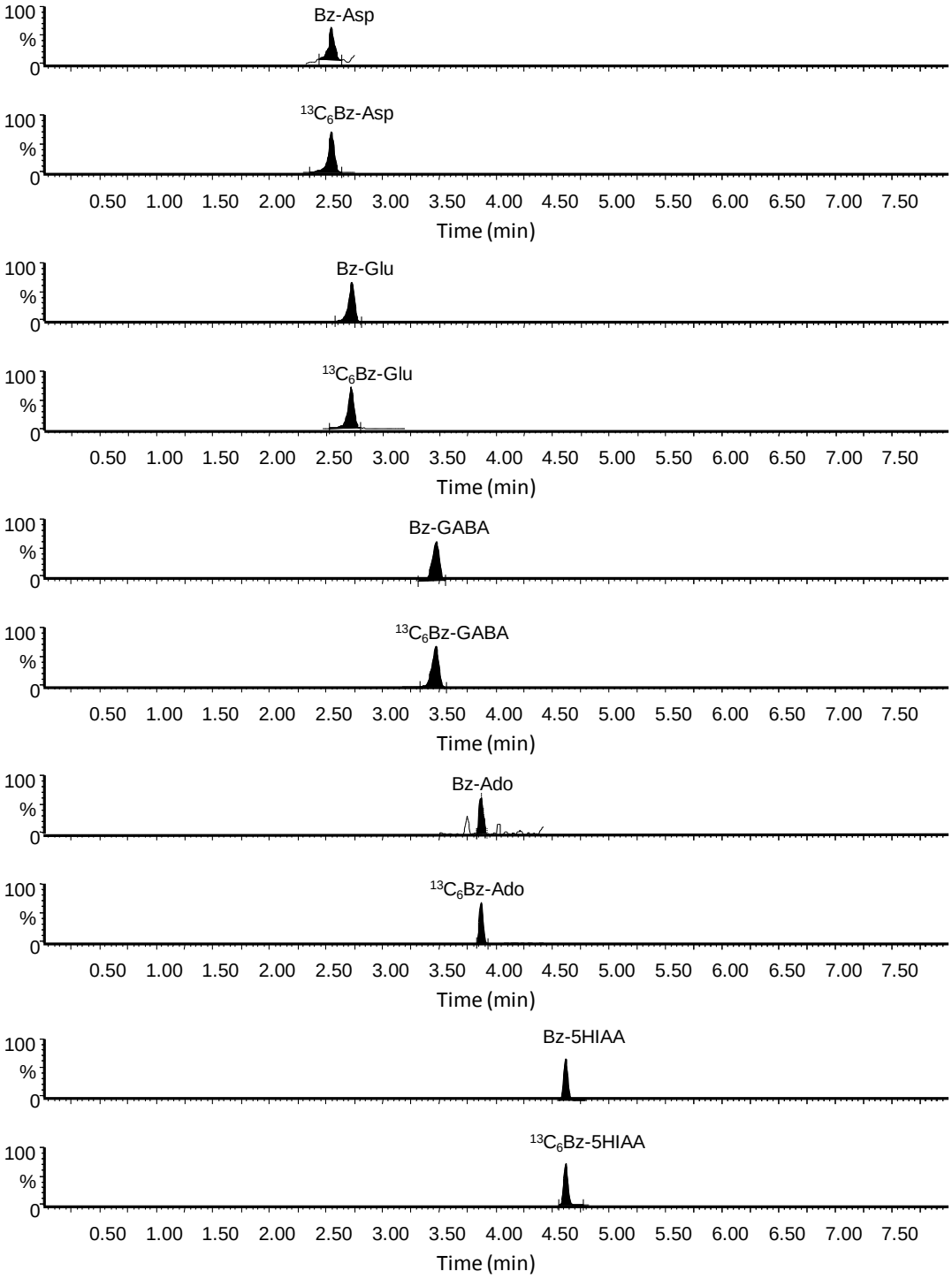
Bz-Asp
$^{13}C_6$Bz-Asp
Bz-Glu
$^{13}C_6$Bz-Glu
Bz-GABA
$^{13}C_6$Bz-GABA
Bz-Ado
$^{13}C_6$Bz-Ado
Bz-5HIAA
$^{13}C_6$Bz-5HIAA
100
%
0
0.50 1.00 1.50 2.00 2.50 3.00 3.50 4.00 4.50 5.00 5.50 6.00 6.50 7.00 7.50
Time (min)

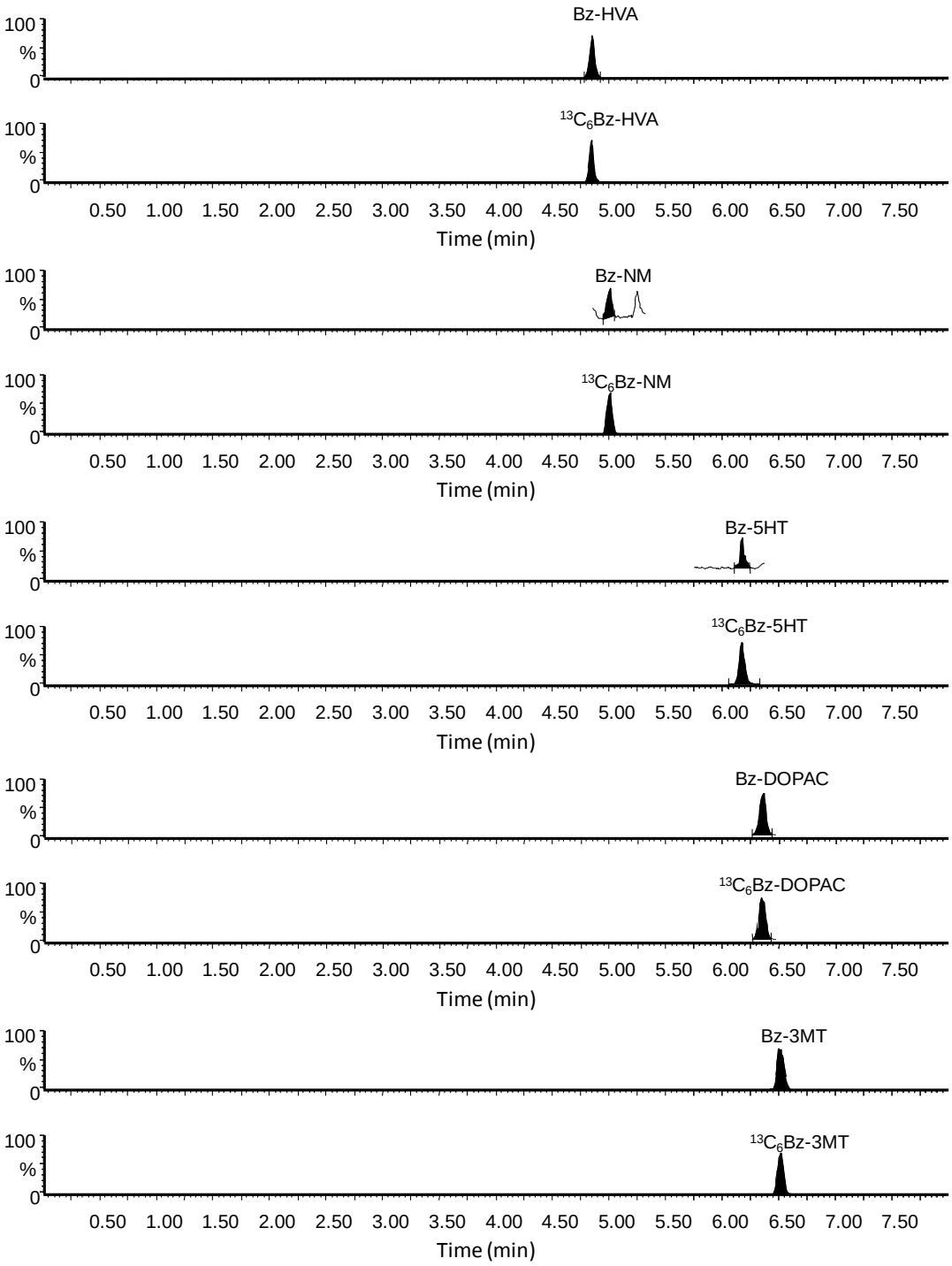
Bz-HVA
$^{13}C_6$Bz-HVA
Bz-NM
$^{13}C_6$Bz-NM
Bz-5HT
$^{13}C_6$Bz-5HT
Bz-DOPAC
$^{13}C_6$Bz-DOPAC
Bz-3MT
$^{13}C_6$Bz-3MT
100
%
0
0.50 1.00 1.50 2.00 2.50 3.00 3.50 4.00 4.50 5.00 5.50 6.00 6.50 7.00 7.50
Time (min)

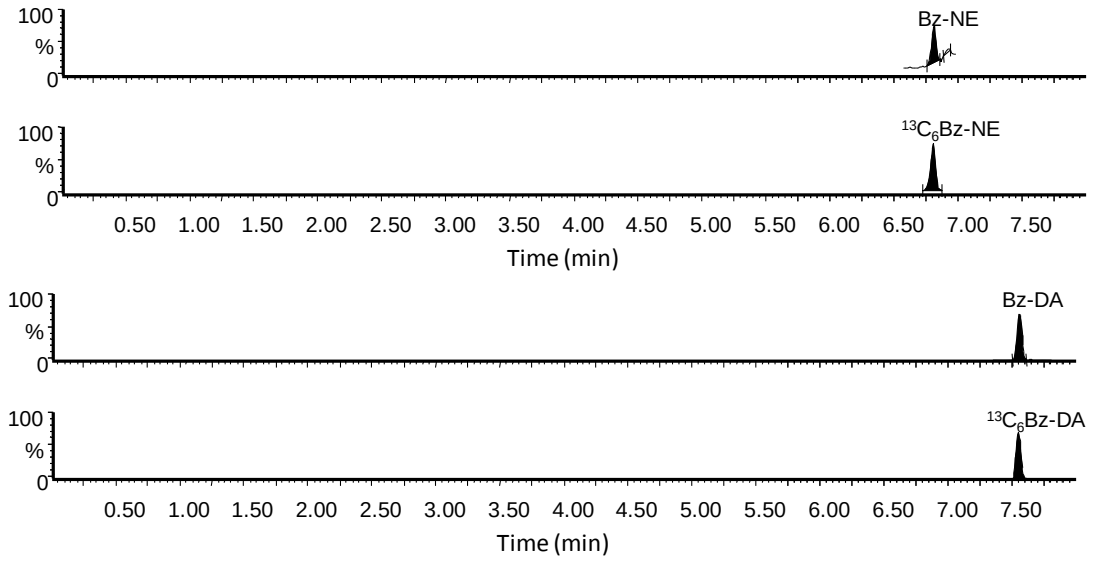

Figure 2.5 Mass chromatogram traces of neurotransmitters and metabolites detected *in vivo* from rat nucleus accumbens. Probe size was 1.5 mm and dialysis flow rate was 0.6 μL/min.

Perfusion of the $GABA_A$ receptor antagonist bicuculline (50 μM) into the VTA (n = 8) yielded a complex set of changes in the neurochemicals measured (Figure 2.6). This treatment stimulated local dendritic (153%; $F_{(7,7)} = 10.15$, $p < 0.0001$) and limbic (106%; $F_{(7,7)} = 5.835$, $p < 0.0001$) DA release, as anticipated [56]. DA release also correlated with an increase in the DA metabolite DOPAC in the VTA (60%; $F_{(7,5)} = 9.209$, $p < 0.0001$), and the NAc (49%; $F_{(7,5)} = 9.641$, $p < 0.0001$). We observed unanticipated increases in VTA 5-HT (146%; $F_{(7,7)} = 5.00$, $p = 0.003$), NE (97%; $F_{(7,7)} = 3.570$, $p = 0.0035$), ACh (153%; $F_{(7,5)} = 3.809$, $p = 0.0036$), Ado (53%; $F_{(7,5)} = 5.086$, $p = 0.0005$), and Gly (66%; $F_{(7,6)} = 3.588$, $p = 0.0041$).

In the NAc we observed unanticipated increases in 5-HT (106%; $F_{(7,6)} = 2.450$, $p = 0.0335$), NE (132%; $F_{(7,7)} = 4.843$, $p = 0.0003$), Glu (73%; $F_{(7,6)} = 6.759$, $p < 0.0001$), ACh (66%; $F_{(7,5)} = 2.782$, $p = 0.0207$), and Hist (95%; $F_{(7,5)} = 3.137$, $p = 0.0111$). We also

observed an unexpected reduction in GABA (34%; $F_{(7,6)} = 2.291$, $p = 0.0452$) in the NAc (Figure 2.6).

To demonstrate the utility of the method under conditions of high temporal resolution, we used 60 s sampling in the medial prefrontal cortex (mPFC) to observe changes in ACh release following a 5 min local perfusion of the ACh esterase inhibitor neostigmine (1 μM; n = 5). Neostigmine perfusion caused a prompt increase in ACh (518%; $F_{(60,4)} = 4.193$, $p < 0.0001$) levels in the mPFC as anticipated (Figure 2.7A). We also observed a large (229%; $F_{(60,4} = 4.443$, $p < 0.0001$) transient increase in Glu concentration (Figure 2.7 B). Neostigmine perfusion had no effect on DA, GABA (Figure 2.7 C, D) or other measured neurotransmitters (data not shown). Basal neurotransmitter concentrations in mPFC dialysate are reported in Table 2.2.

HPLC-MS of neurotransmitters

This study demonstrates that HPLC-MS is suitable for measuring all the most commonly studied low molecular weight neurotransmitters, neuromodulators, and metabolites in a single analysis based on both direct detection (ACh) and benzoylation. Unlike reagents that target only primary amines, benzoyl chloride also labels secondary amines, phenols, and ribose hydroxyl groups. This allows several neurochemicals which do not have primary amine groups, such as DOPAC, 5-HIAA, and HVA, to be labeled. Even though many molecules can be detected directly by MS without derivatization, labeling of polar neurotransmitters has several distinct advantages. Benzoylation enhances reversed phase LC retention, improves ESI-MS sensitivity, and allows for a low-cost stable isotope internal standard.

Although benzoyl chloride has been used for polyamine analysis [57], we found that some specific conditions were necessary to achieve reproducible results for neurotransmitter detection. Borate buffer was preferred over other basic buffers for derivatization because it improved precision in catecholamine measurements. We believe that this is because borate forms a reversible complex with catechol groups [58] and protects them against oxidation under the high pH conditions used for labeling [59]. Another issue is that metabolites labeled at multiple sites became hydrophobic and insoluble in 100% aqueous solution; therefore, 25% organic solvent content in the reaction mixture was used to keep these compounds in solution.

Benzoyl chloride labeling is similar to dansyl chloride labeling previously reported for metabolomics [60] but has several advantages due to its structural simplicity. A preliminary study revealed that monoamines which were multiply-labeled with the dansyl group had low CAD efficiency on our triple quadrupole mass spectrometer, rendering MRM of these analytes unsuitable for high sensitivity analysis. In contrast, multiply labeled benzoylated monoamines are easily fragmented. ^{13}C dansyl chloride must be synthesized for differential labeling using light and heavy isotope reagent [60] while $^{13}C_6$ benzoyl chloride is commercially available at relatively low cost. Dansylation requires 30 min reaction time at elevated temperatures while the benzoylation reaction was instant at room temperature. Unlike dansyl chloride, excess benzoyl chloride is completely hydrolyzed so there is no need to scavenge reagent after the reaction. Importantly, neither benzoyl chloride nor the benzoylated product is light sensitive in contrast to dansyl chloride and its derivatives.

The HPLC separation time is 8 min and total analysis time for each sample is around 12 min, taking into account autosampler injection, elution, and column re-equilibration. Over 80 samples plus standards are routinely analyzed per day in our laboratory using this method. Such throughput is important for microdialysis since hundreds of samples are typically generated per study.

Mesolimbic regulation by GABA

To demonstrate the utility of this system, we investigated GABAergic control of the mesolimbic pathway. The mesolimbic pathway is made up of DA containing cells which originate in the VTA and extend to the NAc. This pathway is intensively studied for its role in reward processing, motivation and addiction since all drugs of abuse activate this pathway [38, 61, 62]. GABA, primarily from VTA interneurons, is an important regulator of the mesolimbic pathway [63, 64] and blockade of $GABA_A$ receptors stimulates mesolimbic DA release [56]. Evidence suggests that the rewarding effects of opiates, cannabinoids, and benzodiazepines rely on their ability to activate the mesolimbic DA pathway by inhibiting GABAergic interneruons in the VTA [64-66]. Neurotransmitters other than dopamine regulated by GABA have received less attention. Here our method has uncovered previously unknown GABAergic involvement in several neurotransmitter systems apart from DA as bicuculline perfusion into the VTA not only evoked the expected increase in NAc DA[23] (and DA metabolite, DOPAC) but also 5-HT, NE, Glu, ACh, and Hist while reducing GABA levels. Locally in the VTA, bicuculline enhanced not only dendritic DA (and DOPAC), but also evoked local 5-HT, NE, ACh, Ado, and Gly release (Figure 2.6). These results show that GABAergic control of the VTA is not limited to limbic DA release and that a complex interplay between several neuronal

substrates is involved in mesolimbic activation, and possibly reward. These measurements also demonstrate compatibility with high spatial resolution experiments. The VTA is ~1 mm in height x ~1 mm in width [67], so a 1 mm long x 250 µm diameter dialysis probe was used. Small probe produces low recovery (~10 %) requiring high sensitivity - a criterion met by the current method.

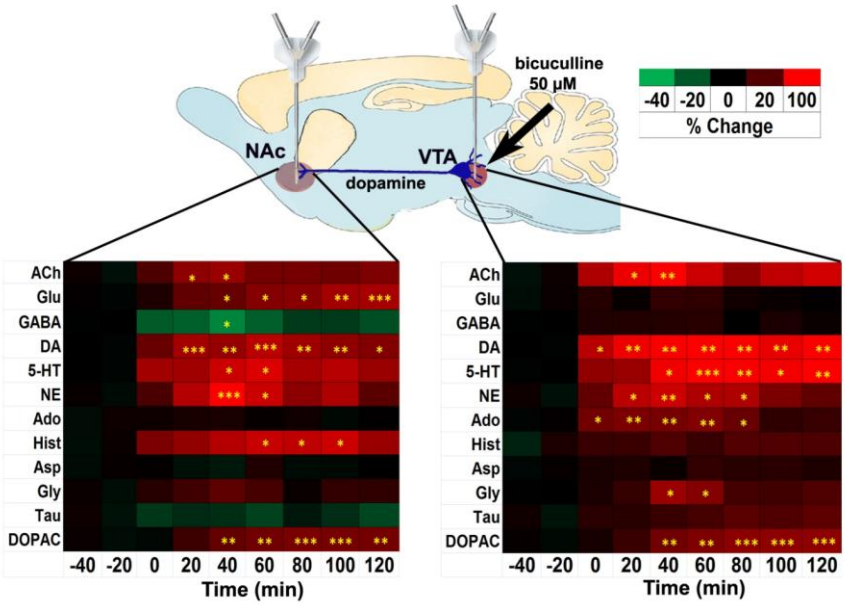

Figure 2.6 Dual probe microdialysis of the mesolimbic pathway. Bicuculline (50 µM) was perfused in the VTA while monitoring neurotransmitters both locally and distally in the NAc. Heat map shows all changes of neurochemicals monitored where colors correlate with changes expressed as percentage of baseline. Times in heat map are referenced to infusion of biculline. RM ANOVA and a post-hoc Tukey test were performed to compare basal levels against post drug levels. *p < 0.05, **p < 0.01, ***p < 0.001 compared to basal level in the respective brain region.

Prefrontal ACh and Glu interaction

We also measured prefrontocortical signaling to test the method under the challenging condition of a high sampling rate. The mPFC is a known center of emotional and cognitive function and is often studied in psychiatric and attentional disorders [68, 69]. To uncover physiologically and behaviorally relevant neurotransmitter interactions in the

mPFC, common microdialysis sampling rates (i.e. 10- 30 min/sample) remain inadequate. Here we have made such measurements every 60 s to better capture concentration dynamics on a more physiologically relevant time scale [69]. Measurement at short intervals requires high sensitivity (1 μL samples are collected containing femtomoles of analyte) and good throughput because of the large number of samples generated (e.g., 80 samples per session in Figure 2.7).

The ACh esterase inhibitor neostigmine (5 min perfusion) elevated ACh concentrations in the mPFC as expected, but also correlated with a transient increase in mPFC Glu concentration. This result suggests that muscarinic or nicotinic ACh receptors in the mPFC are responsible for stimulating Glu release. Past studies have shown that exogenous ACh receptor agonists such as nicotine enhance cognition and stimulate Glu activity in the mPFC [70]. Our data show that stimulated endogenous ACh is capable of enhancing Glu release in this brain area. This ACh-Glu interaction may play a role in cognition and the beneficial effects of drugs which stimulate ACh receptors [70]. Interestingly other neurotransmitter systems, including the monoamines, were left unaffected by neostigmine perfusion. These results show how a comprehensive view of neuropharmacological effects can be assayed by the method. They also show the value of the temporal resolution as the transient rise of Glu would likely be undetected at longer sampling intervals.

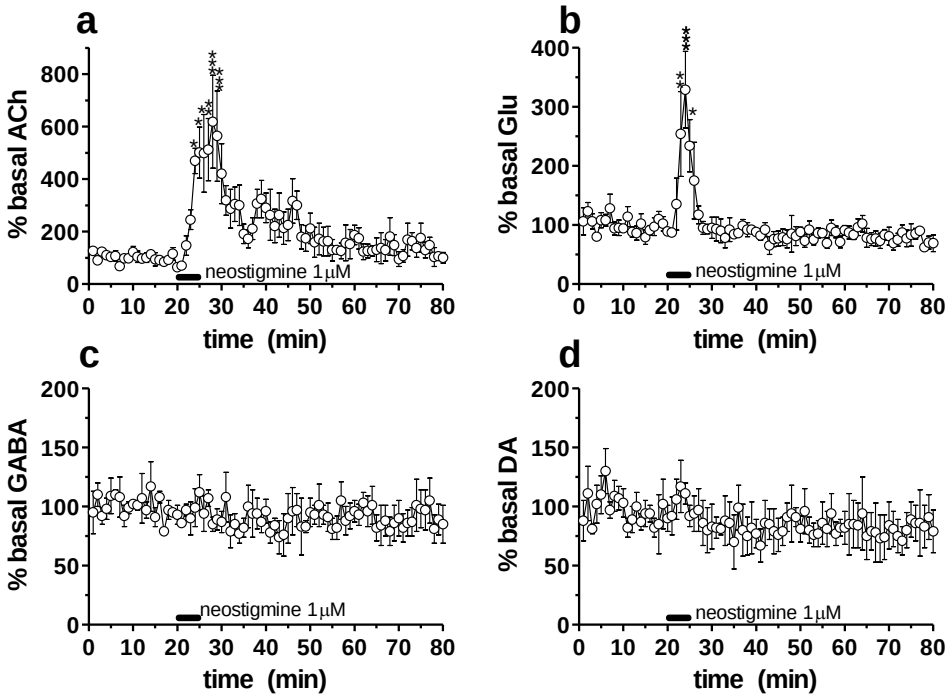

Figure 2.7 Microdialysis in the mPFC. Neostigmine (1 μM) was perfused (black bar) for 5 min in the mPFC while neurotransmitters were monitored locally. Dialysate was collected every 60 s. Error bar is ± 1 SEM (n = 5). Data was expressed as percent of baseline levels. RM ANOVA and a post-hoc Tukey test to compare basal levels against post drug levels. *p < 0.05, **p < 0.01, ***p < 0.001 compared to basal mPFC level.

Conclusion

The results show that benzoylation with HPLC-MS is a robust method for determination of small molecule neurotransmitters and metabolites. The method allows 17 neurotransmitters and metabolites to be detected with 8 min separation at concentrations from picomolar to micromolar. Internal standard is conveniently generated using commercial $^{13}C_6$ reagent, enabling improved quantification. The comprehensiveness, low sample volume requirement, sensitivity, and throughput make this method valuable for neurochemical monitoring under challenging conditions such as small brain regions (VTA) and at short intervals. These properties will make the method widely applicable for pharmacological and brain disorder studies. The good temporal

resolution will be important for correlating neurotransmitter concentrations to behaviors which change on similar time scales.

CHAPTER 3.

A MASS SPECTROMETRY "SENSOR" FOR *IN VIVO* ACETYLCHOLINE MONITORING WITH FIVE SECOND TEMPORAL RESOLUTION

Introduction

Chemical monitoring in a complex microenvironment such as the brain of live subjects requires methods that have high selectivity, low detection limits, and rapid temporal responses. Electrochemical and optical sensors have proven effective for some analytes; however, it is often difficult to develop probes with the necessary performance and many analytes are not amenable to these approaches[71]. Continuous sampling methods, such as microdialysis, coupled to analytical techniques offer an alternative to sensors; but, with only a few exceptions, the relatively slow rate of analysis is a hindrance to achieving comparable temporal resolution to sensors[9, 72]. Mass spectrometry (MS) coupled with continuous ionization methods is an attractive choice for chemical sensing because it allows high-speed analysis with the selectivity and resolving power needed for complex mixtures. The concept of MS-based sensing has been well-documented for volatile organic monitoring[73]. Ambient ionization methods have potential for monitoring condensed phase environments that are accessible to the ionization source[74]. For less

accessible environments, such as *in vivo*, it is necessary to couple the mass spectrometer to a sampling probe. In one example, microdialysis was coupled with fast atom bombardment MS to monitor penicillin G in the bloodstream of a live rat; however, the sample was collected in an injection valve before transferring to the ionization source so that temporal resolution was limited by the time required to collect sufficient sample, which was 20 min[75]. Microdialysis sampling has also been coupled online with liquid chromatography (LC)-MS[76]; but, sample collection and LC separation slow the overall process.

In this report we couple microdialysis sampling directly with electrospray ionization (ESI)-MS to monitor neurotransmitter, metabolite, and drug in the brain of live rats at 5 s temporal resolution. Dilution of the sample stream reduces ionization suppression and fast scanning by MS allows rapid, online assay. Segmenting the sample stream into nanoliter droplets is used to prevent temporal distortion due to Taylor dispersion as concentration pulses collected by the probe are transported to the MS[15] . Segmented flow also facilitates offline analysis by providing a convenient way of storing nanoliter samples for later analysis[10].

The MS "sensor" is applied to monitoring acetylcholine, a neurotransmitter involved in a myriad of functions including cognition[70], memory[77], addiction[78],and movement[79]. Dysregulation of acetylcholine is associated with neurological disorders such as schizophrenia, Parkinson's disease and Alzheimer's disease[80, 81]. Measurement of acetylcholine in the brain of live animals is of great value for better understanding the role of cholinergic neurotransmission in normal and pathological states. Enzyme modified electrochemical sensors for acetylcholine have been reported with temporal

resolution better than 10 s[82, 83]; however, high background from choline, a metabolite of acetylcholine that is rapidly generated by acetylcholinesterase in the extracellular space, compromises this technique so that basal concentrations cannot be detected[83]. Alternatively, choline can be monitored by electrochemistry as a surrogate for acetylcholine[69]. Acetylcholine is frequently monitored *in vivo* using microdialysis sampling and offline analysis by HPLC with electrochemical or MS detection. These methods are highly sensitive and capable of detecting basal acetylcholine levels *in vivo*[12, 84-88]; however, the LC methods are slow and consume microliter samples making them incompatible with high temporal resolution. Recently, matrix assisted laser desorption ionization (MALDI)-MS was used to detect acetylcholine and choline in dialysate samples; however, this method is only compatible with offline analysis and 60 s temporal resolution[89]. We find that microdialysis coupled with segmented flow ESI-MS provides a convenient way to monitor acetylcholine at high temporal resolution. Further, the method allows simultaneous monitoring of drugs or metabolites illustrating the versatility of microdialysis with segmented flow ESI-MS for *in vivo* sensing.

Experimental Section

Chemicals and reagents

All chemicals were purchased from Sigma-Aldrich (St. Louis, MO) unless otherwise specified. HPLC grade water and methanol were from Burdick & Jackson (Muskegon, MI). d4-acetylcholine was purchased from C/D/N isotopes (Pointe-Claire, Canada). Artificial cerebrospinal fluid (aCSF) solution contained 145 mM NaCl, 2.68 mM KCl, 1.0 mM $MgSO_4 \cdot 7H_2O$, 1.22 mM $CaCl_2$, 1.55 mM Na_2HPO_4, 0.45 mM

$NaH_2PO_4 \cdot H_2O$ adjusted to pH 7.4 (salts purchased from Fisher Scientific, Pittsburgh, PA). Tetrodotoxin (TTX) was purchased from Tocris (Minneapolis, MN).

Segmented flow microdialysis

Dialysis probes with side-by-side design were made as previously described[90]. Briefly, two 40 µm ID x 100 µm OD fused silica capillary (Polymicro Technologies, Phoenix, AZ) were glued together with a 2 mm offset at the tip. The capillary tips were ensheathed in an 18 kDa molecular weight cutoff dialysis fiber made from regenerated cellulose (Spectrum Laboratories, Rancho Dominguez, CA). The tip of the fiber was sealed with polyimide sealing resin (Grace, Deerfield, IL).

The outlet of the microdialysis probe was coupled to a fluidic cross for generating segmented flow (Figure 3.1A). The cross was made by inserting a 40 µm ID x 360 µm OD fused silica capillary (Polymicro Technologies, Phoenix, AZ) and the microdialysis probe outlet through the walls of a 55 cm length of 250 µm ID x 1/16" OD perfluoroalkoxyalkane (PFA) tubing (IDEX, Oak Harbor, WA) so that they were juxtaposed as shown in Figure 3.1A. The structure was sealed by epoxy (Quickset™, LOCTITE, Westlake, OH). Dialysate exiting microdialysis probes at 1 µL/min was mixed with diluent flowing from the juxtaposed capillary at 1 µL/min. The combined streams were segmented into droplets by perflurodecalin pumped at 2 µL/min through the PFA tubing as illustrated in Figure 3.1A. This arrangement generated ~32 nL droplets (1 droplet/s) of equal parts diluent and dialysate segmented by perfluorodecalin. Diluent consisted of 50:50 water: methanol (v/v) containing 3 mM EDTA disodium salt and 400 nM d4-acetylcholine.

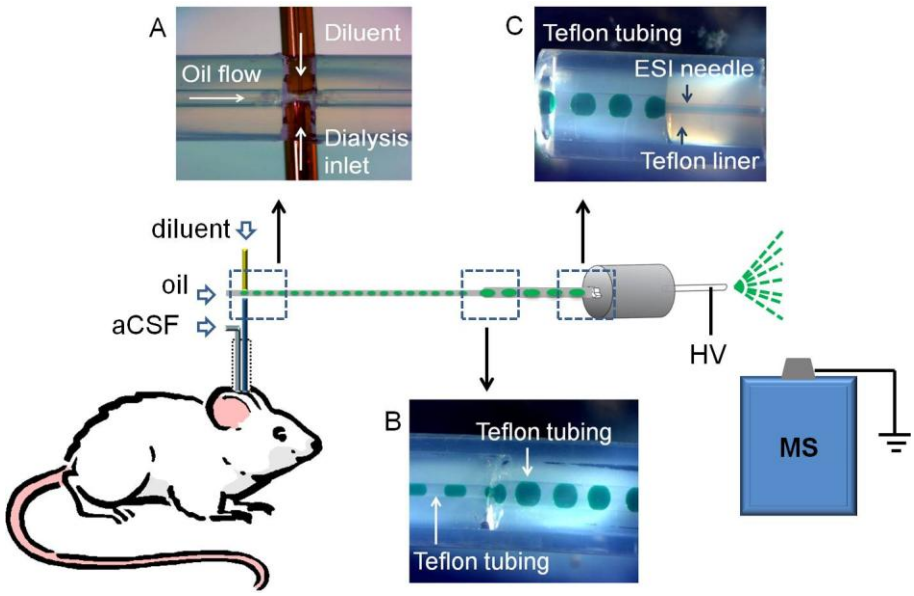

Figure 3.1 Illustration of fluidic design for coupling microdialysis to segmented flow ESI-MS. (A) Droplet generation device before it was sealed with epoxy; (B) Droplet coalescence connection.; (C) Liquid connection at ESI probe. Droplets contained green food dye to facilitate visualization. HV stands for high voltage.

To facilitate online MS analysis, dialysate droplets were coalesced into bigger droplets (~ 160 nL corresponding to a 5 s fraction) by pumping them from the 250 m ID tube into a 5 cm length of 500 µm ID x 1/16" OD PFA tubing (see Figure 3.1B). The coalescence junction was made by sliding a piece of fluorinated ethylene propylene (FEP) tubing (IDEX, Oak Harbor, WA) over the two pieces of 1/16" OD PFA tubing butted together to form a zero dead volume union (Figure 3.1B). For online analysis, wherein droplets were transported directly from the probe to the ESI source, the total infusion flow rate was 4 µL/min. For offline analysis, wherein samples were collected and then pumped into the ESI source, the infusion flow rate was 2 µL/min.

Electrospray ionization – mass spectrometry

Droplets were pumped into a 32 gauge ESI needle for MS analysis. PFA tubing containing samples was interfaced to the ESI needle using a polyether ether ketone

(PEEK) zero dead volume union (ZU1TFPK, Valco, Houston, TX). For better visualization, the PEEK zero dead volume union was replaced with a transparent Teflon tee in Figure 3.1C.

In other experiments, the 32 gauge stainless steel ESI needle was replaced with a modified fused silica capillary of the same size (100 μm ID x 238 μm OD) to reduce carryover between droplets. The fused silica needle was coated on the outside with Au/Pd alloy by a sputter coater (SC7620 Mini, Emitech, Kent, TN). The inner surface was derivatized by infusing 100 μL of 1% trichloro(1H,1H,2H,2H-perfluorooctyl)silane in hexadecane followed by flushing with 300 μL of hexane and then He for 3 min.

The ESI source was interfaced to a Micromass/Waters (Milford, MA) Quattro Ultima triple quadrupole mass spectrometer. ESI voltage was 2.5 kV. The nebulizing gas was at 100 psi for an infusion flow rate of 4 μL/min but was decreased to 60 psi for 2 μL/min. The source temperature was maintained at 100 ℃. The desolvation temperature was 200 ℃. The desolvation gas flow rate was 200 L/h and cone gas flow rate was set at 150 L/h. The MS was operated in multiple reaction monitoring (MRM) mode using conditions listed in Table 3.1. Conditions for LC-MS acetylcholine analysis were described previously[91].

Table 3.1 Analyte MRM conditions

analyte	transition	dwell time (ms)	cone voltage	collision energy
acetylcholine	146→87	70	35	15
d4-acetylcholine	150→91	70	35	15
choline	104→60	70	35	15
neostigmine	223→208	70	35	20

Note: Three analytes were monitored together during *in vivo* experiments: acetylcholine, d4-acetylcholine, and choline or acetylcholine, d4-acetylcholine and neostigmine. Total MS cycle time was ~ 0.2 s.

Temporal resolution and carryover measurement

Carryover of the ESI probe was characterized by infusing discrete droplets containing alternately 0 and 1 μM acetylcholine dissolved in 50:50 aCSF:diluent (v/v). A series of droplets were formed by moving one end of a PFA tubing (500 μm ID x 1/16" OD) up and down between aqueous sample layer and oil layer in a glass vial, while the other end of the tubing was connected to syringe pump operating at pull mode (4 μL/min). Then the tubing was moved to another vial containing different concentrations of sample and a train of new droplets was formed in the same fashion. The tip of the PFA tubing was thoroughly rinsed when switching sampled solutions to eliminate carryover at droplet generation step.

Temporal resolution of the online microdialysis segmented flow ESI-MS system was measured by recording step increases in acetylcholine concentration created by quick transfer of dialysis probes between high and low concentration standard. To determine the effect of segmenting flow, a similar experiment was performed but by-passing the segmenting cross. Instead, the dialysate was mixed with diluent via a tee (C360QTPKG6, Valco, Houston, TX) at 1:1 ratio.

Surgery and in vivo experiments

All animal experiments were performed according to protocols approved by the University of Michigan Committee for the Use and Care of Animals. Male Sprague-Dawley rats (Harlan, Indianapolis, IN) were anesthetized with ketamine (65 mg/kg, intraperitoneal (I.P.) injection) and dexdomitor (0.25 mg/kg, I.P.) and placed in a stereotaxic frame (Kopf Instruments, Tujunga, CA). A burr hole was drilled +0.2 mm anterior-posterior and ±3.0 mm laterally from bregma to target the dorsomedial striatum[67]. The microdialysis probe was lowered so that the active area extended 4.8 mm to 6.8 mm

from the top of the skull. One hour after probe insertion, neostigmine (5 μM) or TTX (100 μM) was microinjected. Boosters of ketamine (30 mg/kg, I.P.) and dexdomitor (0.13 mg/kg, I.P.) were given as needed. For microinjection experiments, a 20 μm ID x 90 m OD capillary was glued so that the outlet was near the middle of the probe active area and 100 μm spaced from the membrane surface. A Picospritzer (General Valve, Fairfield, VA) was used to infuse 200 nL of drug solution over 4 s from the capillary for each microinjection.

Data analysis

Segmented flow ESI-MS data was recorded by Masslynx 4.1 (Waters, Milford, MA) and exported as txt files for plotting and processing. The C-Unipolar Peak Areas detection function of Igor Pro 6.21 (WaveMetrics, Lake Oswego, OR) was used for peak detection and peak height determination. Peak height ratio to internal standard was used for quantification.

Results and Discussion

Direct ESI-MS analysis of acetylcholine in microdialysate droplets

Initial experiments were performed using flow injection analysis (FIA) to determine if acetylcholine dissolved in aCSF could be detected by direct ESI tandem MS (MS/MS). This study showed that signal for acetylcholine in aCSF was about 20-fold lower than that in water (Figure 3.2 A and B), presumably due to ionization suppression. Two-fold dilution of dialysate samples with water reduced ionization suppression and increased the signal ~2.5-fold relative to that in aCSF to yield a low nanomolar detection limit (Figure 3.2 C).

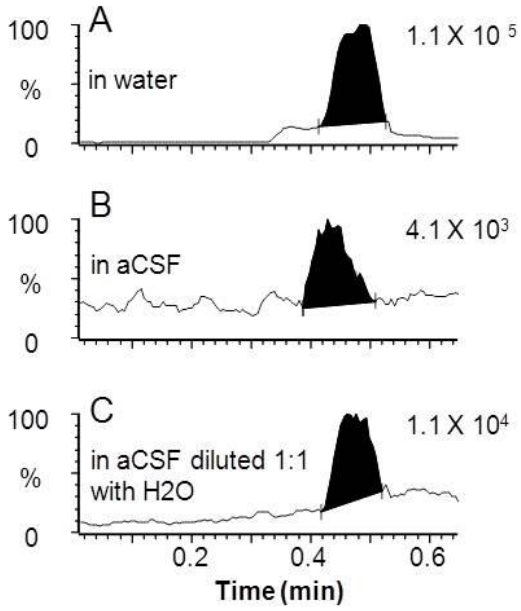

Figure 3.2 Ion suppression of d4-acetylcholine by the inorganic salt in aCSF shown by FIA coupled to ESI-MS/MS (150→91). 50 nM d4-acetylcholine was dissolved in water (A), aCSF (B) and diluted aCSF (C). Ion intensity was shown on the top right corner. FIA flow rate was 100 µL/min. Acquisition started right after sample injection.

Another potential problem faced by direct ESI-MS/MS determination of acetylcholine in aCSF was interference. Using LC-MS/MS analysis of *in vivo* dialysate samples, we detected an additional peak besides acetylcholine corresponding to the same MRM transition (146 → 87), as has been previously reported[84, 86] (Figure 3.3 A). Because this peak would interfere with direct ESI-MS/MS analysis, we further studied its origin. Removing $MgSO_4$ from aCSF eliminated this peak suggesting that it was due to Mg^{2+} cluster ions (Figure 3.3 B). Addition of 3 mM EDTA disodium salt to dialysate samples to chelate Mg^{2+} effectively reduced the interference (Figure 3.3 B) allowing direct detection of acetylcholine by ESI-MS/MS.

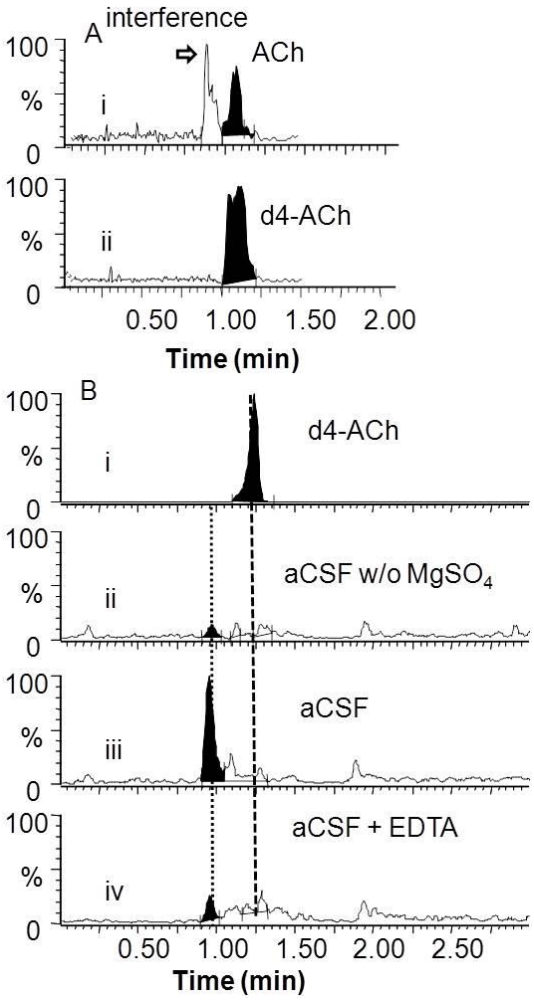

Figure 3.3 Determination of interference of acetylcholine measurement using LC-ESI-MS/MS. (A) Analysis of dialysate samples: (i) MRM (146→87) trace for acetylcholine (ACh) showing interference; (ii) MRM (150→91) trace for d4-acetylcholine. (B) Determination of source of acetylcholine interference and its reduction. (i) LC-ESI-MS/MS (150→91) trace of 1 µM d4-acetylcholine in aCSF; (ii) LC-ESI-MS/MS (146→87) trace of aCSF without $MgSO_4$ showing no interfering peak; (iii) LC-ESI-MS/MS (146→87) trace of regular aCSF blank solution showing interference; (iv) LC-ESI-MS/MS (146→87) trace of regular aCSF blank spiked with 3 mM EDTA showing reduction of interfering peak. Retention time of interference and ACh was aligned with dashed lines.

Based on these experiments, and the desire to obtain high temporal resolution measurements, we designed the system shown in Figure 3.1 to interface microdialysis sampling to ESI-MS. The microdialysis stream was segmented into droplets using perfluorodecalin to avoid dispersion of collected samples during transport and storage

(for offline measurements) as previously demonstrated[10]. As the sample stream was segmented, it was diluted with neat solvent containing EDTA, to chelate Mg^{2+}, and d4-acetylcholine, to provide an internal standard.

The segmented flow dialysate stream was coupled directly to the ESI source as shown in Figure 3.1. Figure 3.4 illustrates that infusion of perfluorodecalin-segmented acetylcholine containing droplets through the ESI source yields distinct current bursts corresponding to each droplet sample. During infusion of samples, perfluorodecalin was removed from the ESI needle by the nebulization gas and produced no signal in the mass spectra. The orthogonal spray geometry was advantageous because oil and non-ionized salt present in the sample were dissipated or deposited on a shield opposing the ESI needle instead of entering the MS inlet. In previous reports of segmented flow ESI-MS, the aqueous droplets were either desegmented prior to ESI-MS[92-95] or directly ionized through nanospray under sufficiently low voltage and flow rate[96]. Compared to previous methods, the ESI format used here proved to be simple (no desegmentation) , robust (no clogging for example) and compatible with a wide range of experimental conditions including different flow rates and voltages.

Direct infusion of droplets containing different acetylcholine concentrations revealed a linear increase in MS/MS signal in the concentration range expected for dialysate samples (Figure 3.4). The limit of detection (LOD) was 5 nM based on the sampled concentration required to achieve signal to noise ratio of 3.

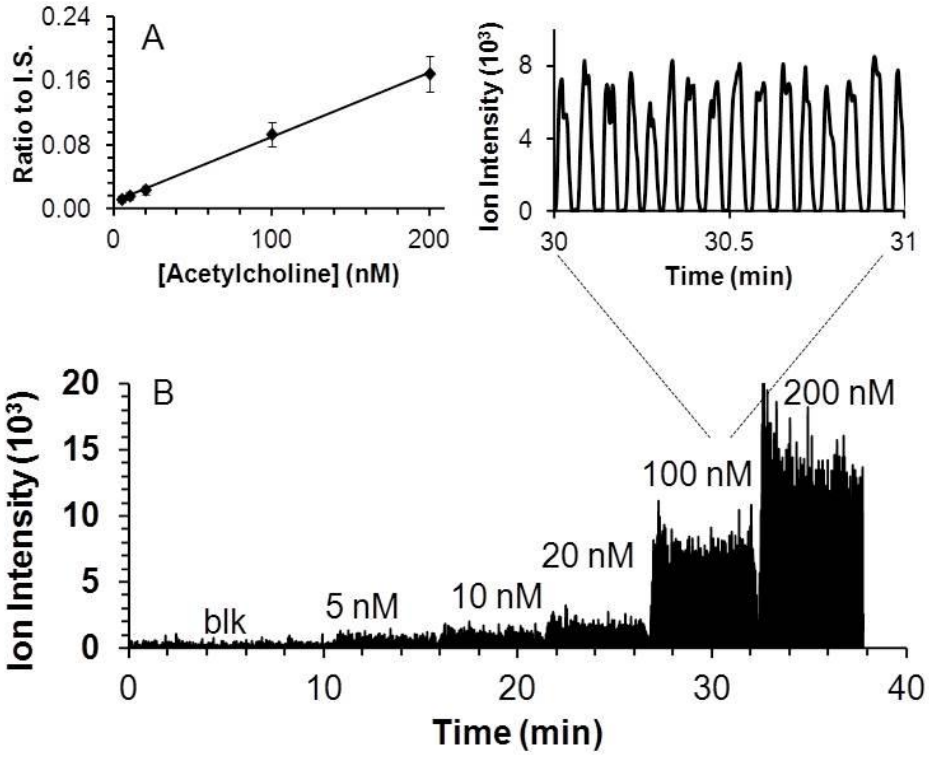

Figure 3.4 Quantitative performance of droplet-microdialysis-ESI-MS acetylcholine detection set up. (A) Calibration curve as ratio of signal for acetylcholine to internal standard (I.S.) Standard was prepared in aCSF. (B) Trace of different concentrations of acetylcholine by segmented flow ESI-MS/MS. Inset shows enlarged view of 16 samples at 100 nM. Result was obtained by sampling from different concentration acetylcholine standard solutions using the system shown in Figure 3.1

System temporal resolution

Temporal resolution is an important consideration for *in vivo* measurements. Choline pulses lasting just a few seconds have been detected *in vivo* by sensors suggesting the need for temporal resolution at that level to capture such dynamics[69]. To preserve temporal resolution, dialysate was segmented at 1 s intervals; but the 0.5 s duration of these droplets (with 0.5 s for oil) was too short for adequate analysis time during online detection. This was because the MS cycle time was 200 ms (time required for MRM scans for acetylcholine, d4-acetylcholine, and either a metabolite, choline, or drug, neostigmine), allowing only 2 to 3 scans per 0.5 s droplet. To obtain more scans per

droplet, we coalesced the 32 nL droplets into 160 nL droplets thus increasing the droplet duration to 2.4 s at a total flow rate of 4 μL/min (2 μL/min of oil, 1 μL/min of dialysate, and 1 μL/min of diluent). Coalescence was reproducible as the RSD of the resulting droplet peak width was 7%; however, it did reduce the best possible temporal resolution. In principle, slower flow rates and narrower ESI needle could be used with droplets that were the original collected size and not coalesced; however, this would increase the overall analysis time and increase the possibility of clogging. As discussed below, the overall temporal resolution was not substantially compromised by this approach.

Once droplets are segmented they should preserve the temporal resolution of the measurement; however, when flowing over hydrophilic surfaces the aqueous samples can wet the surface allowing mixing or carryover between droplets to reduce temporal resolution. The stainless steel needle commonly used for ESI-MS contributed to carryover when segmented samples were pumped through it (Figure 3.5 A,B). In contrast, a modified fused silica capillary (hydrophobic inner surface) eliminated this carryover (Figure 3.5 C).

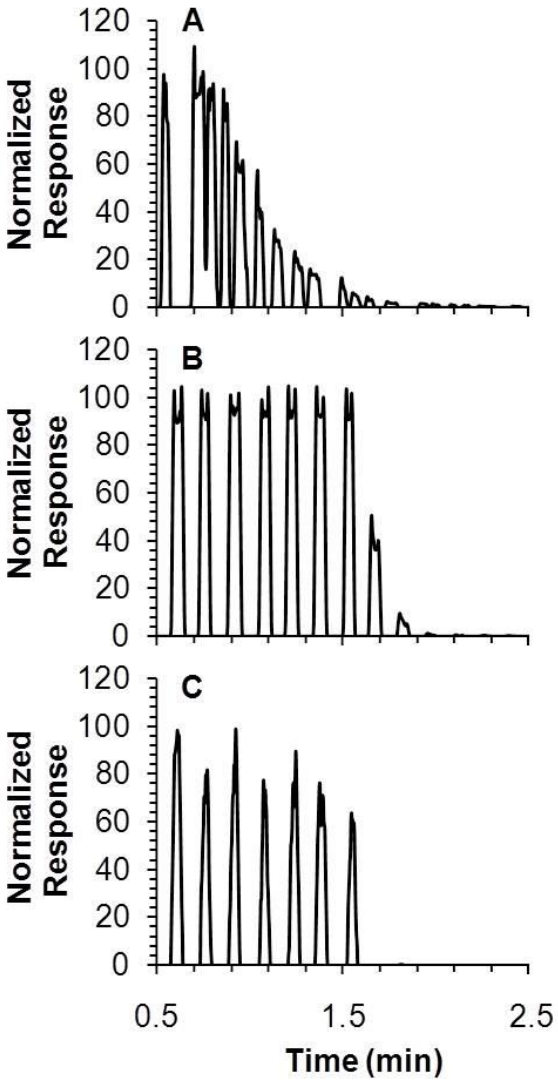

Figure 3.5 Carryover at the ESI probe liquid connection characterized by infusing discrete droplets containing 1 μM acetylcholine and then step decrease to 0 μM using: (A) a low dead volume union and steel ESI needle; (B) a zero dead volume union and steel ESI probe; and (C) a zero dead volume union and modified fused silica ESI needle.

The temporal resolution with continuous flow was 16 s (Figure 3.6 A). In contrast, the temporal resolution of the segmented flow setup under identical microdialysis conditions and using same length of transfer tubing, was 5 s (Figure 3.6 B), which was defined as $t_{res} \approx \varphi/f$ (φ is the number of plugs required to see a change from 10 to 90 %, f is the plug frequency)[97].

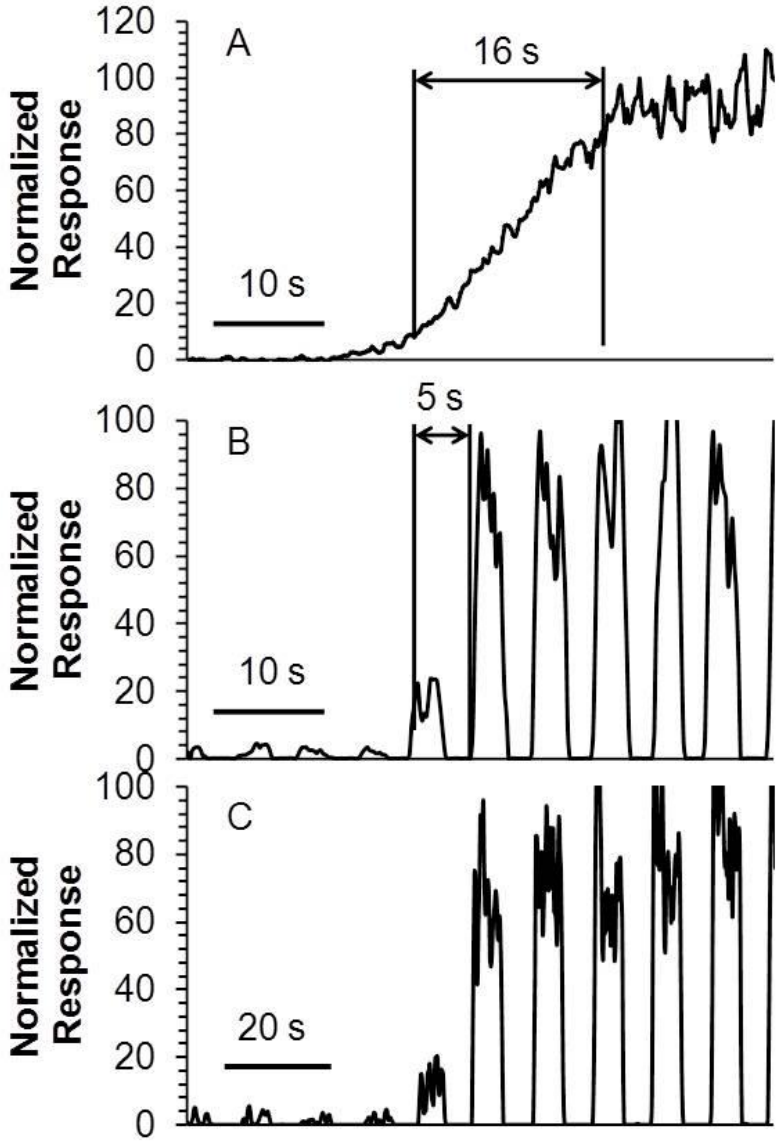

Figure 3.6 Measurement of temporal resolution and comparison. (A) Temporal response to a step change from 500 nM to 5 μM acetylcholine using microdialysis coupled directly to ESI-MS/MS without segmented flow. (B) Temporal response for the same experiment with segmented flow and online analysis. Droplets were analyzed at total flow rate of 4 μL/min. (C) Temporal response for same experiment using segmented flow and offline analysis. Droplets were collected in tubing and analyzed offline at infusion rate of 2 μL/min.

Two factors limit the temporal resolution of the segmented flow ESI-MS system. First is the limited scan speed of the MS. A faster scanning instrument would allow online detection of small droplets without coalescing, a step that sacrificed temporal

resolution. Alternatively, this issue can be solved by analyzing the droplets offline at slower flow rate to accommodate the maximal scan rate. As shown in Figure 3.6 B-C, temporal information was unchanged when analyzing droplet samples at lower flow rate offline showing the potential for this approach. The other factor determining system temporal resolution was the swept volume of the microdialysis probe. Dispersion of concentration gradients crossing the membrane while being swept from the probe limits the temporal resolution to a few seconds[10]. Based on this lower limit for microdialysis, the compromises made to account for the mass spectrometer scan rate were not highly detrimental. It may be possible to achieve sub-second temporal resolution by using alternative sampling methods[98] .

In vivo testing

A typical acetylcholine trace from *in vivo* measurements in an anesthetized rat striatum is shown in Figure 3.7 A.

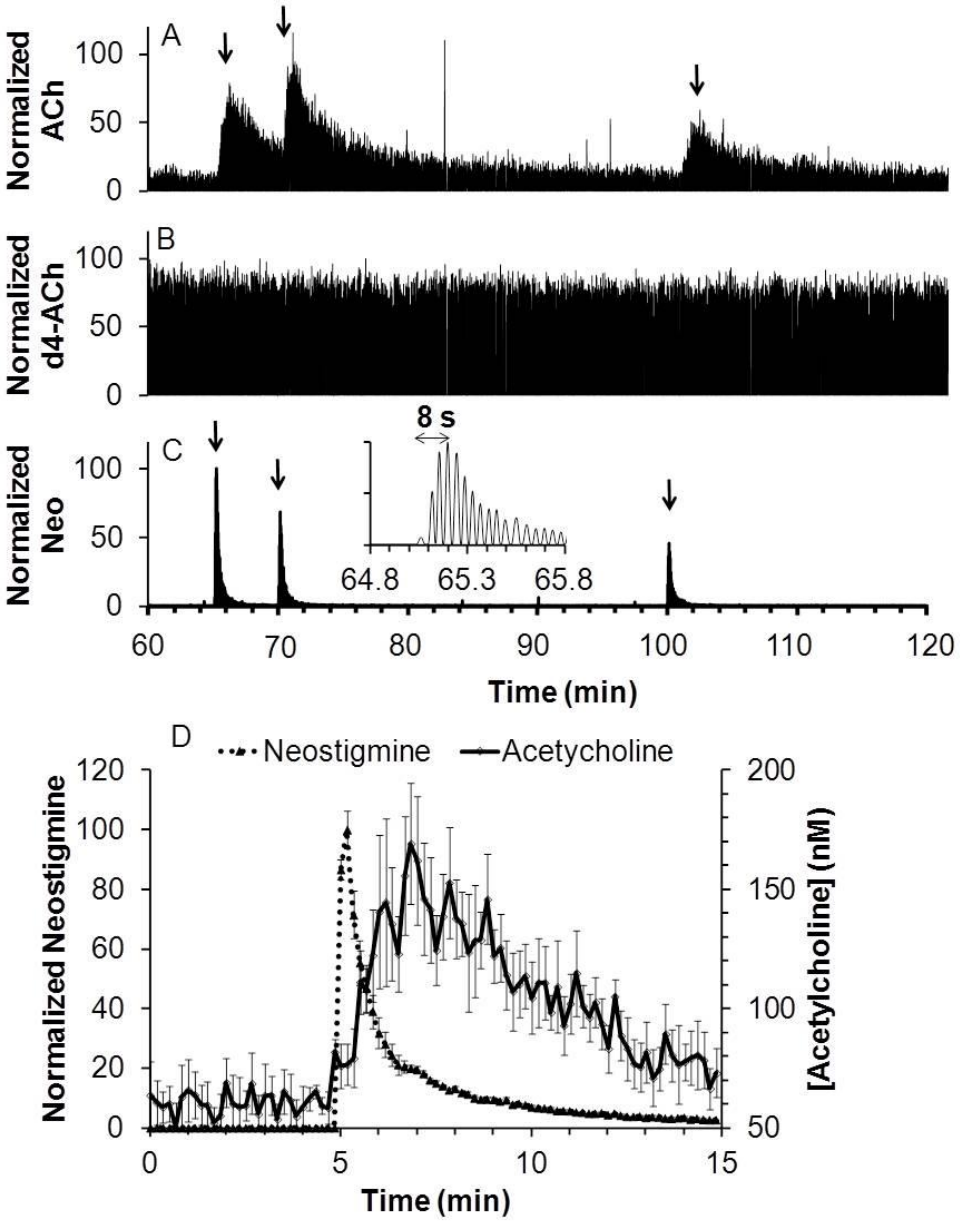

Figure 3.7 Recording of response to *in vivo* microinjection of neostigmine. Figure showed a sample trace for simultaneous detection of (A) acetylcholine (ACh); (B) internal standard, d4-acetylcholine (d4-ACh); and (C) neostigmine (Neo). Arrow indicates beginning of each microinjection. Insert is a magnified view of the 1st microinjection for neostigmine detection. (D) Averaged acetylcholine response to neostigmine microinjection (dotted line) overlaid with averaged neostigmine signal (solid line), (n = 6, error bar = SEM). Response of 2 to 3 droplets were binned in to one data point at 10 s interval for the averaged plot.

After an initial equilibration period (data not shown), a stable signal was achieved that corresponded to an average dialysate concentration of 10 ± 3 nM (SEM, n = 3 rats), in line with reported values[83, 88, 99]. Considering that *in vitro* recovery was 20%, this result corresponds to approximately 50 nM *in vivo* concentration (although *in vitro* recovery is not always a good approximation of *in vivo* recovery[100]).

Microinjection of 200 nL of 5 μM neostigmine, an inhibitor of acetylcholinesterase, yielded a robust acetylcholine transient increase up to 280 ± 71 % of baseline (n = 6 injections from 3 rats). The signal for the internal standard d4-acetylcholine (Figure 3.7 B) remained stable during microinjection showing that the changes in acetylcholine were not due to artifacts such as instrument drift or changes in ionization efficiency.

An advantage of MS detection is that it can be used to monitor multiple analytes simultaneously. For example, neostigmine was readily detected allowing a determination of its dynamics during microinjection (Figure 3.7 C). Neostigmine reached a maximum within 10 s of injection illustrating the high temporal resolution possible *in vivo*. The average response for neostigmine and acetylcholine are overlaid in Figure 3.7 D. The acetylcholine signal is broader than the drug signal possibly reflecting kinetics of inhibition (i.e., we detect the free drug only, so some drug may stay bound to enzyme and continue to inhibit). The broader acetylcholine signal may also reflect the longer distance these molecules had to diffuse through to the probe before detection. Thus, acetylcholine neurons farther from the probe than the microinjector are affected by the neostigmine and the released acetylcholine then diffuses to the probe for detection.

An important test of *in vivo* measurements of neurotransmitters is sensitivity to TTX. TTX binds to neuronal sodium channels to inhibit action potential propagation; therefore, decreases of neurotransmitter concentration with TTX treatment support the conclusion that the signal observed is due to neuronal firing and presumably neuronal release. Figure 3.8 A shows that acetylcholine decreased when TTX was microinjected, in agreement with reports wherein TTX was perfused through a microdialysis probe into the brain[86]. The acetylcholine level remained low for at least 20 min after TTX administration likely due to the persistence of TTX associated with its high affinity for the sodium channel. For these experiments 200 nM neostigmine was perfused through the probe to increase dialysate concentration to 50 ± 10 nM (SEM, n = 5). Without this perfusion, it was difficult to detect a decrease in basal acetylcholine concentration which was typically near the LOD.

Choline was also monitored in these experiments. As shown in Figure 3.8 C, its signal roughly corresponds to that of acetylcholine, supporting the idea that it could be used as a surrogate for acetylcholine under these conditions. These results again illustrate the versatility of MS "sensing" in that different compounds can be selected for monitoring.

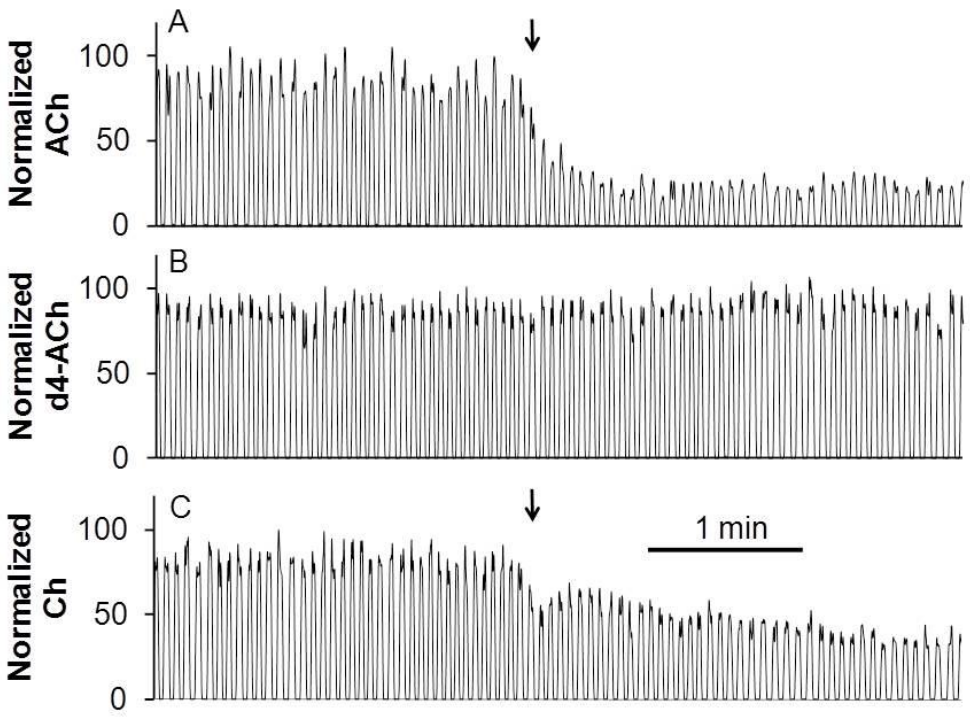

Figure 3.8 Recording of *in vivo* response to a TTX microinjection. Traces showed simultaneous detection of (A) acetylcholine; (B) internal standard, d4-acetylcholine; and (C) choline (Ch) for one experiment. Arrow indicates beginning of microinjection.

Conclusion

Microdialysis coupled with segmented flow ESI-MS provides a powerful *in vivo* sensor with good temporal resolution and selectivity. The method should be suitable for a variety of endogenous and exogenous compounds; however, application will be limited to chemicals that can be readily ionized from complex mixtures. The availability of a stable isotope labeled internal standard enhances quantification and helps account for possible matrix effects. Other sampling probes and online sample pretreatment may further extend the applicability of this approach.

CHAPTER 4.

CAPILLARY UHPLC-MS FOR HIGH THROUGHPUT *IN VIVO* MONITORING

Introduction

Increasing analysis speed has been an enduring theme of HPLC technology development. For in vivo monitoring studies where large sample sets are generated in a short period of time, HPLC method with higher throughput is particularity desirable. The UHPLC-MS method described in Chapter 2 used maximum instrument flow rate to drive the separation on a microbore column (1 mm i.d.), separating 17 compounds of broad polarity range within 8 min. The flow rate limitation of our capillary LC instrument became a hurdle for development of faster analysis. However, speed of LC methods is determined by linear flow velocity, not the volumetric flow rate. Increased linear flow velocity can still be achieved on smaller columns while the volumetric flow rate does not exceed the volumetric flow rate limit imposed by the LC instrument.

HPLC columns with i.d. less than 0.5 mm are commonly referred as capillary columns. Columns with i.d. smaller than 0.1 mm typically operate at nL/min flow rate range, thus are classified as nanoscale columns[101]. Several advantages arise from column miniaturization. Both sample consumption and mobile phase usage drop geometrically as they are proportional to column volume. This is especially useful for sample limited analysis and also substantially reduces the cost of purchasing and disposing LC solvents. Concentration sensitive detectors such as electrochemical detectors, fluorescent detectors

and mass spectrometers, if optimized, give comparable or sometimes superior sensitivity[102, 103]. Another important attribute of smaller columns is related to their thermal property. The heat generated due to frictional heating of the mobile phase as it travel through the micro channels of HPLC columns is distributed unevenly and the radial thermal gradient is detrimental for the separation efficiency. This issue is especially aggravated on long columns or columns packed with small particles. Capillary columns enjoys proportionally reduced heat generation and much improved heat dissipation[24]. Higher separation efficiency was also observed on nanoscale columns[104]. This improvement was proposed to be caused by the more uniform wall effect across entire widths of the columns which resulted in a smaller A term.

Capillary LC, especially nanoscale LC, saw most application sample size limited studies. In proteomics, nanoscale columns coupled to mass spectrometry by sensitive nanospray technique is routinely used to generate high quality data consuming minute amount of proteins[105, 106]. Miniaturized LC techniques were also employed in high temporal resolution monitoring studies for small molecules and peptides[11, 46, 107]. In one example, amino acids in samples collected at 10 s interval were detected, although the analysis of the whole sample set took much longer due to the speed of LC separation[11].

In this chapter, we examined the practical aspect of employing capillary columns packed with high efficiency particles for high speed LC analysis with the ultimate goal of applying the method for in vivo monitoring. Three commercially available capillary columns were evaluated and the best column was further optimized for fast neurotransmitter separation within 4 minutes. The new LC-MS method represented a 2 fold improvement in throughput compared to the old method in Chapter 2 and was

capable of monitoring multiple neurochemicals in real dialysate samples. The pros and cons of the fast LC-MS method are discussed and possible ways of improvement are suggested.

Experimental Section

Chemicals and Reagents

All chemicals, drugs and reagents were purchased from Sigma Aldrich (St. Louis, MO) unless otherwise noted. Water and acetonitrile are Burdick & Jackson HPLC grade purchased from VWR (Radnor, PA). 10 mM stock solution of each analyte was made in HPLC water and kept at -80 ^{o}C. Standard mixture was diluted from stock using aCSF consisting of 145 mM NaCl, 2.68 mM KCl, 1.10 mM $MgSO_4$, 1.22 mM $CaCl_2$, 0.50 mM NaH_2PO_4, and 1.55 mM Na_2HPO_4, adjusted pH to 7.4 with 0.1 M NaOH. Internal standard was 1 mM Gly, Ser and Tau, 100 μM Asp, Glu, GABA, Ado, HVA, 5-HIAA, and DOPAC and 10 μM 5-HT, NE, DA, NM and 3-MT derivatized with $^{13}C_6$ benzoyl chloride using the same procedure as ^{12}C reagent, then diluted 100 fold in DMSO containing 1% concentrated sulfuric acid. d4-ACh (C/D/N isotopes, Pointe-Claire, Canada) was spiked into the reaction mixture to a final concentration of 100 nM.

Microdialysis

A Sprague-Dawley rat weighing 320 g had a concentric 2 mm long microdialysis probe implanted into the globus pallidus externus under ketamine/dexdomitor anesthesia. Microdialysis probe was perfused during implantation surgery at 0.6 ul/min and samples were collected every 4 min (2.4 ul total sample volume). 5 total fractions were collected for analysis.

Benzoylation reaction

Derivatization procedure was similar to that described in chapter 2 with minor modifications. 2 volume of sample or standard was added with 1 volume of buffer, 1 volume of reagent, and 1 volume of internal standard. Then 5 volume of water was added into the mixture to reduce sample elution strength.

HPLC-MS analysis

The HPLC system was a Waters (Milford, MA) nanoAcquity HPLC. Columns used were HSS T3 C18 (1.8 µm particle, 1 mm X 10 cm) from Waters, Waters Atlantis T3 (3 µm particle, 300 µm X 15 cm) from Waters, Pepmap C18 (2 µm particle, 300 µm X 5cm) from Dionex (Sunnyvale, CA)and Halo™ C18 (2.7 µm fused core particle, 500 µm X 10 cm) from Eksigent (Foster City, CA). Connecting tubing in the LC system was 50 um i.d. PEEKSil from IDEX (Oak Harbor, WA). Mobile phase A (m.p.A) was 10 mM ammonium formate, 0.15% (v/v) formic acid in water. Mobile phase B (m.p.B) was straight acetonitrile. Linear gradient from 5 % to 66% m.p.B was used for all columns. Flow rate, injection volume and gradient conditions adjusted for 4 columns were summarized in table 4.1.

Table 4.1 LC conditions for different columns

column	i.d. (µm)	length (cm)	particle (µm)	t_G (min)	flow rate (µL/min)	Inj. vol. (µL)
HSS T3	1000	10	1.8	7	100	5.0
Halo™	500	10	2.7*	7	25	1.3
Pepmap	300	5	2	7	4.5	0.3
dC18	300	15	3	7	13.5	0.7
Halo™	500	10	2.7*	3.5	50	1.3

* fused core particles

Sample injection was done in partial loop injection mode. Autosampler was kept at ambient temperature and column was maintained at 27 ^{o}C. An Agilent (Santa Clara, CA) 6410 triple quadrupole mass spectrometer was used for detection. Atmospheric

pressure ionization source was operated in positive ESI mode at 4 kV. Drying gas flow was 11 L/min at 350 ^{o}C. Nebulizing gas was set at 15 psi. The original stainless steel ESI needle (159 μm i.d.) was replaced with a tapered fused silica needle fabricated from a piece of 50/360 μm fused silica tubing. The original ferrule to adapt stainless steel needle to the 1/16" fittings was also changed to a fused silica adapter from Valco (Houston, TX).

To make the fused silica ESI needle, A 2 cm clear window was burnt on the fused silica tubing. Then it was mounted on a laser pipette puller (P-2000, Sutter Instrument, Novato, CA). The tapered fused silica needle was made using program described in literature[108]. The opening was widened by flattening the tip on a ceramic capillary cutter (Restec, Bellefonte, PA).

Dynamic multiple reaction monitoring (dMRM) conditions are listed in Table 2. Chromatograms were constructed from data points exported from Agilent MassHunter Qualitative Analysis B.04.00.

Table 2. dMRM parameters for neurochemicals and their internal standard

Analyte	Parent Ion	Daughter Ion	Fragment Voltage (V)	Collision Energy (V)	Cell Acc (V)	Ret Time (min)	Ret Window
ACh	146	87	120	15	4	0.7	0.25
Bz-3MT	376	105	120	20	4	3.51	0.2
Bz-5HIAA	313	146	120	15	4	2.89	0.15
Bz-5HT	385	264	140	20	4	3.42	0.15
Bz-Ado	372	136	120	30	4	2.02	0.15
Bz-Asp	238	105	120	10	4	1.54	0.15
Bz-DA	466	105	140	20	4	3.87	0.15
Bz-DOPAC	394	105	140	20	4	3.43	0.15
Bz-GABA	208	105	120	10	4	1.75	0.15
Bz-Glu	252	105	120	20	4	1.61	0.15
Bz-Gly	180	105	120	10	4	1.56	0.15
Bz-Hist	216	105	120	20	4	1.45	0.15
Bz-HVA	304	105	120	15	4	2.99	0.15
Bz-NE	482	105	140	30	4	3.55	0.15
Bz-NM	374	105	140	15	4	3.11	0.15
Bz-Ser	210	105	120	20	4	1.45	0.15
Bz-Tau	230	105	120	10	4	1.38	0.2
C13Bz-3MT	388	111	120	20	4	3.51	0.2
C13Bz-5HIAA	319	146	120	15	4	2.89	0.15
C13Bz-5HT	397	270	140	20	4	3.42	0.15
C13Bz-Ado	378	136	120	30	4	2.02	0.15
C13Bz-Asp	244	111	120	10	4	1.54	0.15
C13Bz-DA	484	111	140	20	4	3.87	0.15
C13Bz-DOPAC	406	111	140	20	4	3.43	0.15
C13Bz-GABA	214	111	120	10	4	1.75	0.15
C13Bz-Glu	258	111	120	20	4	1.61	0.15
C13Bz-Gly	186	111	120	10	4	1.56	0.15
C13Bz-Hist	222	111	120	20	4	1.45	0.15
C13Bz-HVA	310	111	120	15	4	2.99	0.15
C13Bz-NE	500	111	140	30	4	3.55	0.15
C13Bz-NM	386	111	140	15	4	3.11	0.15
C13Bz-Ser	216	111	120	20	4	1.45	0.15
C13Bz-Tau	236	111	120	10	4	1.38	0.2

Results and Discussion

The main goal of this study is to increase the throughput of UHPLC-MS method for neurochemicals and reduce sample consumption by the exploring capillary UHPLC methods. Use of capillary columns was a feasible way of achieving faster separation without exceeding instrument's flow rate limit. According to Van Deemter equation and its derivatives, high velocity inevitability caused loss of separation efficiency due to mass transfer limit. The key for fast and efficient separation invariably involves minimizing the C term. The available technologies to achieve this goal were discussed in detail in

Chapter 1. Here capillary columns packed with small totally porous and fused core particles were evaluated for high speed separation.

Capillary column size

Capillary LC requires low dispersion sample introduction and low flow pumps. Stable nL/min to low μL/min flow and efficient mixing are no longer problems on commercial capillary LC systems (Waters nanoAcquity, Dionex 3000 nano LC, Agilent 1260 capillary LC, Eksigent nanoLC/microLC, Proxeon EASY nLC). However, much remains to be done on the sample introduction part. The injection volume on to a HPLC column can be expressed as[109]

$V_{inj} = \theta K \varepsilon \pi d_c^2 L(k+1)/N^{1/2}$ (Equation 4.1)

V_{inj} is the injection volume; θ is the fractional loss of separation efficiency, usually 5% is considered acceptable ($\theta = 0.05$); K is the constant regarding injector's property, $K = 4$ for rectangular injection profile; ε is column total porosity, usually around 70% ($\varepsilon = 0.7$); d_c is the column i.d; L is column length; k is the retention factor; N is the plate number. Since reduced plate height $h = H/d_p$, H is the plate height and d_p is the particle size.

$N = L/H = L/hd_p$ (Equation 4.2)

Assuming good column efficiency ($h = 2$)

$V_{inj} \approx 0.662 d_c^2 (k+1)(Ld_p)^{1/2}$ (Equation 4.3)

Thus, as Equation 4.3 shows, sample injection volume is determined by analyte retention, column size and to a lesser degree, particle size. Thus, for a 75 um X 15 cm capillary column packed with 3 um particles, the acceptable injection volume of a lightly retained analyte ($k = 3$) is only10 nL. Reproducible injection of such a small volume without

significant dispersion is no easy task and no commercial autosampler today is up to this challenge. Injection of low nL volume is done using split injection (static or dynamic) or pressure vessel[109]. Although capable of injecting very low sample volumes, these techniques are not reproducible, difficult to automate and in the cases of split injections, waste samples. This issue become much easier for analytes with strong retention, such as hydrophobic peptides on reversed phase LC (RPLC) columns. On column focusing are often practiced for these compounds[108]. Dissolved in large volumes of weak solvent, these analytes will stack at the column front without elution, benefiting from thousands fold pre-concentration effect and greatly ease the demand for ultra low volume/dispersion injection system. For this reason, capillary LC and nanoscale LC see most application in the field of proteomics where hydrophobic peptides can be pre-concentrated and efficiently separated. For small hydrophilic bio-molecules, on column focusing is out of the question due to their weak retention on RPLC. Despite the fact that retention of small molecule neurotransmitters is already significantly enhanced after benzoylation, it is not sufficient for all of them if on column focusing is to be used. Care must be taken in matching the autosampler's capability and internal volume to the capillary column size. Considering the minimum aspirated volume by the autosampler is in the hundreds of nL range, only large capillary columns, i.e., columns with i.d. ≥300 um are considered.

Extra column volume

Besides using smaller columns, miniaturized LC techniques also requires reduction of extra column volume in proportion to column volume to reduce band broadening at low flow rate. The original 30 gauge stainless steel ESI needle on the ionization source, cannot be used without causing too much band broadening at low μL/min. A fused silica

needle with narrower i.d was used as replacement. Because Agilent API source grounds the ESI needle assembly while applies high voltage on the MS inlet, a closed circuit can still be formed through the stainless steel union that connects the ESI needle to the LC outlet. The replacement non-conductive fused silica needle was proven to have comparable sensitivity with the original stainless steel one. All other connecting tubing was 50 µm i.d. Assuming analyte's diffusion coefficient to be 1×10^{-5} cm^2/sec and peak width of 6 sec, the 20 cm of 50 µm post column tubing causes 10% increase in peak width at 50 µL/min. Most of the pre-column volume was in the sample loop itself, which was measured to be 6 µL by the instrument. Unfortunately the sample loop volume could not be freely reduced to the desired value and contributed significantly to the band broadening of weakly retained analytes as indicated in results discussed later.

Column comparison

Method development using capillary columns was hampered by their commercial availability. No column with i.d between 300 µm and 500 µm packed with sub 2 µm particles is commercially available. The closest was packed with 2 µm particles (Dionex Pepmap 300 µm X 5 cm column). The only other column packed with high performance particles was the Eksigent column packed with 2.7 µm HALO™ fused core media. As a comparison, a capillary column packed with conventional 3 µm particles was also evaluated. All three capillary columns' performance was pitted against that of the current microbore (1 mm i.d.) UHPLC column (1.8 µm particle). To make the above mentioned columns of different sizes comparable, LC parameters need to be adjusted to the same gradient steepness *b*. Gradient range $\Delta\Phi$, and gradient time *tG* were also maintained the

same. Only flow rate F was adjusted according to various column void volume V_m using equation 4.4.

$b = \Delta\Phi\, S\, V_m / t_G\, F$ (Equation 4.4)

S is the constant for a given compound at fixed experimental conditions, approximately equals to 0.25 $MW^{0.5}$

Meanwhile, injection volume V_{inj} was also adjusted according to equation 4.1. Respective V_{inj} and F of different columns were listed in Table 4.1.

The chromatograms of these columns (Figure 4.1) showed roughly the same spacing and exact elution order as expected[110]. Due to the peak compression effect, peaks in gradient LC usually have the same width, unlike that of isocratic LC where later peaks are broader[111]. But the early eluting peaks of some capillary columns were significantly broader than the late eluters, indicating pre-column band broadening, which affected the weakly retained analytes more than the strongly retained ones[112]. Relatively large sample loop caused mixing of low or sub μL sample plug to mix with transfer solvent (m.p.A), resulting in bigger sample injection plug than desired. The fused core particles have less than half of the surface area compared to fully porous ones[26], therefore retention of the already weakly retained amino acids would have been even less. Despite the HALO™ column's bigger size (500 μm i.d.) compared to the Pepmap and Atlantis (both 300 μm i.d.), the band broadening of early eluting amino acids on the fused core particle column was still obvious. As the smallest column, the Pepmap column also suffered from relatively large extra column volumes. The Atlantis dC18 column, which had the largest stationary phase surface area among all three capillary columns, was not affected by pre-

column band broadening as much. Plumbing issue aside, column efficiency at the same gradient steepness also differed. Surprisingly, the 2 μm particle column failed to be an improvement over column with 3 μm particles, despite its smaller size corresponded to smaller C term. The disparity between theory and experimental results might be due to larger size distribution of the 2 μm particles or the packing heterogeneity. The fused core particle column was the best among all three capillary columns tested. The later eluting analytes had slightly broader peak width compared to the 1 mm UHPLC column packed with sub 2 μm particles. It can be expected that if the pre-column dispersion could be satisfactorily resolved, the HALO™ capillary column would provide high efficiency separation approaching the current UHPLC method described in chapter 2 (Figure 4.2), but consuming only 1/4 of amount of sample and mobile phase. The analytes' peak height of each column was different, contrary to the well established knowledge that ESI-MS is a concentration sensitive technique. The reason for lowered sensitivity on smaller columns was due to the lack of xyz position adjustment system on the API source (ESI emitter could not be placed closer to the MS inlet at lower flow rate).

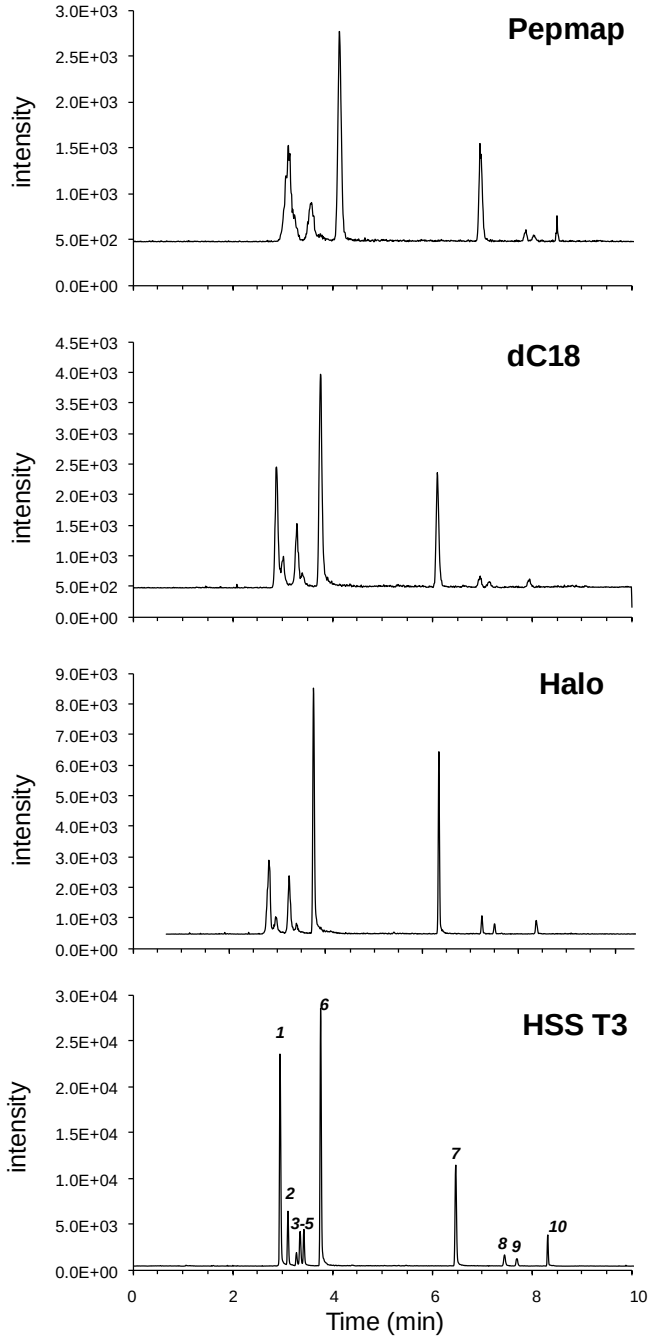

Figure 4.1 Parallel comparison of four HPLC columns for gradient separation of 10 neurotransmitters. All columns were operated at the same gradient steepness. Detailed LC parameters were listed in Table 4.1. All chromatograms are on the same time scale. Analyte key: 1. Tau; 2. Ser, 3. Asp; 4. Gly; 5. Glu; 6. GABA; 7. HVA; 8. 5-HT; 9. NE; 10. DA.

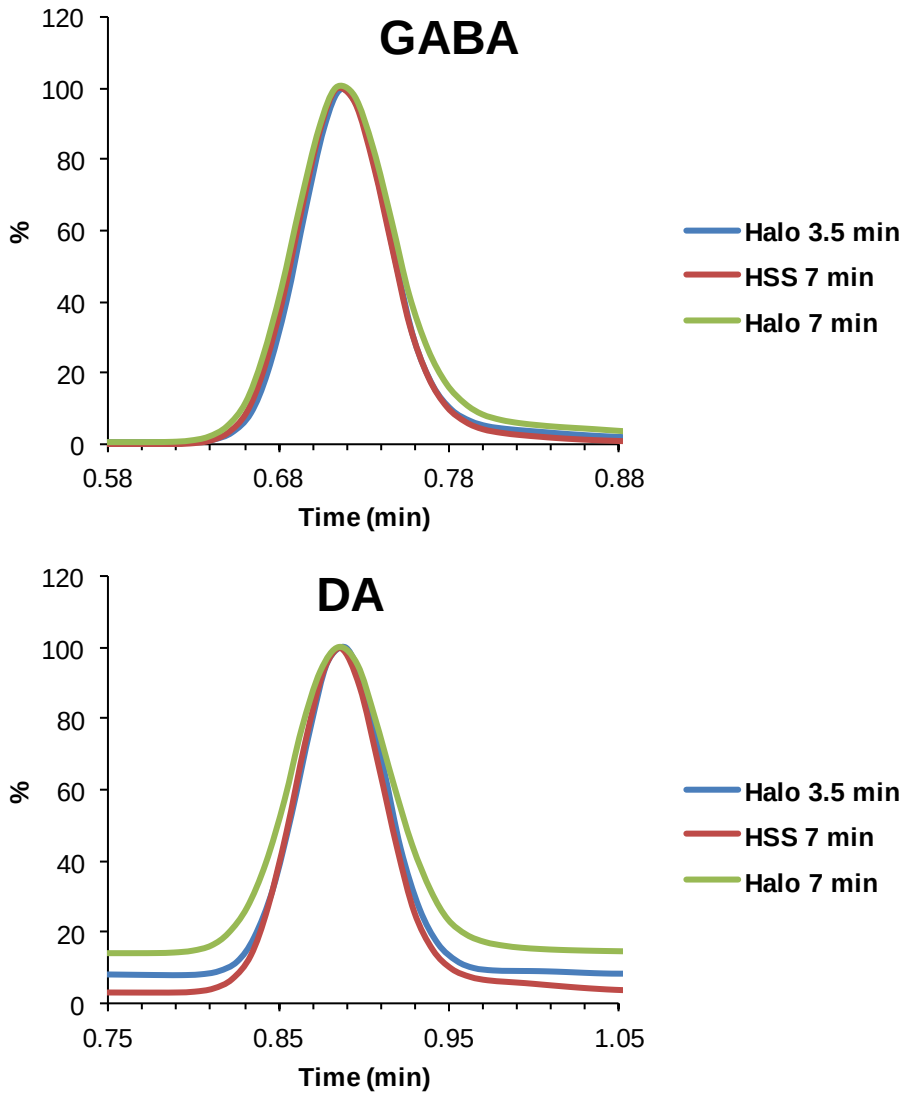

Figure 4.2 Comparison of peak width of early eluting GABA and late eluting DA under different LC conditions. Blue trace was obtained by running fast gradient separation (t_G 3.5 min) on HALO™ column. Red trace was obtained by running regular gradient separation (t_G 7 min) on HSS T3 column. Green trace was obtained by running regular gradient separation (t_G 7 min) on HALO™ column. Note that the y axis was normalized value. The peaks of the same analyte from different LC runs were aligned to have the same peak center.

Increased LC speed and limitations

The best capillary column, the HALO™ (500 µm X 10 cm), was selected for further high speed optimization. The highest flow rate tested on this column was 50 µL/min, which

produced maximum backpressure ~ 8000 psi at 27^{o}C. Highest flow rate achievable was limited by the mechanical strength of the packing material, which could withstand up to 9000 psi, and the pressure capability of the LC instrument (10,000 psi). The option of higher temperature to column backpressure was not pursued because it also reduced retention of amino acids, exacerbated the pre-column band broadening issue. At the highest flow rate/linear velocity permitted, the gradient time t_G was reduced to 3.5 min while maintaining the same peak spacing. The peak capacity in the shortened LC method was reduced compared to longer runs, as shown in Figure 4.3. This result indicated the increasing toll taken by mass transfer resistance. Although peaks did get sharper at higher flow rate (Figure 4.2), the reduction of peak width was not two fold as gradient time t_G was halved.

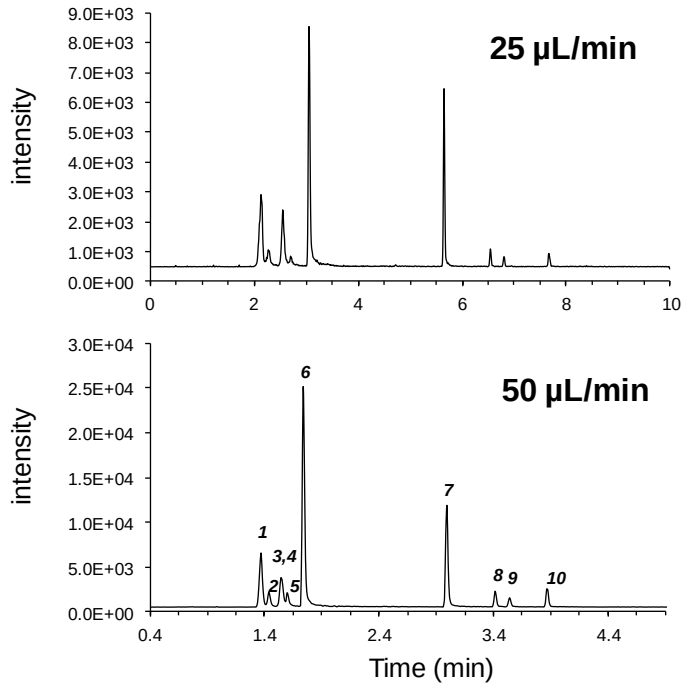

Figure 4.3 Chromatograms of 7 min gradient at 25 µL/min (top) and 3.5 min gradient at 50 µL/min (bottom) using HALO™ 500 µm X 10 cm column.

In addition to the loss of peak capacity, approximately 50% loss of concentration sensitivity was observed running the 3.5 min capillary LC method compared to the 7 min microbore LC method (Figure 4.4).

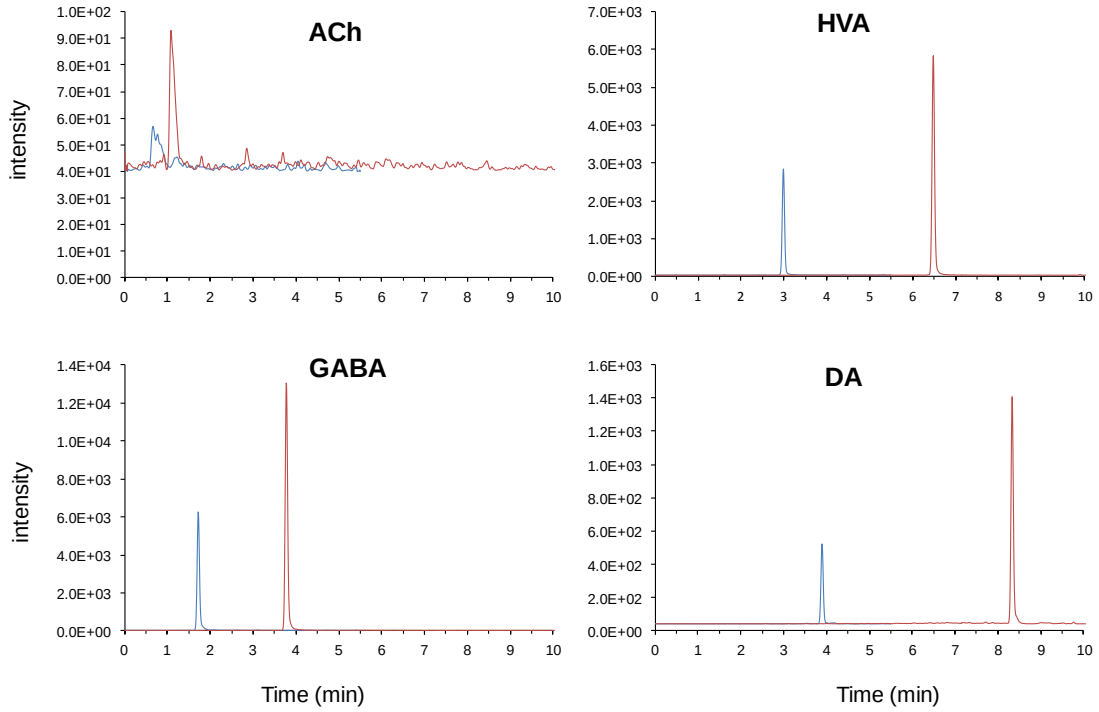

Figure 4.4 Loss of concentration sensitivity of the 3.5 min capillary LC method (blue trace) compared to the 7 min microbore LC method (red trace). Injection volume was adjusted for column void volume. Detailed parameters were listed in Table 4.1.

The ESI sensitivity at 50 µL/min was verified to be the same as 100 µL/min by post column flow splitting experiment (data not shown). The comprise in sensitivity by running the fast capillary LC method can be explained by chromatographic dilution factor *D*, the ratio of initial sample concentration C_0 and the peak maximum concentration C_{max}[101].

$$D = \frac{C_0}{C_{max}} = \frac{\varepsilon\,\pi\,r^2\,(1+k)\sqrt{2\pi LH}}{V_{inj}} = \frac{V_m\,(1+k)\sqrt{2\pi/N}}{V_{inj}} \qquad \text{(Equation 4.5)}$$

ε is the column porosity, r is the column radius, k is the retention factor, L is the column length, H is peak height and N is the plate number. The injection volume V_{inj} was already adjusted for column void volume V_m. Assuming the same retention factor k between the HALO™ 500 µm X 10 cm column and the HSS T3 1 mm X 10 cm column, the dilution factors of these two columns were inversely proportional to $N^{1/2}$. Plate number N is proportional to the square of the ratio of retention time t_R and peak width W.

$$N \propto \frac{t_R^2}{W^2} \qquad \text{(Equation 4.6)}$$

Thus the dilution factors are proportional to W/t_R

$$D \propto \frac{W}{t_R} \qquad \text{(Equation 4.7)}$$

The peak widths between the two LC methods were roughly the same (Figure 4.2). But the retention time of the fast LC method was about half of that of the slower LC method. So the dilution factor of the fast capillary LC method was two times of that of the slower microbore LC method. The two fold chromatographic dilution agrees with two fold loss in concentration sensitivity. However, considering only ¼ sample volume was injected on the capillary column, the mass sensitivity of the fast capillary LC method was still twice better than that of the microbore LC method.

Application for in vivo monitoring and practical aspects

Rat dialysate samples was used to evaluate the new method's suitability for *in vivo* monitoring. The whole LC-MS cycle, including column equilibration, sample loading and injection, was now halved from original 12 min of current method to 6 min. Although 2.4 µL fraction was collected, only 0.5 µL was consumed for analysis. All

amino acids, ACh, Ado, dopamine, 5-HT, metabolites including HVA, DOPAC, 3-MT, 5-HIAA were detected (Figure 4.5). The loss of NE could be partially due to the lower sensitivity of the new method. The ACh peak, broadened by the pre-column band broadening and lower sensitivity, was more difficult to quantify (Figure 4.5). With doubled throughput and doubled mass sensitivity, but halved concentration sensitivity, the fast capillary UHPLC method would be most suited for experiments that generate large number of low volume samples with reasonable analyte concentration such as high temporal resolution monitoring using large microdialysis probes.

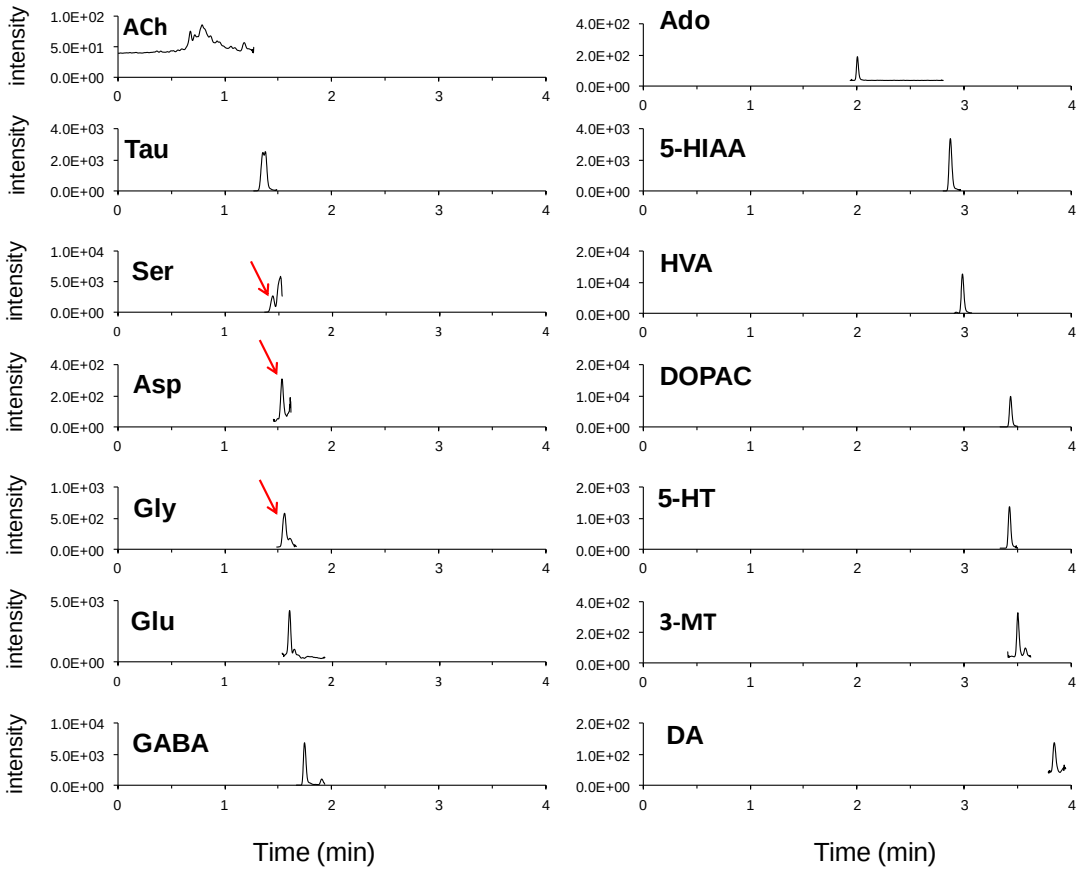

Figure 4.5 Traces of detected neurochemicals from rat brain dialysate.

Conclusion

In this chapter, we explored the possibility of further improving the throughput of the LC-MS method described in Chapter 2. Large capillary column packed with high efficiency fused core particles was proved to be a suitable platform for this purpose. Operating at very high linear velocity (10 mm/sec), gradient time was reduced to 3.5 min with acceptable peak capacity. On the other hand, the difficulty of fitting a smaller sample loop (< 2 μL) caused band broadening of early eluting analytes, reduced their chromatographic resolution and sensitivity. The smaller C term of fused core particles still did not fully compensate for the loss of efficiency due to mass transfer resistance.

Several steps need be taken to fully utilize the advantage of fast capillary UHPLC separation. The internal volume of the capillary UHPLC instrument and connecting tubings need to kept at minimum to reduce the extra column effect. More efficient column is still needed to mitigate the loss of separation power due to mass transfer resistance at high flow velocity. Higher pressure capability of the instrument (> 10,000 psi) will be desirable as both the high efficiency columns and narrow tubings causes increased backpressure. Fast LC separation also placed stringent requirement on the mass spectrometer. The internal volume of the ESI needle need to be small enough as not to cause significant increase in peak width. The mass spectrometer will need to be able to achieve cycle time less than 100 ms with adequate sensitivity to provide enough data points for each peak.

CHAPTER 5.

FUTURE DIRECTIONS

In this dissertation, we describes two mass spectrometry approaches for *in vivo* neurochemical monitoring. Online HPLC coupled to MS allows separation of interferences, enabling comprehensive determination of all classical neurotransmitters in one run. State of the art high speed LC technologies were employed to increase the throughput of sample analysis. Stable isotope labeled internal standard was also used to improve the accuracy and consistency of the analysis. In the second approach, an elaborate segmented flow liquid handling setup replaced HPLC to enable high temporal resolution online MS monitoring of acetylcholine, choline and drugs in brain. Sensitivity was compromised due to lack of liquid phase separation, but was still sufficient to detect basal analyte levels and capture fast *in vivo* chemical changes in the brain at 5 second temporal resolution. The technologies developed in the above mentioned projects can be further refined and expanded into other areas with improved analytical performance.

Benzoylation of Neuropeptides

Neuropeptides are the largest class of neurotransmitters. Over 200 different neuropeptides are involved in signaling in the brain[113]. Highly sensitive and specific LC-MS methods are becoming increasingly popular for detection of neuropeptides in dialysate[12]. Due to peptides' low pM concentration in dialysate samples, nanoLC-tandem MS setup with pre-concentration and nanospray are commonly used to boost the

sensivity[108]. Benzoylation LC-MS described in chapter 2 and chapter 4 focused only on classical small molecule neurotransmitters. Preliminary data showed that neuropeptides such as enkaphalins can also be benzoylated at the N terminus, lysine and tyrosine side chains. Figure 5.1 shows the chromatographic trace of doubly benzoylated leu-enkaphalin and its MS/MS spectrum. The main advantage of pre-column benzoylation for peptides is not increase in hydrophobicity, because the peptides are usually hydrophobic enough for large ratio pre-concentration and excellent ESI response. The major benefit is the ability of incorporating an isotopic tag to these molecules to obtain stable isotope internal standard. Custom synthesized stable isotope incorporated peptides are very expensive and not stable for extended period of time. Not all LC-MS methodologies use these internal standards peptides routinely, leaving matrix effects and instrument drift unaccounted for. Another possible advantage of benzoylating peptides after sample collection is the improved stability. It has been noted that neuropeptides such as the enkaphalins and angiotensin collected in dialysate degrade rapidly even under refrigerated conditions[108, 114]. If the cause of degradation is the peptidase in the environment, chemical modification of the peptides could potentially protect them from decomposing[115]. Following the same derivatization protocol as the small molecules, the LOD of doubly benzoylated leu-enkaphalin was 0.5 nM on the Quattro Ultima, similar to that of monoamines. With the new Agilent 6410 QqQ, which was proven to be > 50 fold more sensitive, it is not unreasonable to expect a LOD of ~ 10 pM for Bz_2-leu-enkaphalin. This level of sensitivity would allow reproducible detection of neuropeptides sampled *in vivo*, together with all the classical neurotransmitters. This will be another step forward in monitoring neurochemicals *in vivo*. Preliminary results also showed that under conditions optimized

for small molecules, the yield of fully benzoylated leu-enkaphalin was not 100%. Both unlabeled and singly labeled peaks were observed. Use of the succinimidyl ester of benzoyl chloride (N-benzoylsuccinimide, or 1-benzoyl-pyrrolidine-2,5-dione by Sigma-Aldrich) is likely to produce more uniform labeling. Reacting at slower rate and lower pH, succinimidyl esters label peptides with good yield sometimes approaching or exceeding 90% and is a very popular chemistry for amine labeling. Driving reaction towards completion will further improve the sensitivity of benzoylated neuropeptides.

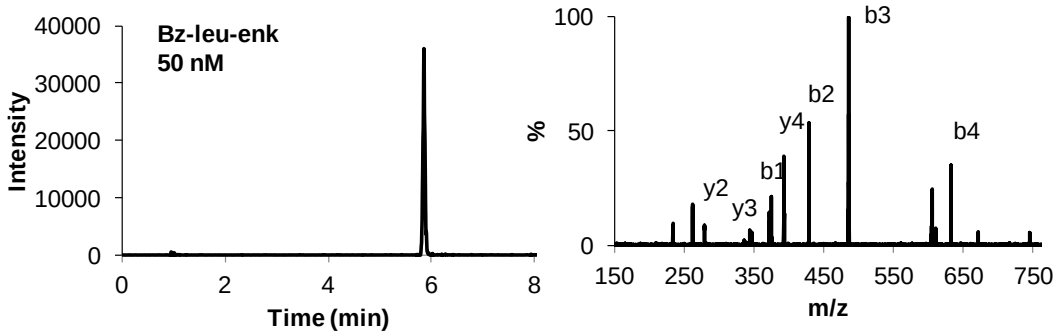

Figure 5.1 Chromatographic traces of doubly benzoylated leu-enkaphalin (left) and its MS/MS spectrum (right). 50 nM unlabeled leu-enkaphalin was mixed with borate buffer and benzoyl chloride solution at 1: 0.5: 0.5 ratio at room temperature. 5 µL of reaction mixture was injected on 1 mm X 10 cm HSS T3 1.8 µm UHPLC column. Data was obtained using Waters nanoAcquity UHPLC coupled to Quattro Ultima QqQ.

Acetylcholine MS Sensor with Higher Spatial and Temporal Resolution

As explained in Chapter 3, the temporal performance of ACh MS sensor current setup is partially limited by the microdialysis. Its internal volume causes mixing of dialysate prior to segmentation, limiting the temporal resolution to the low seconds level[10]. Low flow push pull perfusion, as an alternative sampling technique, has no such limitations and was demonstrated to be capable of sub second temporal resolution[98].

Nano or micro electrospray setup which is capable of lower flow rate is needed to analyze low nL droplets formed by push pull perfusion.

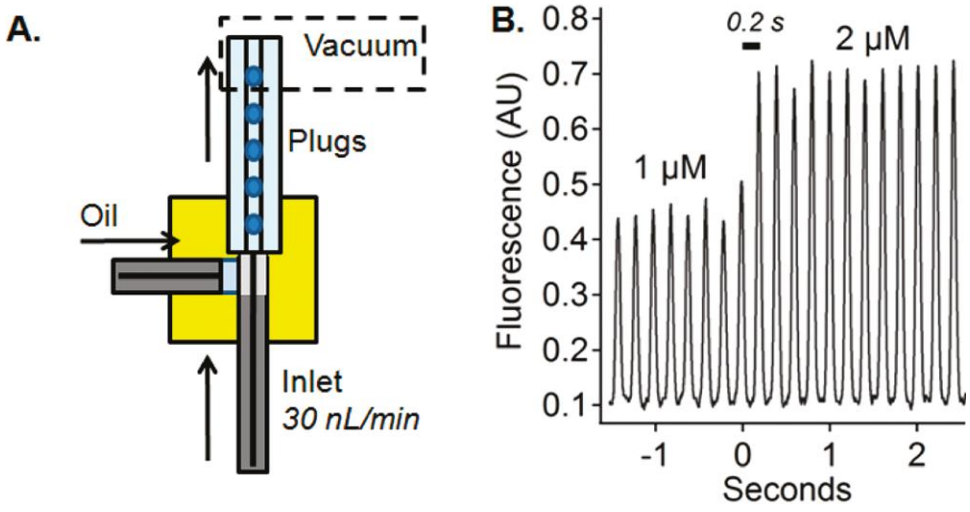

Figure 5.2 System for high temporal resolution sampling. (A) Droplet generation using push-pull perfusion setup; (B) *in vitro* experiment demonstrating 0.2 s temporal resolution[98]. Reproduced with permission from ACS.

MS Sensor for Other Neurotransmitters

There is potential for other small molecule neurotransmitters to be detected using the droplet microdialysis-mass spectrometry setup similar to ACh. Preliminary data showed that elevated level of adenosine can be detected from the brain *in vivo* (Figure 5.3). But as it dropped down to basal level, the sensitivity of the same setup no longer suffice. A more sensitive mass spectrometer or ionization method will allow the MS sensor detect basal level *in vivo* adenosine. Amino acid neurotransmitters lacked the permanent ion group or hydrophobicity of ACh and adenosine. Their ESI-MS sensitivity and ability to overcome ionization suppression is much inferior. To use the MS sensor method, they need to be derivatized to enhance ESI response. In addition to enhancing the ESI-MS delectability of amino acids by increasing the hydrophobicity or charge

derivatization, reagent itself should not cause too much suppression when it is used in excess.

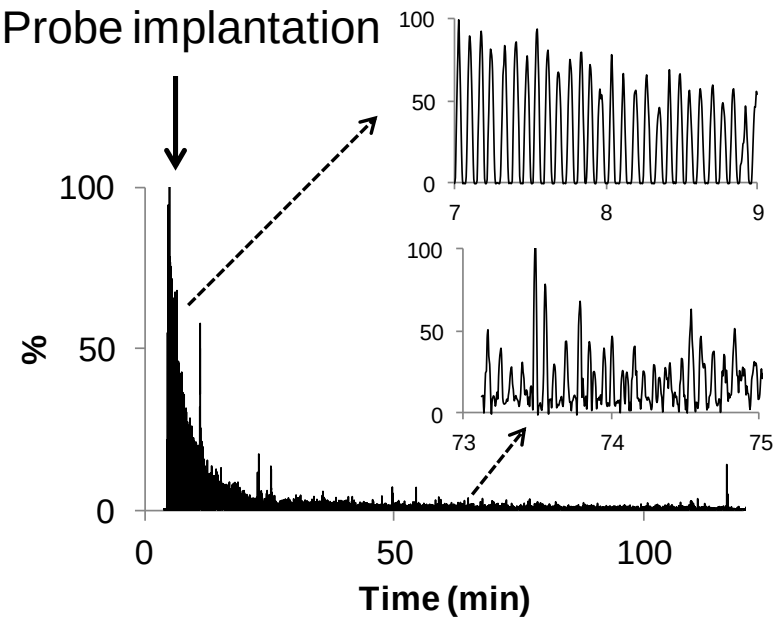

Figure 5.3 Adenosine signal detected by mass spectrometry "sensor" *in vivo*. Elevated level of adenosine following microdialysis probe implantation can be detected by same setup used as ACh MS sensor. But detecting basal adenosine needs more sensitivity.

Quantitative Metabolomics Using C12/C13 Differential Benzoylation

Because of the availability of $^{13}C_6$ benzoly chloride, the benzoylation reaction could be applied to the field of quantitative metabolomics where differential isotope labeling is a powerful tool. As previously mentioned, matrix effect hampers the quantitative results of LC-MS analysis. Use of stable isotopes is generally considered to be the golden standard to overcome such a problem. Compared to purchasing individual stable isotope incorporated standard for all metabolites of interest, differential isotope labeling uses light and heavy reagent to tag the same metabolites in different samples. The chemical labeling step derivatize the same functional group of multiple metabolites,

thus presents a more economical and universal approach[60, 116, 117]. Compared to previously reported differential labeling methods, benzoyl chloride labeling has some unique qualities. First of all, both light and heavy reagents are both commercially available at relatively cheap price, saving the hassle of in house synthesis. Secondly, it is a very reactive and universal reagent. Benzoyl chloride not only labels primary, secondary amines, phenols, but to a less degree, hydroxyl groups, the yield of which can be improved be performing the reaction in a non aqueous environment. Diverse class of metabolites, including amines, phenols and steroids can be benzoylated under appropriate conditions. Third, the product is more stable due to the structural simplicity of benzoyl group. It does not degrade upon exposure to light, unlike reagents originating from fluorescent tags. Fourth, the benzoyl tag is of intermediate hydrophobicity. Smaller isotopic tags such as dimethyl or diethyl labeling do not afford enough hydrophobicity of polar metabolites for reversed phase LC separation, while retention of some bigger tags may be excessive and can cause elution problems.

Metabolomics study used high resolution mass spectrometer, some at fullscan mode after differential isotope labeling[60], others at data dependant MS/MS mode[118]. The former gave high confidence identification of metabolites, but produced very large data sets. The extraction of chromatographic peaks has to be done using software. Labeled metabolites, unlabeled metabolites, background ions were all picked up and integrated. The un- discriminative data processing demanded high computing power and could potentially result in overlooking the low level analytes of interest. Isobaric labeling and data dependant MS/MS acquisition allowed simultaneous quantitative analysis of multiple samples and reduced the data size. But it also overlooked the low abundance

ions and placed high demand on the MS acquisition speed, especially when online high speed LC was used.

Here we propose a method that combines the elements of both high resolution fullscan and MS/MS acquisition but has unique advantages. Initial sample preparation was the same as previous methods. Two samples under different treatment are labeled with light and heavy benzoyl chloride respectively and mixed prior analysis (Figure 5.4).

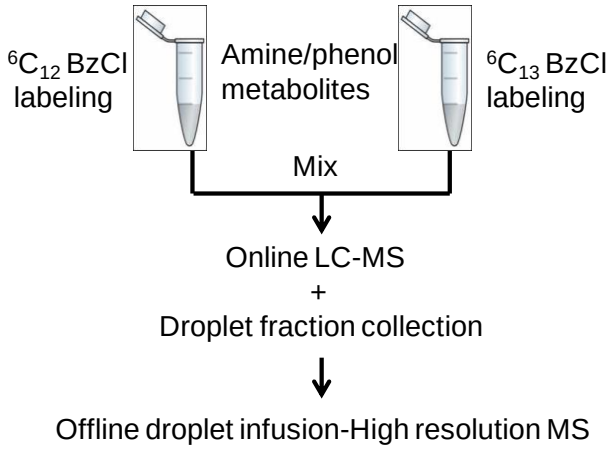

Figure 5.4 Workflow of metabolomics experiment using differential benzoylation and parallel MS acquisition.

The MS analysis is of two steps. In the first step, HPLC is coupled to QqQ operating at parent scan mode for daughter ion 105 (C12 benzoyl group) and 111 (C13 benzoyl group) (Figure 5.5).

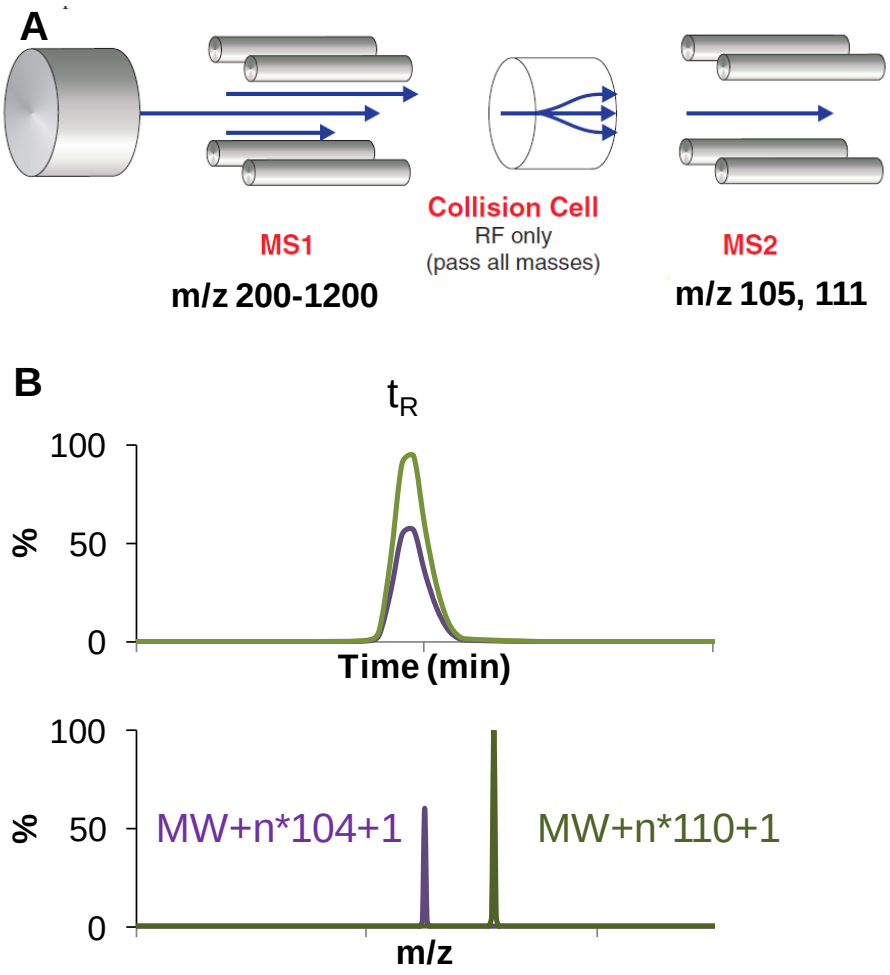

Figure 5.5 Experimental setup (A) and data (B) obtainable from online HPLC with QqQ in parent ion scan mode. The same metabolite molecules in two samples are labeled with light and heavy benzoyl groups respectively, which co-elute on the chromatogram but differentiate on the mass spectrum.

At the same time, a small portion of the LC effluent (1-10 μL/min) will be diverted to a tee where it is mixed with immiscible oil to form droplets similar to the fashion described in chapter 3 (Figure 5.6 A). Droplet fraction collection allows complete preservation of separation resolution. In the second MS step, droplets containing tubing is connected to a high resolution mass spectrometer and the LC effluent segmented by oil droplets is directly pumped through the ESI and analyzed by the MS (Figure 5.6 B).

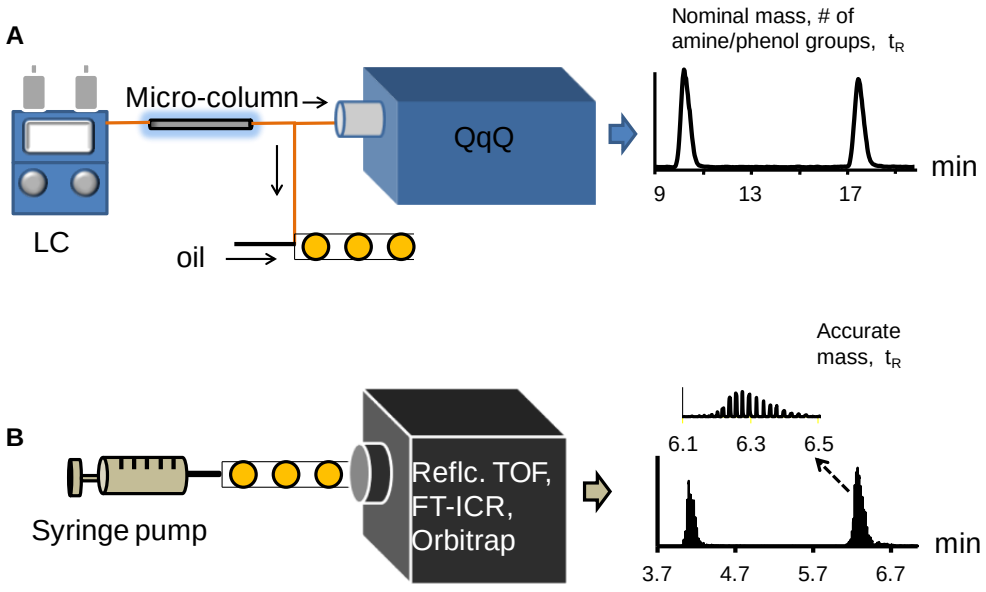

Figure 5.6 Two step metabolomics MS experiment coupled by droplet LC fraction collection. A small fraction of online LC effluent is collected as oil segmented droplets while the majority is diverted to the QqQ (A). The droplets are then pumped into a high resolution MS (B). Since segmentation prevented mixing of droplet content, the LC resolution is preserved. The chromatographic "peak" is made of individual droplet signal.

As the data from the first step MS experiment being processed, labeled metabolites will be picked up by software such as XCMS, same way as previously done. The ones that changes will be identified by statistics and a list of candidates is generated. From the mass difference between the light and heavy species, we will be able to know the number of functional groups and the nominal molecular weight. Then the high mass resolution data from the second step fullscan MS experiment will be examined using the known nominal mass of the candidate metabolites. The high mass resolution and accuracy will allow further narrowing down candidate metabolites. Once a tentative identification is made, standard compound can be obtained to compare retention time t_R for further confirmation.

Since all small molecules produced characteristic benzoyl group fragment ion, only the benzoylated metabolites will generate signals on the MS. This protocol eliminates background ions and non-labeled species. Doing so reduces the data size and complexity, it will easier for the software to pick up from much fewer features contained in the raw data. The parent ion scan does not discriminate low abundance ions like the data dependant acquisition. So their chance of being identified should be improved both from the data acquisition point of view and data processing part. Metabolite identification also benefits from the use of high mass resolution data. But processing of such data can be easily done manually because the list of candidates with their nominal mass is already generated from the low resolution QqQ data. Only a few targeted m/z will be looked at. Droplet fraction collection has convincingly demonstrated its ability of preserving chromatographic resolution[96] (also Appendix A). This simple arrangement eliminated the need of setting up another HPLC instrument to the high resolution MS while ensuring identical chromatographic information (Figure 5.6). It requires no additional LC-MS runs or sample consumption. One injection will suffice in obtaining all information from one sample.

APPENDICES

Appendix A: Droplet nanoLC Fraction Collection

HPLC effluent fraction collection allows more flexible analysis of separated analytes. It is commonly done by transferring LC effluent to individual containers. For nano LC separation, the conventional approach is no longer feasible due to evaporation and handling problems associated with nL volume fractions. nanoLC fraction collection in droplet format was reported and showed its ability to couple with slower offline analysis without losing much chromatographic resolution[96]. Here we further expanded this methodology to demonstrate its compatibility with both slow or fast MS detection.

Negative ion electron capture dissociation (niECD) is a novel MS/MS mode that is advantageous in analyzing negatively charged bio-molecules with labile functional group such as phosphorylated peptides. niECD, at its current stage of development, takes several seconds to obtain one high quality spectrum, which makes it not readily compatible with high efficiency online HPLC separation. But with droplet fraction collection and offline infusion, longer MS acquisition was possible without excessive loss of chromatographic resolution. Each chromatographic peak was segmented into five to six ~30 nL droplets. When infused at 20 nL/min into the FTICR MS for niECD, each droplet lasted more than 1 min to allow more acquisition time for niECD.

Sample: 5 uM phosphopeptide mixture from Anaspec (Bovine ß-Casein, PKA Regulatory Subunit II Substrate, UOM9, Phosphorylated PKC Substrate-3, DAM1 [221-241] peptide, Kinase Domain of Insulin Receptor-singly phosphorylated, Kinase Domain of Insulin Receptor-triply phosphorylated). PKA Regulatory Subunit II substrate signal low, sometimes not observed.

LC condition: column 75 um X 10 cm packed with Waters dC18 3um particle, m.p. A: 10 mM ammonium formate, 0.15% formic acid, B: 0.15% formic acid in MeOH, 0% to 70 % m.p.B in 22 min, flow rate 340 nL/min, injection volume ~ 40 nL.

Droplet generation: LC effluent was mixed with oil by a 1/16" microvolume tee (Valco, MT1XCPK). Capillary column was adapted to the tee using 1/16" Teflon sleeve. Droplet was collected in 250 um i.d. 1/16" o.d. tubing (IDEX). LC effluent ~340 nL/min, oil 150 nL/min, droplet size ~30 nL.

Droplet analysis condition on FTICR: initial flow rate 100 nL/min, upon elution of the first peptide containing droplet, flow rate dropped to 20 nL/min to facilitate niECD. Spray tip was 20/360 um with 5 um opening from New Objective (FS360-20-5-CE). Droplet containing tubing was adapted to spray tip by a reducing union (IDEX, P882). Voltage was applied by attaching wires to the conductive tip front.

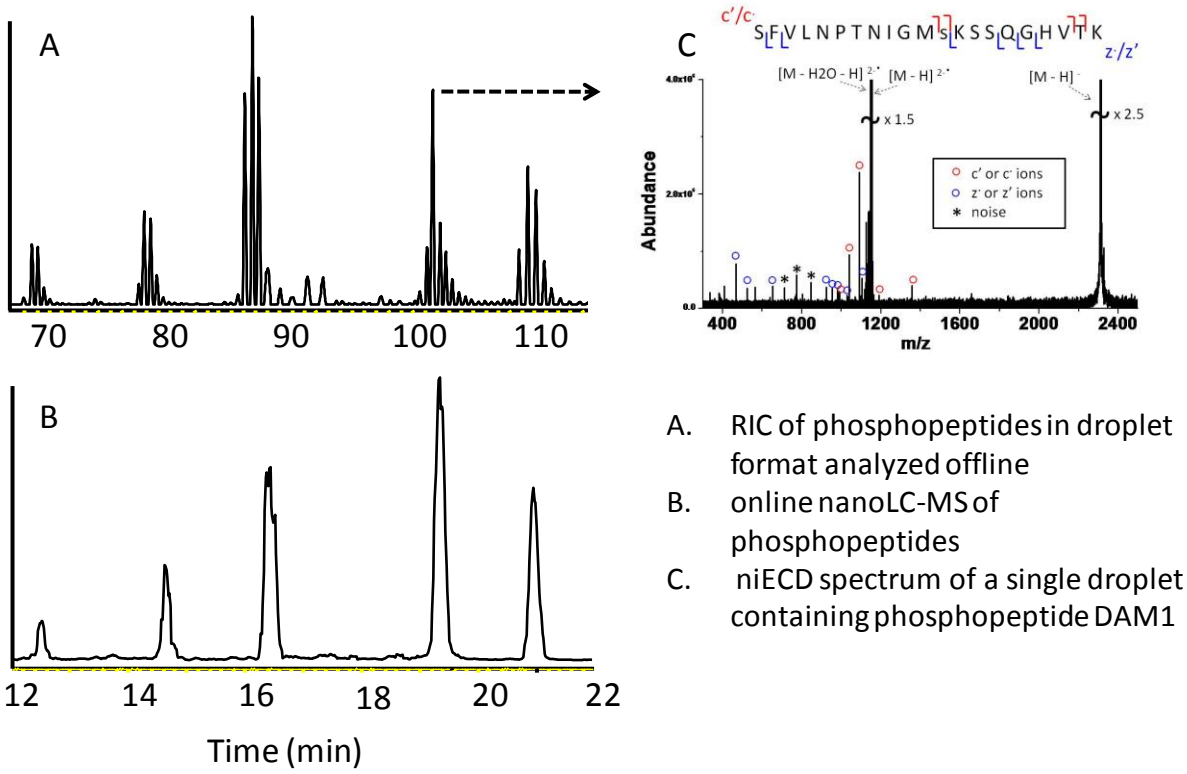

A. RIC of phosphopeptides in droplet format analyzed offline
B. online nanoLC-MS of phosphopeptides
C. niECD spectrum of a single droplet containing phosphopeptide DAM1

Figure A.1 niECD performed by peak parking using droplet capillary LC fraction collection. Phosphopeptide ion trace in droplet format (A) responded to that obtained from online capillary LC-MS (B). niECD spectrum (C) was obtained from DAM1 contained in a single droplet.

In cases where the mass spectrometer is capable of fast scanning, the LC effluent in droplet format can be analyzed at high speed with the chromatographic resolution intact.

Sample: dansylated amino acids, taurine and GABA, each at 50 µM. 20 mg/mL dansyl chloride was made in acetonitrile. The labeling reaction was carried out by mixing amino acid standard with 100 mM sodium tetraborate (in water) and dansyl chloride solution at 1:1:1 volume ratio. Reaction mixture was kept at 60^{o}C for 30 min.

LC condition: column 75 um X 10 cm packed with Waters dC18 3um particle, m.p. A: 10 mM ammonium formate, 0.15% formic acid, B: 0.15% formic acid in MeOH, 0% to 70 % m.p.B in 22 min, flow rate 340 nL/min, injection volume ~ 40 nL

Droplets generation: LC effluent was mixed with oil by a 1/16" microvolume tee (Valco, MT1XCPK). Capillary column was adapted to the tee using 1/16" Teflon sleeve. Droplet was collected in 250 um i.d. 1/16" o.d. tubing (IDEX). LC effluent ~340 nL/min, oil 300 nL/min, each peak segmented into ~ 10 droplets.

MS acquisition: online nanoLC-MS performed on LCQ in fullscan mode, positive nanoESI, droplets infusion on QqQ at 2.4 μL/min. QqQ operated in MRM mode at ~ 19 Hz. Each droplet got ~ 10 data points. nanoESI source was installed on QqQ. Cone gas 150 L/Hr, nebulizing gas 50 L/Hr, source temperature 100 ^{o}C. spray tip was fabricated in house from 75/360 μm fused silica capillary, etch to have an opening of ~ 30 μm. Voltage was applied at the end of the tip by a 1/16" metal union. Tip was adapted to the union via a fused silica adapter ferrule (Valco, FS1.3PK-5).

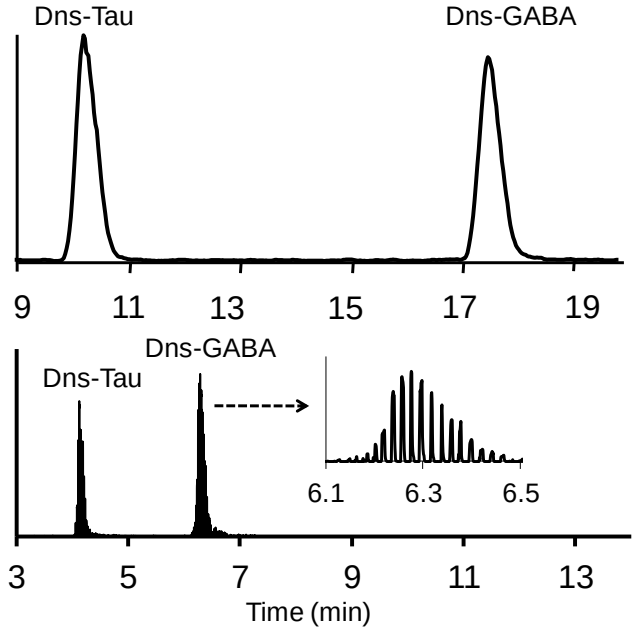

Figure A.2 Fast capillary LC fraction analysis by MS in droplet format. Chromatographic resolution of online LC (top) was fully preserved by the droplet format (bottom).

Droplet infusion rate was ~3.75 fold of original combined oil + effluent flow rate (300 nL/min + 340 nL/min). The separation time of online nanoLC was ~ 3.47 fold of that of fast offline droplet analysis. The difference between observed value and expected value is likely due to inaccuracy of nanoLC flow rate measurement .

Appendix B: MALDI-TOF Amino Acids Analysis

Matrix assisted laser desorption (MALDI) is another popular soft ionization method for mass spectrometry and is widely used in bio-analysis. Compared to continuous ESI, MALDI is pulsive ionization method and is more tolerant to ionization suppression. Although in many cases, desalting is still needed for high quality spectrum. One disadvantage of MALDI is the high background ions associated with the matrix in the low mass range obscuring small molecule signal. We adapted a charge derivatization method that shifted m/z of amino acids to above 500 and allowed us to detect multiple amino acids from rat brain dialysate.

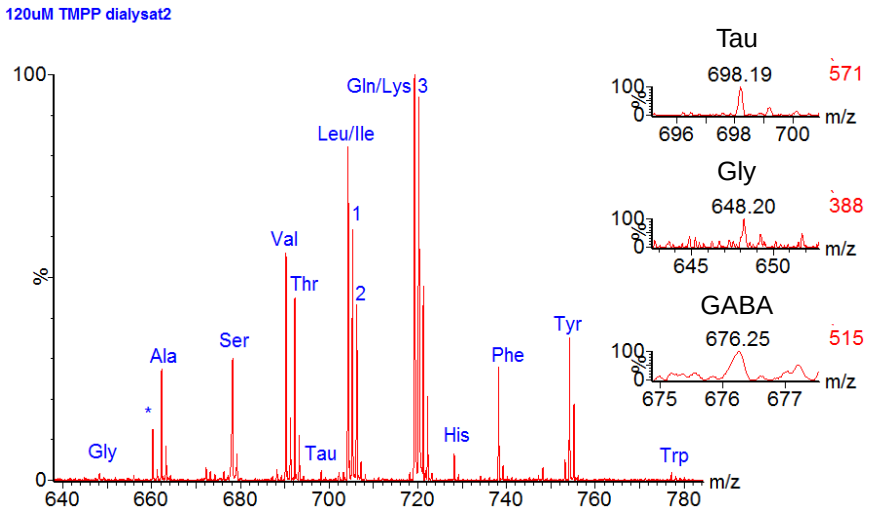

Figure A.3 Mass spectrum of amino acids from rat brain dialysate. 1. Combined signal of Leu/Ile 2nd isotopic peak + Asn; 2. Combined signal of Asn 2nd isotopic peak + Asp; 3. Combined signal of Gln/Lys 2nd isotopic peak + Glu.

Sample preparation: 1 μL dialysate was mixed with 1 μL 20 mM sodium tetraborate (in water) and 1 μL 0.12mM TMPP-Ac-OSu (in ACN). After 30 min reaction at room temperature, mixture was added equal volume of matrix solution (CHCA 10 mg/mL 50% 0.1% TFA in water 50% MeOH), and 1 μL was deposited on MALDI plate.

Mass spectrometry: Micromass MALDI Tofspec-2E, reflectron mode. Operating voltage: 20 kv, positive, suppression 500 AMU, pulse time 39, pulse voltage 2200 V. Sampling rate 2 G Hz, sensitivity 300 mV, shorts 5, mass range 1000

11 amino acids (Gly, Ala, Ser, Val, Thr, Tau, Leu/Ile, His, Phe, Tyr, Trp) can be unequivocally detected within 1-2 s from less than 100 nL of rat brain dialysate. No salt adduct signal was observed due to the permanent charge fixed on the molecule by derivatization. Due to the limited mass resolution of this instrument, amino acids which are 1 Da apart in molecular weight such as the group of Gln/Glu and Leu/Asn/Asp could not be differentiated due to isotopic distribution. Minimum resolution of 36, 000 is required to tell these amino acids apart from each other. The sensitivity of GABA was not adequate for routine analysis. Despite these limitations for in vivo neurotransmitter monitoring, this method with some modifications is suitable for other areas such as newborn PKU screening to take advantage of its simplicity, high throughput and low sample consumption. With high resolution tandem MS instrument, Caprioli's group used the same reaction for neurotransmitter imaging of rat brain[119].

Appendix C: LC-MS Method of Water Soluble Vitamin Analysis

Column: Waters Atlantis T3 3 μm, 1 mm X 15 cm

Temperature: 27 ^{o}C

Mobile phase: A. 10 mM ammonium formate, 0.15% formic acid in water; B. 10 mM ammonium formate, 0.15% formic acid in methanol

Gradient: 0-5 min, 0-50% m.p.B; 5-7min, 50-70% m.p.B

Flow rate: 50 µL/min

Injection volume: 2 µL

Sample preparation: extracted from tear strips using 50 uL of mobile phase A. 30 uL of extract was placed in autosampler vials for LC-MS analysis.

Table A.1 MS acquisition conditions for water soluble vitamins

Analyte	Parent Ion	Daughter Ion	Dwell Time (ms)	Frag (V)	CE (V)	Cell Acc (V)	Polarity
B1	265.1	122.1	50	125	10	7	Positive
B6 pyridoxine	170.1	134.1	50	125	15	7	Positive
B6 pyridoxamine	169.2	134.1	50	125	15	7	Positive
B6 pyridoxal	168.1	150.1	50	115	10	7	Positive
B3 NA	124.1	80.1	50	135	20	7	Positive
B3	123.1	80.1	50	125	10	7	Positive
B12	678.7	147.2	50	155	35	7	Positive
B9	442.1	295.1	50	115	10	7	Positive
B2	377.1	243	50	115	20	7	Positive
B7	245.1	227.2	50	115	10	7	Positive
B5	220.1	90.1	50	115	10	7	Positive

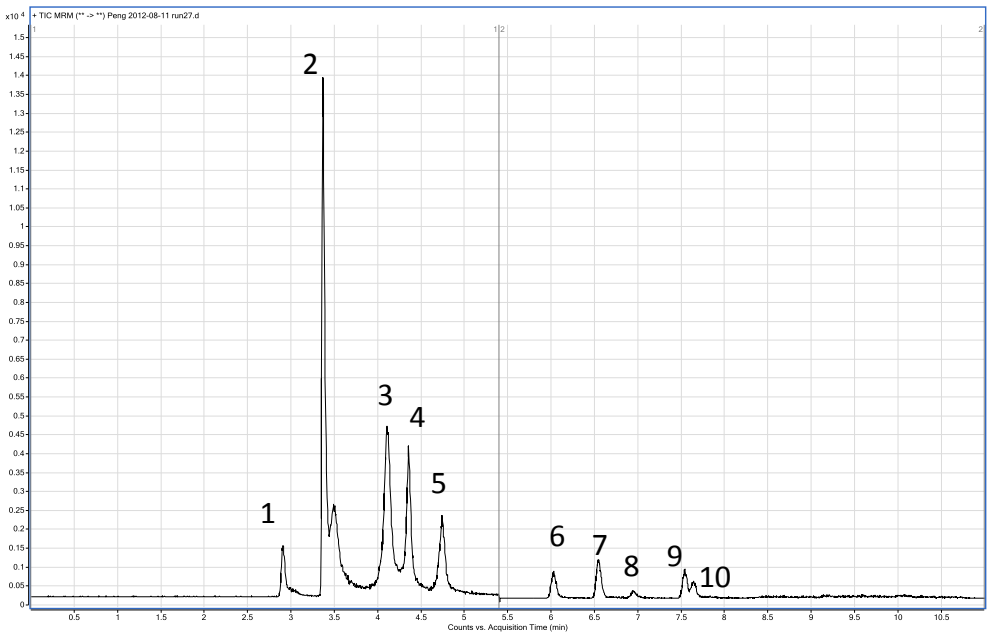

Figure A.4 Overall chromatogram of 11 waters soluble vitamin standard using finalized LC-MS method. 1.B6 pyridoxamine; 2. B1; 3. B3 nictonic acid (NA) and B6 pyridoxal; 4. B6 pyridoxine; 5. B3 nicotinamide (NM); 6. B5; 7. B12; 8. B9; 9. B7; 10. B2.

Appendix D: Common LC-MS Instrument Troubleshooting

Quattro Ultima Mass Spectrometer

Reset communication:

1. Press windows key + R on the keyboard
2. Type in “telnet epc” from the command window that pops up
3. Type in “reboot” in the DOS window to reboot the embedded computer in the mass spectrometer. 3 beeping sound will be heard.
4. Check re-establishment of communication by press windows key + R and type in “ping-epc”. Communication is established after the response time is less than 1 ms.

nanoAcquity UHPLC

Calibrating loop and needle volume:

Often when a new sample loop or needle is fitted, the autosampler fails to perform the required volume calibration. This is primarily due to the un-coordinated movement of the wash syringes and sample syringes. For 5 µL sample loops, loop and needle volume calibration can be successfully performed after the following steps

1. Power down the autosampler
2. Open the instrument panel cover
3. Re-connect the bubble detector's cable
4. Power up the autosampler and redo the volume calibration

Operating at flow rate below 50 µL/min:

Another curious feature of the nanoAcquity is its flow meter feedback mechanism. By default, ~ 20 cm long 25 µm i.d. PEEKSil tubing is used to connect the two flow meters (one for each mobile phase) to the mixing tee. However, this narrow tubing causes too much backpressure (> 1000 psi) when high flow rate (> 50 µL/min) is used and is replaced by bigger i.d. tubing for running LC method at 100 µL/min. Interestingly, when bigger tubing is used to connect the flow meter to the mixing tee in solvent line B, B pump does not deliver the right amount of m.p.B at flow rate below 20 µL/min. Thus for running gradient LC methods with flow rate ≤ 50 µL/min, the 25 µm i.d. tubing is still to be used to ensure the correct delivery of gradient.

REFRENCES

(1) Aebersold, R., Mann, M. *Nature* **2003**, *422*. 198-207.
(2) Dettmer, K., Aronov, P. A., Hammock, B. D. *Mass Spectrom. Rev.* **2007**, *26*. 51-78.
(3) Raman, R., Raguram, S., Venkataraman, G., Paulson, J. C., Sasisekharan, R. *Nat. Methods* **2005**, *2*. 817-824.
(4) Nadja B. Cech, C. G. E. *Mass Spectrom. Rev.* **2001**, *20*. 362-387.
(5) Stroobant, E. d. H. a. V. *Mass Spectrometry - Principles and Applications*. 3 ed.; John Wiley & Sons, Ltd: Chichester, UK, 2007.
(6) Mark F. Bear, B. W. C., Michael A. Paradiso *Neuroscience Exploring the Brain*. 3rd ed.; Lippincott Williams & Wilkins: Baltimore, MD, 2007.
(7) Schultz, K. N., Kennedy, R. T. *Annu. Rev. Anal. Chem.* **2008**, *1*. 627-61.
(8) Venton, B. J., Robinson, T. E., Kennedy, R. T. *J. Neurochem.* **2006**, *96*. 236-246.
(9) Lada, M. W., Vickroy, T. W., Kennedy, R. T. *Anal. Chem.* **1997**, *69*. 4560-4565.
(10) Wang, M., Slaney, T., Mabrouk, O., Kennedy, R. T. *J. Neurosci. Methods* **2010**, *190*. 39-48.
(11) Boyd, B. W., Witowski, S. R., Kennedy, R. T. *Anal. Chem.* **2000**, *72*. 865-871.
(12) Perry, M., Li, Q., Kennedy, R. T. *Anal. Chim. Acta* **2009**, *653*. 1-22.
(13) Miao, H., Rubakhin, S. S., Sweedler, J. V. *Anal. Chem.* **2005**, *77*. 7190-7194.
(14) Shou, M. S., Ferrario, C. R., Schultz, K. N., Robinson, T. E., Kennedy, R. T. *Anal. Chem.* **2006**, *78*. 6717-6725.
(15) Wang, M., Roman, G. T., Schultz, K., Jennings, C., Kennedy, R. T. *Anal. Chem.* **2008**, *80*. 5607-5615.
(16) Hows, M. E. P., Lacroix, L., Heidbreder, C., Organ, A. J., Shah, A. J. *J. Neurosci. Methods* **2004**, *138*. 123-132.
(17) Zhang, M. Y., Beyer, C. E. *J. Pharm. Biomed. Anal.* **2006**, *40*. 492-499.
(18) Zhang, X. Z., Rauch, A., Lee, H., Xiao, H. B., Rainer, G., Logothetis, N. K. *Rapid Commun. Mass Spectrom.* **2007**, *21*. 3621-3628.
(19) Ji, C. J., Li, W. L., Ren, X. D., El-Kattan, A. F., Kozak, R., Fountain, S., Lepsy, C. *Anal. Chem.* **2008**, *80*. 9195-9203.
(20) Taylor, P. J. *Clin. Biochem.* **2005**, *38*. 328-334.
(21) Garden, R. W., Moroz, L. L., Moroz, T. P., Shippy, S. A., Sweedler, J. V. *J. Mass Spectrom.* **1996**, *31*. 1126-1130.
(22) Gerber, S. A., Rush, J., Stemman, O., Kirschner, M. W., Gygi, S. P. *Proc. Natl. Acad. Sci. U. S. A.* **2003**, *100*. 6940-6945.
(23) Colin F. Poole, S. A. S. *Contemporary practice of chromatography*. Elsevier Science Publishers B.V.: Amsterdam, The Netherlands, 1984.
(24) Jorgenson, J. W., in *Annual Review of Analytical Chemistry, Vol 3*. 2010, vol. 3, pp 129-150.
(25) DeStefano, J. J., Langlois, T. J., Kirkland, J. J. *J. Chromatogr. Sci.* **2008**, *46*. 254-260.
(26) Gritti, F., Guiochon, G. *J. Chromatogr., A* **2007**, *1176*. 107-122.
(27) Cunliffe, J. M., Maloney, T. D. *J. Sep. Sci.* **2007**, *30*. 3104-3109.
(28) Unger, K. K., Skudas, R., Schulte, M. M. *J. Chromatogr., A* **2008**, *1184*. 393-415.

(29) Guiochon, G. *J. Chromatogr., A* **2007**, *1168*. 101-168.
(30) Cabrera, K. *J. Sep. Sci.* **2004**, *27*. 843-852.
(31) Heinisch, S., Rocca, J.-L. *J. Chromatogr., A* **2009**, *1216*. 642-658.
(32) McNeff, C. V., Yan, B., Stoll, D. R., Henry, R. A. *J. Sep. Sci.* **2007**, *30*. 1672-1685.
(33) Yan, B. W., Zhao, J. H., Brown, J. S., Blackwell, J., Carr, P. W. *Anal. Chem.* **2000**, *72*. 1253-1262.
(34) Xiqin Yang, L. M., Peter W. Carr *J. Chromatogr., A* **2005**, *1079*. 213–220.
(35) Tossman, U., Ungerstedt, U. *Acta Physiol. Scand.* **1986**, *128*. 9-14.
(36) Robinson, T. E., Justice, J. B. J. *Techniques in the behavioral and neural sciences*. Elsevier: Amsterdam, Netherlands, 1991.
(37) Westerink, B. H. C., Cremers, T. I. F. H. *Handbook of microdialysis*. Elsevier: Amsterdam, Netherlands, 2007.
(38) Di Chiara, G., Imperato, A. *Proc. Natl. Acad. Sci. U. S. A.* **1988**, *85*. 5274-5278.
(39) Cornish, J. L., Kalivas, P. W. *J. Neurosci.* **2000**, *20*. RC89.
(40) LaLumiere, R. T., Kalivas, P. W. *J. Neurosci.* **2008**, *28*. 3170-3177.
(41) PorkkaHeiskanen, T., Strecker, R. E., Thakkar, M., Bjorkum, A. A., Greene, R. W., McCarley, R. W. *Science* **1997**, *276*. 1265-1268.
(42) During, M. J., Ryder, K. M., Spencer, D. D. *Nature* **1995**, *376*. 174-177.
(43) Feuerstein, D., Manning, A., Hashemi, P., Bhatia, R., Fabricius, M., Tolias, C., Pahl, C., Ervine, M., Strong, A. J., Boutelle, M. G. *J. Cereb. Blood Flow Metab.* **2010**, *30*. 1343-1355.
(44) Bullock, R., Zauner, A., Woodward, J., Young, H. F. *Stroke* **1995**, *26*. 2187-2189.
(45) Felice, L. J., Felice, J. D., Kissinger, P. T. *J. Neurochem.* **1978**, *31*. 1461-1465.
(46) Liu, Y., Zhang, J., Xu, X., Zhao, M. K., Andrews, A. M., Weber, S. G. *Anal. Chem.* **2010**, *82*. 9611-9616.
(47) Yoshitake, T., Yoshitake, S., Fujino, K., Nohta, H., Yamaguchi, M., Kehr, J. *J. Neurosci. Methods* **2004**, *140*. 163-168.
(48) Zhou, S. Y., Zuo, H., Stobaugh, J. F., Lunte, C. E., Lunte, S. M. *Anal. Chem.* **1995**, *67*. 594-599.
(49) Robert, F., Bert, L., Denoroy, L., Renaud, B. *Anal. Chem.* **1995**, *67*. 1838-1844.
(50) Maidment, N. T., Brumbaugh, D. R., Rudolph, V. D., Erdelyi, E., Evans, C. J. *Neuroscience* **1989**, *33*. 549-557.
(51) Eckstein, J. A., Ammerman, G. M., Reveles, J. M., Ackermann, B. L. *J. Neurosci. Methods* **2008**, *171*. 190-196.
(52) Hong, S., Pedersen, P. L. *Microbiol. Mol. Biol. Rev.* **2008**, *72*. 590-641.
(53) Skorka, G., Shuker, P., Gill, D., Zabicky, J., Parola, A. H. *Biochemistry* **1981**, *20*. 3103-3109.
(54) You, Z. B., Wang, B., Zitzman, D., Azari, S., Wise, R. A. *J. Neurosci.* **2007**, *27*. 10546-10555.
(55) Parsons, L. H., Justice, J. B. *J. Neurochem.* **1993**, *61*. 1611-1619.
(56) Westerink, B. H. C., Kwint, H. F., deVries, J. B. *J. Neurosci.* **1996**, *16*. 2605-2611.
(57) Redmond, J. W., Tseng, A. *J. Chromatogr.* **1979**, *170*. 479-481.
(58) Higa, S., Suzuki, T., Hayashi, A., Tsuge, I., Yamamura, Y. *Anal. Biochem.* **1977**, *77*. 18-24.
(59) Miki, K., Sudo, A. *Clin. Chem.* **1998**, *44*. 1759-1762.
(60) Guo, K., Li, L. *Anal. Chem.* **2009**, *81*. 3919-3932.
(61) Nestler, E. J. *Nat. Neurosci.* **2005**, *8*. 1445-1449.
(62) Koob, G. F., Le Moal, M. *Neurobiology of addiction*. Elsevier: Amsterdam, Netherlands, 2006.
(63) Dobi, A., Margolis, E. B., Wang, H. L., Harvey, B. K., Morales, M. *J. Neurosci.* **2010**, *30*. 218-229.
(64) Johnson, S. W., North, R. A. *J. Neurosci.* **1992**, *12*. 483-488.
(65) Szabo, B., Siemes, S., Wallmichrath, I. *Eur. J. Neurosci.* **2002**, *15*. 2057-2061.

(66) Tan, K. R., Brown, M., Labouebe, G., Yvon, C., Creton, C., Fritschy, J. M., Rudolph, U., Luscher, C. *Nature* **2010**, *463*. 769-U78.
(67) Paxinos, G., Watson, C. *The rat brain in stereotaxic coordinates*. 6 ed.; Elsevier: Amsterdam, Netherlands, 2007.
(68) Lipska, B. K., Weinberger, D. R. *Neuropsychopharmacology* **2000**, *23*. 223-239.
(69) Parikh, V., Kozak, R., Martinez, V., Sarter, M. *Neuron* **2007**, *56*. 141-154.
(70) Hasselmo, M. E., Sarter, M. *Neuropsychopharmacology* **2010**, *36*. 52-73.
(71) Wilson, G. S., Gifford, R. *Biosens. Bioelectron.* **2005**, *20*. 2388-2403.
(72) Nandi, P., Lunte, S. M. *Anal. Chim. Acta* **2009**, *651*. 1-14.
(73) Lindinger, W., Hansel, A., Jordan, A. *Int. J. Mass Spectrom.* **1998**, *173*. 191-241.
(74) Cooks, R. G., Ouyang, Z., Takats, Z., Wiseman, J. M. *Science* **2006**, *311*. 1566-1570.
(75) Caprioli, R. M., Lin, S. N. *Proc. Natl. Acad. Sci. U. S. A.* **1990**, *87*. 240-243.
(76) Wong, P. S. H., Yoshioka, K., Xie, F., Kissinger, P. T. *Rapid Commun. Mass Spectrom.* **1999**, *13*. 407-411.
(77) Van der Zee, E. A., Luiten, P. G. M. *Prog. Neurobiol.* **1999**, *58*. 409-471.
(78) Dani, J. A., Ji, D. Y., Zhou, F. M. *Neuron* **2001**, *31*. 349-352.
(79) Day, J., Damsma, G., Fibiger, H. C. *Pharmacol. Biochem. Behav.* **1991**, *38*. 723-729.
(80) White, K. E., Cummings, J. L. *Compr. Psychiat.* **1996**, *37*. 188-195.
(81) Felician, O., Sandson, T. A. *J. Neuropsychiatr. Clin. Neurosci.* **1999**, *11*. 19-31.
(82) Burmeister, J. J., Pomerleau, F., Huettl, P., Gash, C. R., Wemer, C. E., Bruno, J. P., Gerhardt, G. A. *Biosens. Bioelectron.* **2008**, *23*. 1382-1389.
(83) Mitchell, K. M. *Anal. Chem.* **2004**, *76*. 1098-1106.
(84) Zhu, Y. X., Wong, P. S. H., Cregor, M., Gitzen, J. F., Coury, L. A., Kissinger, P. T. *Rapid Commun. Mass Spectrom.* **2000**, *14*. 1695-1700.
(85) Hows, M. E. P., Organ, A. J., Murray, S., Dawson, L. A., Foxton, R., Heidbreder, C., Hughes, Z. A., Lacroix, L., Shah, A. J. *J. Neurosci. Methods* **2002**, *121*. 33-39.
(86) Zhang, M. Y., Hughes, Z. A., Kerns, E. H., Lin, Q., Beyer, C. E. *J. Pharm. Biomed. Anal.* **2007**, *44*. 586-593.
(87) Shackman, H. M., Shou, M., Cellar, N. A., Watson, C. J., Kennedy, R. T. *J. Neurosci. Methods* **2007**, *159*. 86-92.
(88) Huang, T. H., Yang, L., Gitzen, J., Kissinger, P. T., Vreeke, M., Heller, A. *J. Chromatogr. B-Biomed. Appl.* **1995**, *670*. 323-327.
(89) Persike, M., Zimmermann, M., Klein, J., Karas, M. *Anal. Chem.* **2010**, *82*. 922-929.
(90) Church, W. H., Justice, J.B. *Anal. Chem.* **1987**, *59*. 712-716.
(91) Song, P., Mabrouk, O. S., Hershey, N. D., Kennedy, R. T. *Anal. Chem.* **2012**, *84*. 412-419.
(92) Kelly, R. T., Page, J. S., Marginean, I., Tang, K., Smith, R. D. *Angew. Chem. Int. Ed.* **2009**, *48*. 6832-6835.
(93) Zhu, Y., Fang, Q. *Anal. Chem.* **2010**, *82*. 8361-8366.
(94) Fidalgo, L. M., Whyte, G., Ruotolo, B. T., Benesch, J. L. P., Stengel, F., Abell, C., Robinson, C. V., Huck, W. T. S. *Angew. Chem. Int. Ed.* **2009**, *48*. 3665-3668.
(95) Baker, C. A., Roper, M. G. *Anal. Chem.* **2012**, *84*. 2955-2960.
(96) Li, Q., Pei, J., Song, P., Kennedy, R. T. *Anal. Chem.* **2010**, *82*. 5260-5267.
(97) Chen, D., Du, W., Liu, Y., Liu, W., Kuznetsov, A., Mendez, F. E., Philipson, L. H., Ismagilov, R. F. *Proc. Natl. Acad. Sci. U. S. A.* **2008**, *105*. 16843-16848.
(98) Slaney, T. R., Nie, J., Hershey, N. D., Thwar, P. K., Linderman, J., Burns, M. A., Kennedy, R. T. *Anal. Chem.* **2011**, *83*. 5207-5213.
(99) Uutela, P., Reinila, R., Piepponen, P., Ketola, R. A., Kostiainen, R. *Rapid Commun. Mass Spectrom.* **2005**, *19*. 2950-2956.

(100) Benveniste, H., Hansen, A. J., Ottosen, N. S. *J. Neurochem.* **1989**, *52*. 1741-1750.
(101) Vissers, J. P. C., Claessens, H. A., Cramers, C. A. *J. Chromatogr., A* **1997**, *779*. 1-28.
(102) Vissers, J. P. C. *J. Chromatogr., A* **1999**, *856*. 117-143.
(103) Edwards, J. L., Edwards, R. L., Reid, K. R., Kennedy, R. T. *J. Chromatogr., A* **2007**, *1172*. 127-134.
(104) Kennedy, R. T., Jorgenson, J. W. *Anal. Chem.* **1989**, *61*. 1128-1135.
(105) Gatlin, C. L., Kleemann, G. R., Hays, L. G., Link, A. J., Yates, J. R. *Anal. Biochem.* **1998**, *263*. 93-101.
(106) Shi, Y., Xiang, R., Horvath, C., Wilkins, J. A. *J. Chromatogr., A* **2004**, *1053*. 27-36.
(107) Emmett, M. R., Andren, P. E., Caprioli, R. M. *J. Neurosci. Methods* **1995**, *62*. 141-147.
(108) Li, Q., Zubieta, J. K., Kennedy, R. T. *Anal. Chem.* **2009**, *81*. 2242-2250.
(109) Johannes P.C. Vissers*, A. H. d. R., Mario Ursem, Jean-Pierre Chervet *J. Chromatogr., A* **1996**, *746*. 1-7.
(110) Lloyd R. Snyder, J. W. D. *High-Performance Gradient Elution The Practical Application of the Linear-Solvent-Strength Model*. John Wiley & Sons, Inc: Hoboken, NJ, 2007.
(111) Neue, U. D., Marchand, D. H., Snyder, L. R. *J. Chromatogr., A* **2006**, *1111*. 32-39.
(112) Gritti, F., Guiochon, G. *J. Chromatogr., A* **2012**, *1238*. 77-90.
(113) Wotjak, C. T., Landgraf, R., Engelmann, M. *Pharmacol. Biochem. Behav.* **2008**, *90*. 125-134.
(114) Lanckmans, K., Van Eeckhaut, A., Sarre, S., Smolders, I., Michotte, Y. *J. Chromatogr., A* **2006**, *1131*. 166-175.
(115) Dass, C., Mahalakshmi, P. *Life Sci.* **1996**, *58*. 1039-1045.
(116) Katja Dettmer, P. A. A., Bruce D. Hammock *Mass Spectrom. Rev.* **2007**, *26*. 51–78.
(117) Michael R. Shortreed, S. M. L., Brian L. Frey, Margaret F. Phillips, Madhusudan Patel,, Peter J. Belshaw, a. L. M. S. *Anal. Chem* **2006**, *78*. 6398-6403.
(118) Yuan, W., Anderson, K. W., Li, S., Edwards, J. L. *Anal. Chem.* **2012**, *84*. 2892-2899.
(119) Caprioli, L. M. R. M., presented in part at 60th ASMS Vancouver, Canada, Yea.